SHORT NOTES ON ALASKAN GEOLOGY
1981

GEOLOGIC REPORT 73

Recent research on Alaskan geology

STATE OF ALASKA

Jay S. Hammond, *Governor*

John W. Katz, *Commissioner, Dept. of Natural Resources*

Geoffrey Haynes, *Deputy Commissioner*

Ross G. Schaff, *State Geologist*

'Short Note' Editorial Policy

This document comprises short contributions on recent investigations of a limited scope on Alaskan geology. Manuscripts are accepted for review with certain qualifications: that manuscripts must not have been published or submitted for publication elsewhere; that all persons listed as authors have given their approval for submission of the paper; and that any person cited as a source of personal communication has approved such a citation.

Two copies of the manuscript, typed double spaced including references and figure captions, should be submitted to Editor, Alaska Division of Geological & Geophysical Surveys, Box 80007, College, AK 99708. No more than seven double-spaced manuscript pages (2000 words), including references, figures, and tables, will be accepted. All figures should be camera ready and suitable for black-and-white reproduction at a maximum size of 6-1/2 by 8-1/2 inches—foldout or color art will not be accepted. Contributors should keep one copy of material submitted. All manuscripts will be examined and approved by Alaska DGGS reviewers. *Substantial changes by the author—whether scientific or editorial—will not be allowed once the manuscript is in galley form.*

Deadline for manuscripts for the next Short Notes on Alaska Geology is September 1, 1982.

Cover photo: Holocene maar crater, Buzzard Creek area, north flank of Alaska Range; view to north. Photo by Mary D. Albanese.

For sale by Alaska Division of Geological and Geophysical Surveys, P.O. Box 80007, College, 99708; 323 E. 4th Ave., Anchorage, 99501; P.O. Box 7438, Ketchikan, 99901; and 230 S. Franklin, Juneau, 99811. Cost: $3.

CONTENTS

METRIC CONVERSION FACTORS

To convert feet to meters, multiply by 0.3048. To convert inches to centimeters, multiply by 2.54.

ALKALINE IGNEOUS ROCKS IN THE EASTERN ALASKA RANGE

By Jeffrey Y. Foley[1]

INTRODUCTION

Previously unreported, alkaline igneous rocks occur in the eastern Alaska Range as two dike swarms, one near the West Fork of the Robertson River and another to the east near the Tok River. These rocks intrude the underlying Precambrian and possibly younger, crystalline metamorphic terrane and are believed to be the youngest igneous rocks in the area. A single potassium-argon age date (69.2 ± 1.5 m.y.) on biotite indicates that a local, Late Cretaceous thermal event was associated with a stage of alkaline magmatism.

SUMMARY OF GEOLOGY

The upper West Fork of the Robertson River (figs. 1, 2) drains a crystalline terrane consisting largely of polymetamorphic pelitic schists and associated metamorphosed mafic flows. These rocks are correlated with the Birch Creek Schist (Mertie, 1937; Moffit, 1954; Richter and Jones, 1973) of Precambrian age (Wahrhaftig, 1968; Forbes, 1971). Mineral assemblages within the pelitic and mafic schists are restricted to the greenschist facies, as defined by Winkler (1967, p. 88-106) and Miyashiro (1973, p. 67). Quartz-mica schist is most abundant, with subordinate quartz-mica-garnet schist, chlorite-albite-epidote schist, actinolite schist, quartzite, and marble. These rocks are largely sedimentary in origin and contain minor mafic volcanic interlayers. A younger(?) metavolcanic and metasedimentary section to the east, between the Robertson and Tok Rivers, is associated with the stratiform massive-sulfide deposits of the 'Delta Mineral Belt' (Clynton Nauman, oral commun.).

Large metamorphosed diorite and gabbro sills---up to tens of meters thick---show relict, phaneritic igneous textures with metamorphic overprinting in the form of a weakly developed, preferred orientation of prismatic minerals. Postmetamorphic alkaline igneous rocks intrude the above-described lithologies.

PETROLOGY OF THE ALKALINE ROCKS

Potassic alkaline igneous rocks within the study area include a swarm of biotite-lamprophyre dikes and sills, associated breccia dikes, and a heterogeneous stock of alkali gabbro and alkali diorite. The lamprophyre dikes are most common and typically strike northeast. This recurring strike direction is generally controlled by a northeast-striking joint set, but in some cases, the dikes are controlled by normal faults that are oblique to the joint set.

Although these alkaline igneous rocks show a wide range of textures, the most common is fine- to medium-grained, panidiomorphic to porphyritic. Many narrow dikes and sills are continuous in strike and outcrop for tens of meters, but others bifurcate and show discontinuous thicknesses ranging from centimeters to several meters. Mineralogically, these rocks contain euhedral biotite, augite, olivine, and occasional hornblende in a groundmass of fine-grained plagioclase, potassium feldspar, and ankeritic carbonate with up to 5 percent euhedral ilmenite and magnetite (samples 257, 349, 355, 377; table 1). Alteration resulted in corrosion of mafic phenocrysts, and olivine typically displays a web texture characteristic of serpentinization. Alteration products include chlorite and iron oxides after mafic minerals; pyroxene and olivine are replaced by antigorite, talc, and carbonate. Feldspars are extensively fractured and replaced by carbonate along these fractures. Accessory minerals include abundant

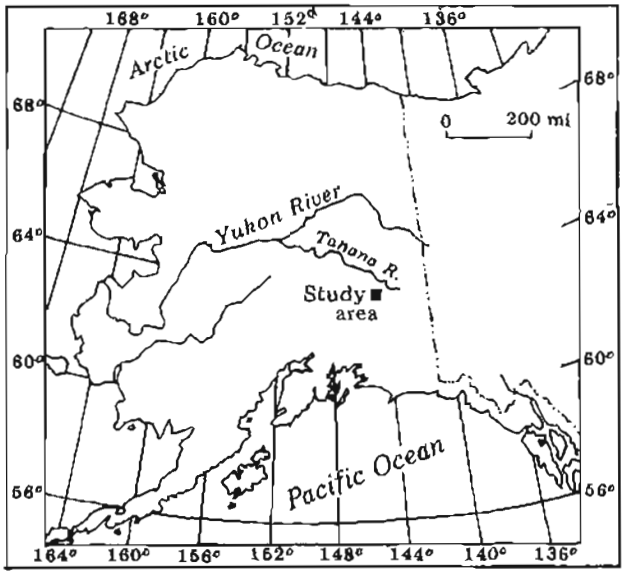

Figure 1. Location of study area in the east-central Mt. Hayes Quadrangle, Alaska.

[1]U.S. Bureau of Mines, Fairbanks, Alaska 99701.

needles of apatite in feldspar and fine, fish-egg-like aggregates of sphene.

Locally, some dikes exhibit the ocellar texture (sample 375, table 1) peculiar to lamprophyric, volcanic rocks (Carmichael and others, 1974, p. 66; Philpotts, 1972). Ocelli are spheroidal aggregates--from microns to centimeters in diameter--with the same mineralogy as the remainder of the rock, but with a greater proportion of carbonate and felsic minerals in a glassy groundmass. Theories of ocelli origin include a) formation by segre-

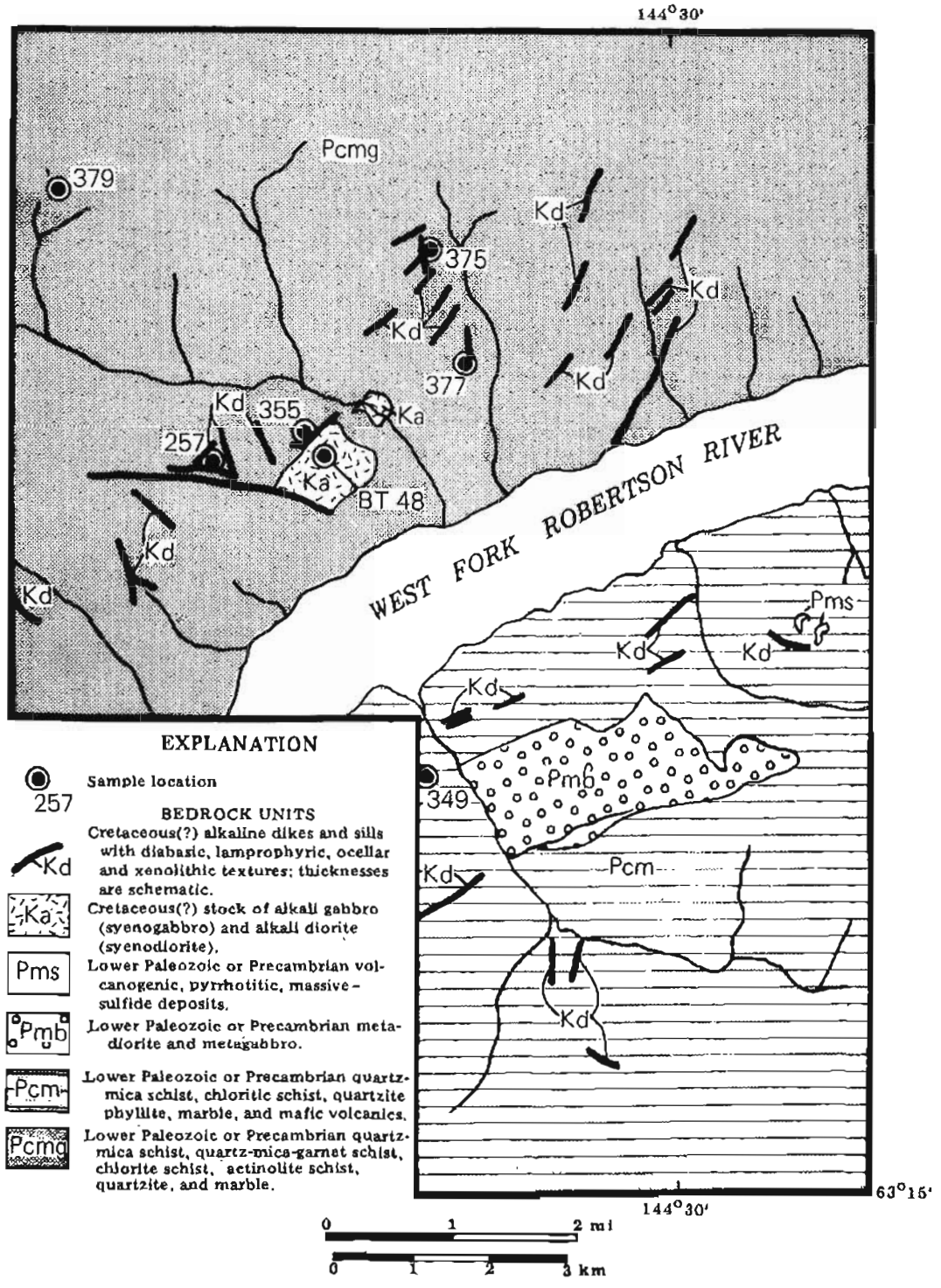

Figure 2. Generalized bedrock geology, West Fork Robertson River, Alaska.

Table 1. *Chemical analyses*[1] *(wt %) and CIPW norms of seven igneous rocks from Robertson River area.*

	257 Porphyritic, panidiomorphic biotite-augite lamprophyre	349 Porphyritic biotite-augite-olivine lamprophyre	355 Porphyritic, panidiomorphic biotite-augite-olivine lamprophyre	375 Ocellar biotite-augite lamprophyre	377 Porphyritic biotite-augite-olivine lamprophyre	379 Siliceous, hornblende-porphyry dike	BT48 Phaneritic alkali diorite
SiO_2	47.50	51.80	51.80	47.50	50.10	56.90	55.00
TiO_2	0.85	1.60	1.10	1.10	0.87	0.94	0.67
Al_2O_3	10.10	15.00	10.90	11.80	12.90	14.90	14.20
FeO^1	8.20	10.60	8.70	10.40	8.30	6.90	5.40
MnO	0.16	0.90	0.14	0.18	0.18	0.09	0.06
MgO	8.70	0.72	9.10	8.80	7.10	3.90	3.10
CaO	9.20	6.60	8.30	7.90	7.90	6.10	5.20
Na_2O	2.70	4.10	2.50	0.99	2.50	3.50	4.00
K_2O	1.60	5.20	3.90	3.20	4.80	3.80	5.10
P_2O_5	0.15	0.21	0.15	0.12	0.14	0.17	1.05
BaO	0.15	0.21	0.15	0.15	0.20	0.16	0.13
SrO	0.08	0.09	0.07	0.06	0.11	0.11	0.02
H_2O^2	8.60	1.20	0.80	7.70	4.40	1.20	4.90
CO_2	5.00	0.40	0.10	3.30	2.40	0.10	2.80
Total	102.99	98.63	97.71	103.20	101.90	98.77	101.63
			CIPW norms				
qz	1.12	0.00	0.00	0.72	0.00	1.79	2.83
or	9.81	32.17	23.61	19.77	28.76	23.03	30.70
ab	25.15	22.40	19.70	9.29	22.76	32.24	36.59
an	11.12	7.51	7.18	18.42	9.94	14.08	1.26
co	0.00	0.00	0.00	0.29	0.00	0.00	1.83
di	2.16	18.54	26.91	0.00	10.80	12.30	0.00
hy	35.06	0.00	0.00	40.94	0.50	14.66	16.93
ol	0.00	5.99	18.57	0.00	19.56	0.00	0.00
il	1.23	2.33	1.57	1.60	1.23	1.34	0.95
ap	0.24	0.31	0.24	0.24	0.30	0.30	2.24
cc	13.12	1.06	0.26	8.73	6.61	0.26	7.21
			Thornton-Tuttle Differentiation Index (Thornton and Tuttle, 1960)				
DI[2]	36.08	54.57	43.31	29.78	51.52	57.06	70.12

[1]Resource Associates of Alaska, Fairbanks, and Skyline Laboratories, Wheat Ridge, Colorado.
[2]H_2O measured upon ignition at 1000°C; total iron measured as FeO.

Table 2. *Analytical data for biotite ^{40}K-^{40}Ar age determination on alkali diorite (sample BT48). Analysis by D.L. Turner and Diane Duvall, Geophysical Institute, University of Alaska, Fairbanks.*

K_2O (wt %)	Sample weight (g)	$^{40}Ar_{rad}$ (moles/gm) x 10^{-11}	$\frac{^{40}Ar_{rad}}{^{40}K \times 10^{-3}}$	$\frac{^{40}Ar_{rad}}{^{40}Ar_{total}}$	Age ± 1σ (m.y.)
8.017	0.1194	81.179	4.099	0.811	69.2 ± 1.9
8.010					
7.960					
7.983					
$\bar{x}$ = 7.993					

gation of residual magma that migrates into vesicles prior to complete solidification of the host rock, and b) formation as droplets of immiscible feldspathic melt separate from a cooling basic magma (Carmichael and others, 1974; Philpotts, 1972).

Although the lamprophyric dikes and sills represent the most common mode of occurrence of alkaline rocks in the map area, chemically and mineralogically related rocks occur as breccia dikes containing xenoliths of quartz-rich schist and gneiss suspended in a mafic, biotite-rich matrix. The breccia-dike groundmass is mineralogically and texturally similar to the typical lamprophyric dike rock except resorption of siliceous xenoliths has resulted in silica enrichment of the mafic groundmass. The abundance of quartz-rich xenoliths (fig. 3) and carbonate suggests forceful emplacement of rapidly ascending, volatile-rich magma.

A single stock of medium- to coarse-grained, panidiomorphic alkali gabbro and alkali diorite (fig. 2; sample BT48, table 1) is interpreted as the plutonic equivalent of the alkaline dike rocks on the basis of proximity and mineralogical and chemical similarities. Mafic minerals in the plutonic rocks include varying proportions of biotite and augite; biotite is partly altered to chlorite and augite to carbonate, talc, and antigorite. Plagioclase and orthoclase are largely altered to carbonate, sericite, and kaolin. Some coarse euhedral and twinned carbonate grains do occur but replacement textures predominate, indicating a late paragenesis for the carbonate. Accessories include quartz, magnetite, ilmenite, olivine, and apatite. A potassium-argon age of 69.2 ± 1.9 m.y. was obtained from biotite in sample BT48 (table 2). This conforms with the Late Triassic or Early Jurassic through Late Cretaceous thermal event reported by Foster and others (1973).

Table 1 shows chemical analyses and CIPW norms for selected samples of alkaline igneous and related rocks collected in the Robertson River area (fig. 2). Figure 4 is an alkali-silica diagram illustrating the alkaline nature of these samples. Lamprophyres characteristically have a high content of both FeO + MgO and $Na_2O + K_2O$; are rich in volatiles, including H_2O and CO_2; and are enriched in BaO, SrO, and P_2O_5. Evidence of deuteric activity is also common, including bleached biotite crystals, alteration of feldspar to carbonate, and serpentine-talc-carbonate pseudomorphs after olivine (Turner and Verhoogen, 1951, p. 334). All rocks listed in table 1 resemble lamprophyres by containing abundant biotite, augite, and olivine with occasional barkevikitic hornblende. Samples 355, 375, and 377 are potash-rich lamprophyres. Sample 257 has a lower potash content and sample 349 contains anomalously low MgO but is texturally, mineralogically, and otherwise chemically similar to lamprophyres. Sample 379 is a siliceous hornblende porphyry with a carbonatized, feldspathic groundmass. Sample BT48 is a phaneritic, hypidiomorphic, biotite-alkali diorite with abundant orthoclase and plagioclase; biotite is the primary mafic constituent. A sample of float collected near sample BT48—a biotite *peridotite* distinguished by its cumulate texture—is representative of the deep-seated magmatic source of the rocks described in this paper.

DISCUSSION

Numerous mechanisms have been proposed for the genesis of lamprophyric magmas (Turner and Verhoogen, 1960, p. 254-256; Carmichael and others, 1974,

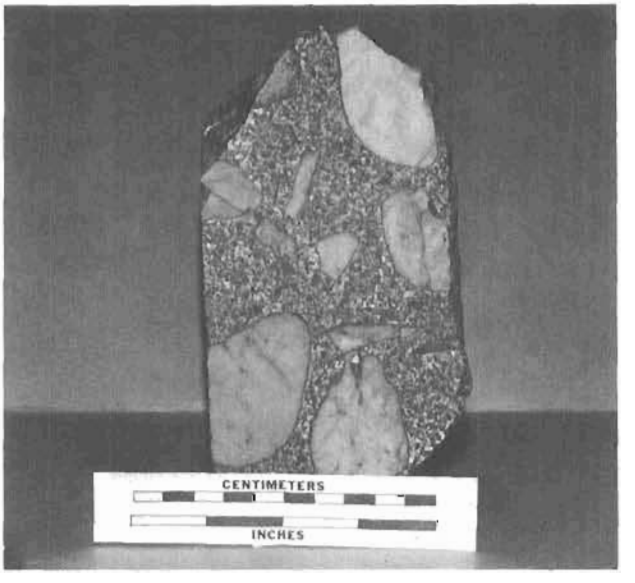

Figure 3. Sample of breccia dike showing quartz-rich xenoliths.

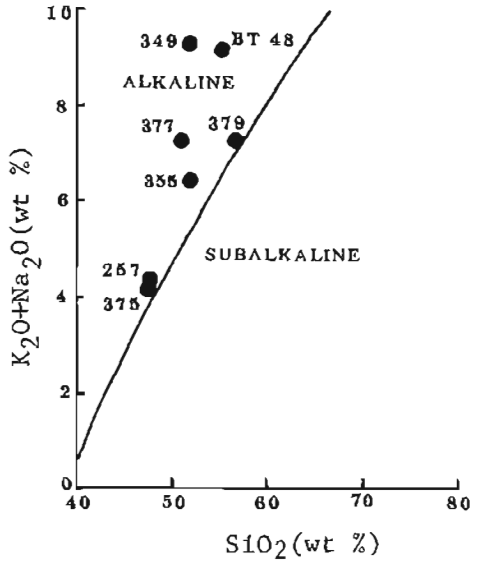

Figure 4. Alkali-silica diagram (after Irvine and Baragar, 1971) for seven rocks from Robertson River area, Alaska.

p. 508-510). Among these are differentiation from alkaline, olivine basaltic magmas, differentiation from granitic magmas, and assimilation of wall rock by magma. Most authors favor multiple modes of origin because lamprophyres have a wide range of composition; in fact, the term lamprophyre is generally texturally defined. A combination of these mechanisms may account for a specific variety of lamprophyre, and this may be the case with the alkaline rocks in the Robertson River area. It is unclear what type of primary magma is responsible for the evolution of these rocks, but remelting of ferromagnesian minerals at the base of a body of differentiating magma in the presence of a hydrous phase could account for alkali enrichment of the liquid phase and result in the production of abundant biotite with simultaneous crystallization of pyroxene and olivine (Bowen, 1928, p. 258-273). It is clear that a CO_2-rich volatile phase played a significant role in the late-stage, deuteric alteration of these rocks. Oftedahl (1957) explains potassic lamprophyres as products of fusion of a shale roof by hot gases emanating from an underlying magma. This hypothesis may account for the high content of BaO, SrO, H_2O, P_2O_5, and CO_2 characteristic of potassic lamprophyres and explains the high incidence of quartz-rich xenoliths in these rocks.

ACKNOWLEDGMENTS

Charles Green, James Mason, and Don Cannon, formerly with Asamera Oil, Inc., provided the author with the opportunity to undertake this project. Asamera Oil, Inc., provided logistical support during the 1978 field season. I thank Don Turner and Diane Duvall for the potassium-argon age determination. Bear Creek Mining Company and the University of Alaska School of Mineral Industry assisted in paying for chemical analyses. Special thanks go to T.K. Bundtzen for his continuous aid and encouragement and thoughtful review, and to reviewers J.T. Dillon, T.E. Smith, S.E. Swanson, and Clynton Nauman. Helpful comments were also offered by Paul Metz.

REFERENCES CITED

Bowen, N.L., 1928, Evolution of the igneous rock: Princeton, Princeton University Press, 332 p.

Carmichael, I.S.E., Turner, F.J., and Verhoogen, John, 1974, Igneous petrology: New York, McGraw-Hill, 739 p.

Forbes, R.B., 1971, Preliminary investigations of the petrology and structure of the Birch Creek Schist in the Fairbanks and Circle districts, Alaska: Geological Society of America Bulletin, v. 71, no. 2, p. 2085.

Foster, H.L., Weber, F.R., Forbes, R.B., and Brabb, E.E., 1973, Regional geology of the Yukon-Tanana Upland, Alaska, *in* Pitcher, M.G., ed., Arctic geology: American Association of Petroleum Geologists Memoir 19, p. 388-395.

Irvine, T.N., and Baragar, W.R.A., 1971, A guide to the chemical classification of common volcanic rocks: Canadian Journal of Earth Science, v. 8, p. 523-548.

Mertie, J.B., 1937, The Yukon-Tanana Region, Alaska: U.S. Geological Survey Bulletin 872, 276 p.

Miyashiro, Akiho, 1973, Metamorphism and metamorphic belts: Great Britian, Unwin Brothers Limited, 492 p.

Moffit, F.H., 1954, Geology of the eastern Alaska Range and adjacent area: U.S. Geological Survey Bulletin 989-D, 218 p.

Oftedahl, C., 1957, Studies on the igneous rock complex of the Oslo region, *in* Turner, F.J., and Verhoogen, John, 1960, Igneous and metamorphic petrology (2d ed.): New York, McGraw-Hill, p. 254-255.

Philpotts, A.R., 1972, Density, surface tension and viscosity of the immiscible phase in a basic, alkaline magma: Lithos, v. 5, p. 1-18.

Richter, D.H., and Jones, D.J., 1973, Structure and stratigraphy of eastern Alaska Range, Alaska, *in* Pitcher, M.G., ed., Arctic geology: American Association of Petroleum Geologists Memoir 19, p. 408-420.

Thornton, C.P., and Tuttle, O.F., 1960, Chemistry of igneous rocks, I. Differentiation index: American Journal of Science, v. 258, p. 664-684.

Turner, F.J., and Verhoogen, John, 1951, Igneous and metamorphic petrology (1st ed.): New York, McGraw-Hill, 602 p.

_____, 1960, Igneous and metamorphic petrology (2d ed.): New York, McGraw-Hill, 694 p.

Wahrhaftig, Clyde, 1968, Schists of the central Alaska Range: U.S. Geological Survey Bulletin 1254-E, 22 p.

Winkler, H.G.F., 1967, Petrogenesis of metamorphic rocks (2d ed.): New York, Springer-Verlag, 237 p.

SHEAR MODULI AND DAMPING RATIOS FOR THE BOOTLEGGER COVE FORMATION AS DETERMINED BY RESONANT-COLUMN TESTING

By Randall G. Updike[1], David A. Cole, Jr.[2], and Cathy Ulery[1]

INTRODUCTION

The physical properties of soils underlying a site or region have a profound influence on the response of that area to earthquakes. Techniques to assess the dynamic behavior of soils during a seismic event have only recently approached the sophistication required to assess the characteristics of site-specific response to seismic-induced excitation; in fact, no single technique provides the precise simulation of both *in situ* conditions and the responses of a soil sequence during a seismic event (Woods, 1978). Resonant-column testing, however, has proven instructive in determining the dynamic behavior of the Bootlegger Cove Formation, a glaciomarine clayey silt that underlies much of the Anchorage area.

The Bootlegger Cove Formation played a critical role in the ground failures that occurred in the bluffs within the city during the 1964 Prince William Sound earthquake. Although some studies were performed immediately after the earthquake (Shannon and Wilson, 1964), additional research was not conducted until recently (Updike and Carpenter, 1981). However, high seismic exposure and pressure for urban development are prompting renewed interest in the dynamic behavior of the Bootlegger Cove Formation and other sedimentary units. This paper is the result of one study to develop siting criteria for the Anchorage community.

STRESS-STRAIN PROPERTIES OF SOILS

Predicting the response of the Bootlegger Cove Formation to earthquake-loading conditions requires an understanding of the nonlinear stress-strain properties of individual sedimentary units during cyclic loading. Material properties that describe the dynamic behavior of a soil are its shear modulus and damping ratio. For small shear-strain amplitudes, the shear modulus is generally equal to the mean slope of its stress-strain curve (secant modulus). However, as the level of strain increases, the stress-strain behavior becomes increasingly nonlinear ('softer'), and typically results in a marked decrease in shear modulus. Similarly, material damping, or the energy-absorbing characteristics of soil, is also strain dependent. Damping modeled in ground-response studies is generally expressed as a fraction of critical viscous damping, termed the damping ratio. The damping ratio for soil typically increases nonlinearly with increasing cyclic shear-strain amplitude. Shear strain developed in unconsolidated deposits during earthquakes may increase from about 10^{-3} percent during low-level ground shaking to 10^{-1} percent for strong motions. Within this range, nonlinear strain dependency is generally most pronounced; the lower part of that range ($10^{-3}<\gamma>10^{-1}$) is examined in this paper.

ENGINEERING-GEOLOGIC FACIES OF THE BOOTLEGGER COVE FORMATION

The Bootlegger Cove Formation is a clastic sedimentary unit of late Pleistocene (~14,000 years B.P.) age (Schmoll and others, 1972). Formerly referred to as the 'Bootlegger Cove Clay,' the formation actually consists of silt with some clay and fine sand. Recent research (Updike, 1981) indicates that the various sedimentary facies that constitute the formation developed in response to subtle changes in the glaciomarine depositional environment. Each facies is the product of a distinct set of depositional and postdepositional environmental factors, and retains a characteristic suite of mappable engineering properties.

Engineering geologic facies defined within the Bootlegger Cove Formation include: a) F.I., clay, with very minor silt and sand; b) F.II, silty and/or clayey silt; c) F.III, silty clay and/or clayey silt, sensitive; d) F.IV, silty clay and/or clayey silt, with thin silt and sand lenses; e) F.V, silty clay and/or clayey silt, with random pebbles; f) F. VI, silty fine sand with silt and clay layers; and g) F.VII, fine to medium sand, with traces of silt and gravel.

Data from engineering tests conducted over the past 25 yr were processed to establish characteristic static properties for each facies (table 1). The only dynamic testing of the formation was the Shannon and Wilson (1964) cyclic triaxial testing.

SAMPLING AND TEST PROCEDURE

Test samples were taken from a site in downtown Anchorage that is typical of that part of the city, namely, it is not directly influenced by free-face topography and has not had landslide failures.

Undisturbed core samples from several boreholes

[1]DGGS, Anchorage, Alaska 99501.
[2]DOWL Engineers, Anchorage, Alaska 99503.

were collected in modified Shelby tubes at prespecified depths. The cores were extracted by Alaska Testlab, and routine soils classification and indexes, including Torvane, pocket penetrometer, moisture content, and Atterberg limits, were obtained. Some samples were selected for more advanced testing. The liquid limit (W_L), plastic limit (Wp), and natural moisture content (W_N) were determined in the DGGS Anchorage laboratory. A representative engineering geologic-soils profile of the site was made from field and laboratory logs, facies discrimination, and Atterberg limits (fig. 1).

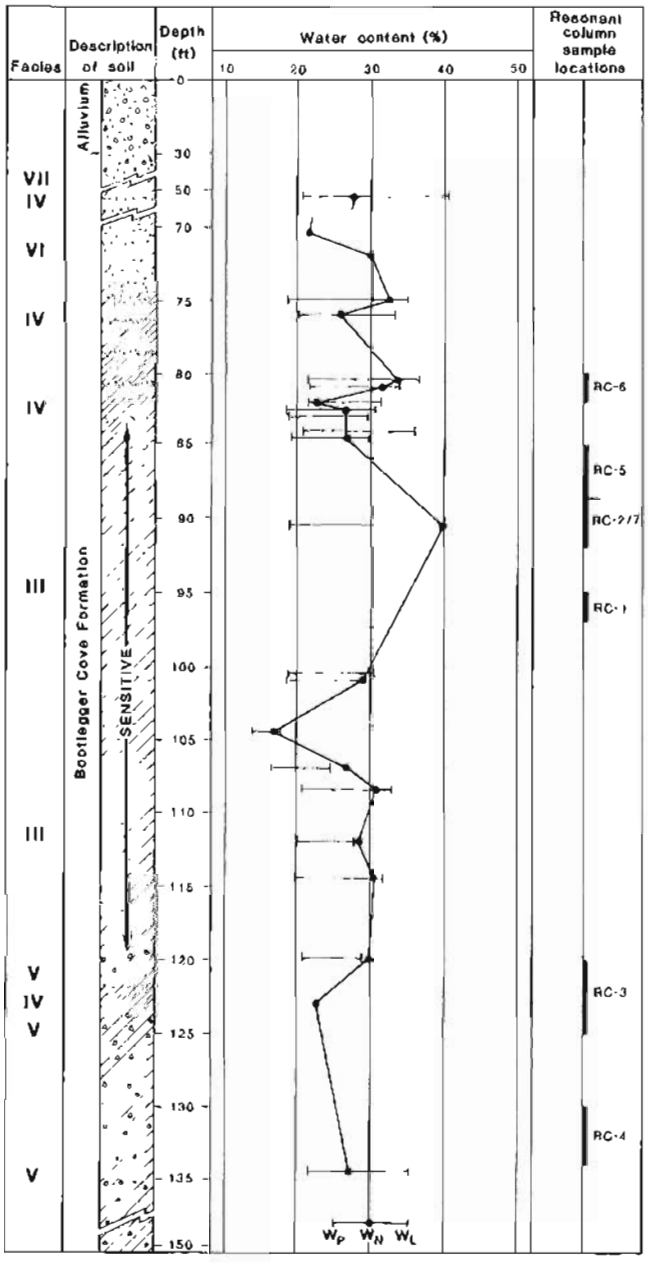

Figure 1. Composite geotechnical profile of two boreholes at downtown Anchorage sampling site (elevation 100.5 ft above mean sea level). Central column of graph shows Atterberg Limits (Wp = plastic limit, W_N = natural moisture content, W_L = liquid limit).

Table 1. *Mean values of physical parameters of engineering geologic facies, Bootlegger Cove Formation.*

FACIES	I	II	III	IV	V	VI	VII
Mean grain size (mm)	0.0014	0.004	0.004	0.015	0.006	0.15	0.37
Moisture content (%)	29.8	28.4	29.8	28.0	28.5	25.0	29.1
Plastic limit (%)	23.0	22.1	22.0	20.5	22.2	np	np
Liquid limit (%)	39.0	37.2	28.3	34.8	36.9	nv	nv
Plasticity index	16.0	15.1	7.0	16.0	14.7	np	np
Liquidity index	0.43	0.42	1.10	0.47	0.42	nv	nv
Shear strength (tsf)	0.49	0.79	0.52	0.69	1.09	0.61	nd
Compressive strength (tsf)	1.69	1.49	0.92	1.16	1.91	1.32	nd
Sensitivity ratio	8.9	2.8	19.7	6.1	4.1	ns	ns

NOTE: *np*—nonplastic, *nv*—nonviscous, *ns*—nonsensitive, *nd*—no data available

Undisturbed samples of the major facies beneath the site were selected for resonant-column testing from two boreholes. The samples were hand carried to the Harding-Lawson Laboratories in Novato, California, for testing.

The heart of the testing apparatus is the Harding Oscillator, which vibrates a cylindrical column of soil in a torsional mode at very small amplitudes (fig. 2). The frequency of vibration was changed until resonance in the soil column occurred. A sinusoidal signal supplied by an Exact function generator was fed into a Hewlett-Packard 50-watt power amplifier; the amplified signal drove the oscillator. The output signal from an accelerometer on the oscillator was amplified through a Columbia Research Laboratory charge amplifier and was fed, along with some of the amplitude of the driving signal, into a Tektronix storage oscilloscope, where input and output frequencies were compared and matched at resonance.

Six test samples were prepared by trimming the Shelby tube sample to a diameter of 2.46 in. and a length of 6.00 in., enclosing it in a membrane, and placing it in the test apparatus, where it was allowed to consolidate for 48 hr. Each sample was subjected to isotropic consolidation based on a calculated effective overburden pressure at the depth of sample recovery. A uniform soil density of 130 lb/ft^3 and saturated conditions below a depth of 18 ft were assumed. Water exuded from the sample during the consolidation phase was measured. During the consolidation process, the vertical pressure (σ_1) was increased above the assumed confining pressure by 300 lb/ft^2 to achieve proper coupling between the oscillator and the sample.

After consolidation occurred, the actual test began when a small-amplitude signal was applied to the oscillator. Oscillation frequency was altered until resonance, when accelerometer-amplitude output, resonant frequency, and driving signal were recorded. The test continued at various induced amplitudes. The damping

coefficient was determined by turning off the driving signal and allowing the oscillation to decay. This decay was recorded on the storage oscilloscope screen and a logrithmic decrement was calculated. After each test, an undrained and unconfined triaxial compression test was performed on the sample to establish its undrained shear strength (τ, figs. 3-10). (Because a very low level of strain was induced during resonant-column testing, we assume the triaxial compression tests were performed on undisturbed samples.) On completion of these tests, each sample was weighed to determine field density and dried to obtain natural moisture content (W_N). Samples RC-1 and RC-5 were thoroughly remolded---to destroy the original soil structure---before they were tested in the same manner as the undisturbed samples. All samples are stored in the DGGS Anchorage laboratory.

RESULTS

Six samples subjected to resonant-column testing represent facies F.II, F.III, and F.V (figs. 3-10). Facies F.I occurred in layers too thin for testing and facies F.IV was abundant in the upper half of the formation but was considered too inhomogeneous for this study. Sample RC-5 (facies F.II) is from a distinct horizon in a part of the section that, on the larger scale, is indicated as facies F.IV; it is typical of the upper Bootlegger Cove Formation.

Aside from the direct application of the curve-to-response analysis, the following general conclusions are supported:

(1) Shear-moduli curves for the undisturbed specimens of facies F.II and F.III are quite similar. At a given strain, the shear modulus for facies F.V is about twice that of the other facies, which probably reflects a more rigid soil fabric or a higher degree of consolidation or both.

(2) The shear modulus of the soft cohesive facies (F.III) decreases when the soil is remolded. After remolding, sample RC-1 appears to have lost significant moisture during reconsolidation. Thixotropic hardening may have influenced the increased remolded shear modulus of sample RC-1.

(3) At low values of strain (to about 10^{-2} percent), the damping ratio is consistently about 2 percent of critical, regardless of facies. This suggests the formation is uniform with respect to damping for moderately strong shaking.

ACKNOWLEDGMENTS

The Alaska Division of Emergency Services (ADES) funded this project as part of a grant from the Federal Emergency Management Agency. The perception of long-term needs in earthquake-hazard preparedness by Col. Ed Newberry, Harold Wolverton, Christie Miller, and Duane Bessette, all of ADES, is appreciated. The Earthquake Hazard Reduction Program of the U.S.

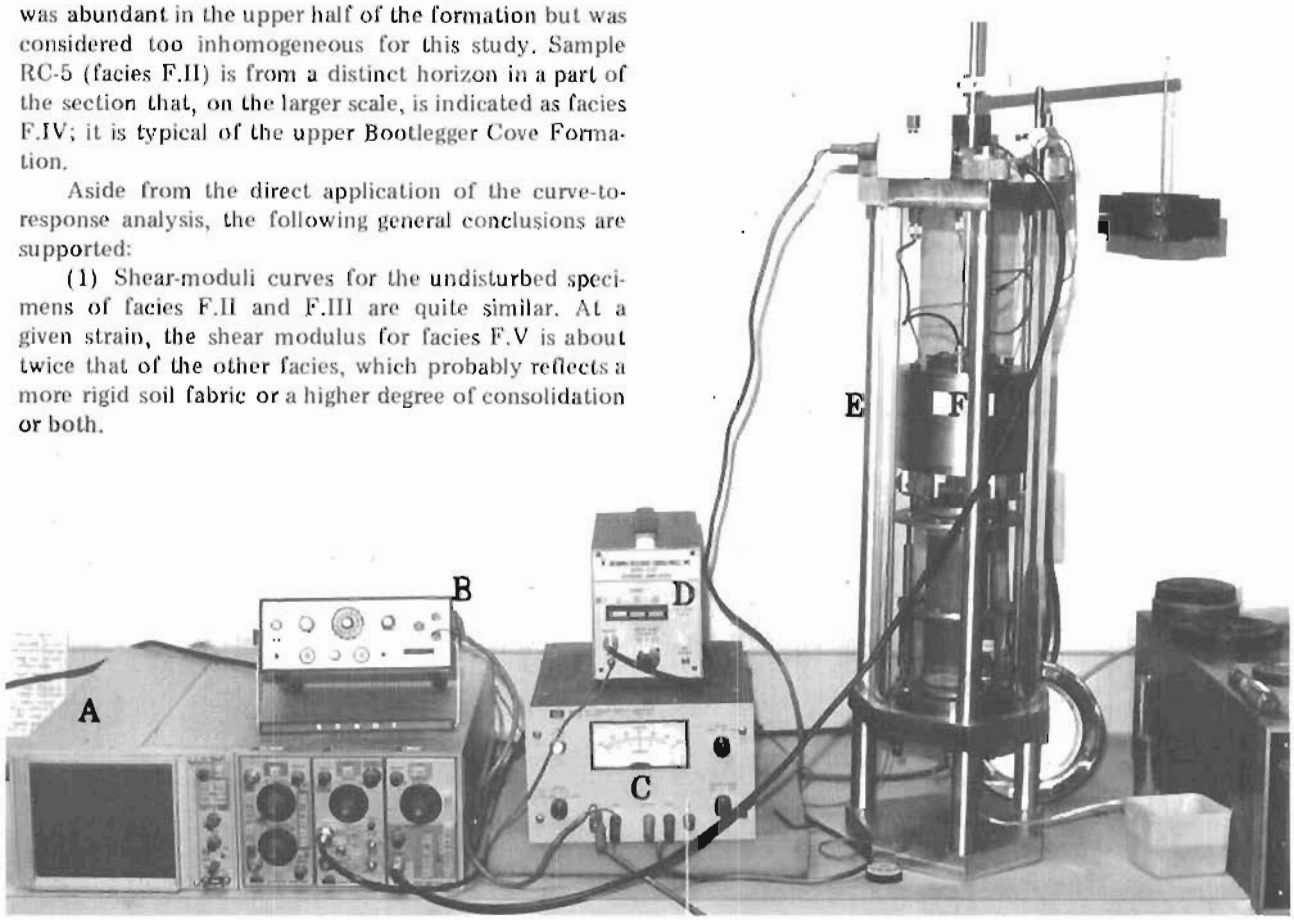

Figure 2. Resonant-column instrument array used in study. A - Tektronix storage oscilloscope, B - Exact-function generator, C - Hewlett-Packard power amplifier, D - Columbia Research charge amplifier, E - Harding resonant-column apparatus, F - Undisturbed sample, Bootlegger Cove Formation.

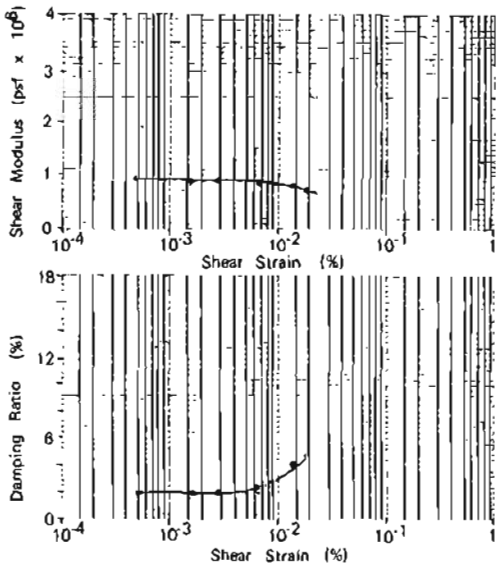

FACIES F. II	INITIAL	FINAL
Sample number	RC-5	
Moisture content (%)	34.0	32.6
Dry density (pcf)	87.3	89.1
σ_1, σ_3 (psf)	7500, 7200	
τ (psf) TX UU	2100	
Undisturbed/remolded	Undisturbed	
Field moisture/saturated	Field moisture	

Figure 3. Shear modulus and damping-ratio results for sample RC-5, facies F.II, *in situ* condition.

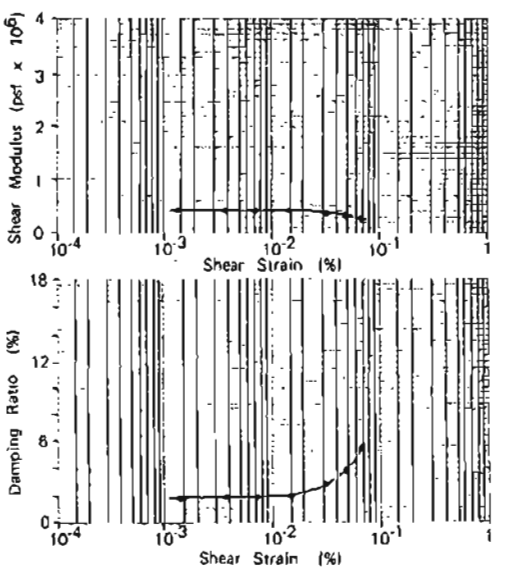

FACIES F. II	INITIAL	FINAL
Sample number	RC-5	
Moisture content (%)	32.6	30.4
Dry density (pcf)	89.1	92.0
σ_1, σ_3 (psf)	7500, 7200	
τ (psf) TX UU	1500	
Undisturbed/remolded	Remolded	
Field moisture/saturated	Field moisture	

Figure 4. Shear modulus and damping-ratio results for sample RC-5, facies F.II, remolded condition.

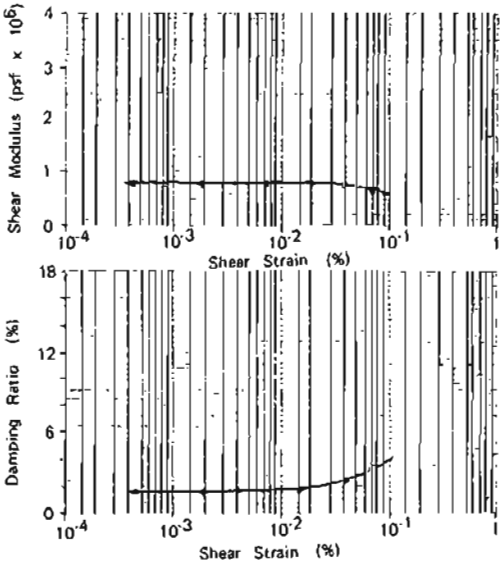

FACIES F. III	INITIAL	FINAL
Sample number	RC-1	
Moisture content (%)	37.5	36.7
Dry density (pcf)	83.9	86.4
σ_1, σ_3 (psf)	7500, 7200	
τ (psf) TX UU	1800	
Undisturbed/remolded	Undisturbed	
Field moisture/saturated	Field moisture	

Figure 5. Shear modulus and damping-ratio results for sample RC-1, facies F.III, *in situ* condition.

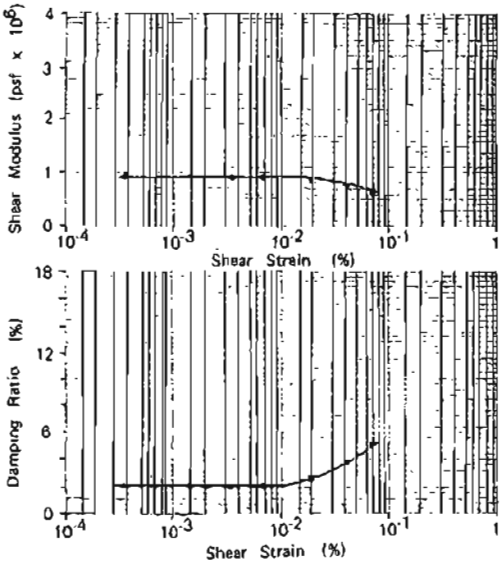

FACIES F. III	INITIAL	FINAL
Sample number	RC-1	
Moisture content (%)	36.7	31.6
Dry density (pcf)	86.4	88.8
σ_1, σ_3 (psf)	7500, 7200	
τ (psf) TX UU	2060	
Undisturbed/remolded	Remolded	
Field moisture/saturated	Field moisture	

Figure 6. Shear modulus and damping-ratio results for sample RC-1, facies F.III, remolded condition.

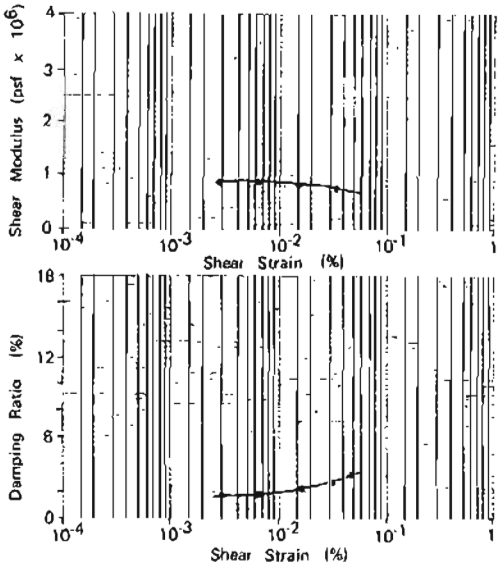

FACIES F. III	INITIAL	FINAL
Sample number	RC-2	
Moisture content (%)	40.8	36.4
Dry density (pcf)	79.6	85.3
σ_1, σ_3, (psf)	7500, 7200	
τ (psf) TX UU	2090	
Undisturbed/remolded	Undisturbed	
Field moisture/saturated	Field moisture	

Figure 7. Shear modulus and damping-ratio results for sample RC-2, facies F.III, *in situ* condition.

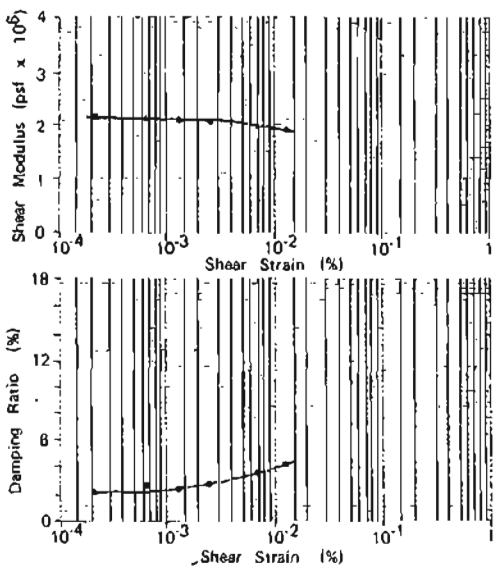

FACIES F. V	INITIAL	FINAL
Sample number	RC-3	
Moisture content (%)	25.4	22.1
Dry density (pcf)	102.3	108.1
σ_1, σ_3, (psf)	9660, 9360	
τ (psf) TX UU	4500	
Undisturbed/remolded	Undisturbed	
Field moisture/saturated	Field moisture	

Figure 8. Shear modulus and damping-ratio results for sample RC-3, facies F.V, *in situ* condition.

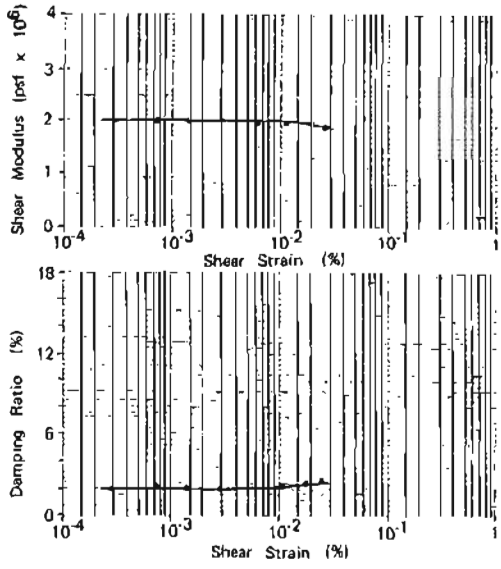

FACIES F. V	INITIAL	FINAL
Sample number	RC-4	
Moisture content (%)	27.6	25.7
Dry density (pcf)	97.3	100.3
σ_1, σ_3, (psf)	10,380, 10,080	
τ (psf) TX UU	4000	
Undisturbed/remolded	Undisturbed	
Field moisture/saturated	Field moisture	

Figure 9. Shear modulus and damping ratio for sample RC-4, facies F.III, *in situ* condition.

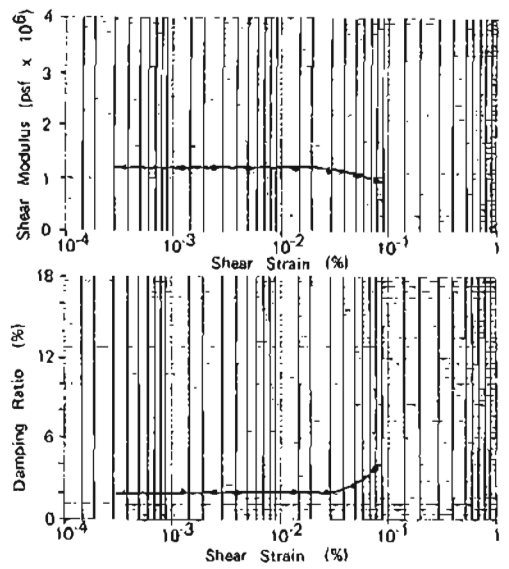

FACIES F. III	INITIAL	FINAL
Sample number	RC-7	
Moisture content (%)	39.7	34.7
Dry density (pcf)	82.2	88.0
σ_1, σ_3, (psf)	7500, 7200	
τ (psf) TX UU	1850	
Undisturbed/remolded	Undisturbed	
Field Moisture/saturated	Field moisture	

Figure 10. Shear modulus and damping ratio for sample RC-7, facies F.V, *in situ* condition.

Geological Survey also contributed to the project. The authors especially thank DOWL Engineers, Anchorage, and Harding-Lawson Engineers, Novato, California, for their technical support. This report was reviewed by R.D. Reger, DGGS, and Hans Pulpan, University of Alaska, Fairbanks.

REFERENCES CITED

Schmoll, H.R., Szabo, B.J., Rubin, Meyer, and Dobrovolny, Ernest, 1972, Radiometric dating of marine shells from the Bootlegger Cove Clay, Anchorage area, Alaska: Geological Society of America Bulletin, v. 83, no. 4, p. 1107-1114.

Shannon and Wilson, 1964, Report on Anchorage area soil studies, Alaska: Seattle, Washington, Shannon and Wilson, Inc., 109 p.

Updike, R.G., 1981, Engineering geologic maps, Government Hill area, Alaska: U.S. Geological Survey I-series maps [in press].

Updike, R.G., and Carpenter, B.A., 1981, Engineering geology of the Government Hill area, Anchorage, Alaska: U.S. Geological Survey Bulletin [in press].

Woods, R.D., 1978, Measurement of dynamic soil properties: American Society of Civil Engineers, Geotechnical Division, Conference on Earthquake and Soil Dynamics, Pasadena, Calif., 1978, Proceedings, v. 1, p. 91-178.

CLINOPTILOLITE AND MORDENITE DEPOSITS OF POSSIBLE ECONOMIC VALUE AT ILIAMNA LAKE, ALASKA

By James A. Madonna[1]

INTRODUCTION

In the early 1970's, the increased industrial use of zeolites stimulated the search for commercial zeolite deposits in Alaska. As a result, extensive zeolitized volcanic tuffs were located in the upper Matanuska Valley (Hawkins, 1973), and Tertiary tuffs and tuffaceous sedimentary rocks containing zeolites were identified on the Alaska Peninsula near Iliamna Lake (Madonna, 1973). This report describes the potentially economic clinoptilolite- and mordenite-bearing tuffs and tuffaceous sediments at the latter location.

BACKGROUND

Mumpton (1973) classified zeolites according to environment of formation as follows:

a) from volcanic material in 'closed' systems of ancient and present-day saline lakes,

b) from volcanic material in 'open' systems of freshwater lakes or ground-water systems,

c) from volcanic material in nearshore or deep-sea marine environments,

d) by low-grade burial metamorphism of volcanic and other material in thick sedimentary sequences,

e) by hydrothermal or hot-spring activity, and

f) in lacustrine or marine environments without direct evidence of volcanic precursor material.

Zeolite formation is favored by the presence of fluids of high pH and high alkali- to hydrogen-ion ratios in contact with reactive silicate material such as vitric volcanic tuff. Deffeys (1959) suggested that zeolites form in sedimentary tuff deposits by solution of volcanic glass followed by precipitation of the zeolite from solution. Sheppard (1971) suggested that high pH conditions account for the solubility of the glass and that reactivity of alkali ions is responsible for precipitation of the zeolites.

Because zeolites are extremely porous, hydrous mineral phases of low specific gravity, they are particularly sensitive to pressure and temperature changes, which accounts for the vertical zonation often found in thick sequences of tuffaceous sediments. The most hydrous and least dense zeolites form in the lower pressure-temperature conditions---at the top of the sequence---and the least hydrous and most dense zeolites form in the higher pressure-temperature conditions at the bottom of the sequence. Alteration due to burial diagenesis proceeds from fresh glass to clinoptilolite and mordenite to analcime and heulandite and finally to laumontite. The zeolites become unstable with increased pressure and temperature, and are ultimately transformed to minerals such as the feldspars.

These observations suggest that four conditions must be met before extensive sedimentary zeolitization and preservation are possible:

a) presence of reactive parent material such as vitric tuff,

b) presence of 'active' fluids such as marine, saline-lake, or hydrothermal waters,

c) passage of a geologically short time span, so that previously formed metastable zeolites have not been altered to more stable mineral phases, and

d) relatively shallow burial, so that burial diagenesis has not transformed the metastable zeolites into more stable mineral phases.

These conditions are diagrammatically shown in figure 1. Zeolite formation and preservation are most

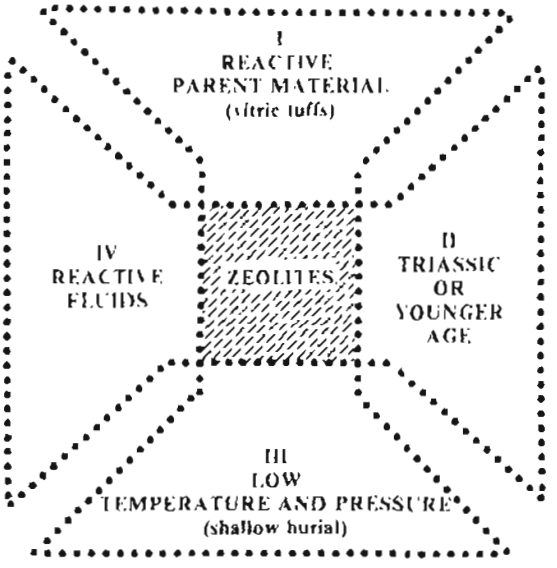

Figure 1. Diagram showing conditions which favor sedimentary zeolite formation and preservation.

[1] Alaskan Prospectors and Geologists Supply, Fairbanks, Alaska 99701.

favored when all four conditions are simultaneously satisfied.

DISCUSSION

The search for zeolites in the Iliamna area was restricted to those lithologic units that satisfy the basic conditions for zeolite formation and preservation (Madonna, 1973, 1975). Selected samples collected in 1972 were analyzed by X-ray diffraction techniques and several highly zeolitized units along the south shore and in the foothills bordering Iliamna Lake were thus identified (fig. 2).

The 1972 investigation of Tertiary andesites, tuffs, and tuffaceous sediments revealed several rock units with high concentrations of clinoptilolite and mordenite, but the extent of the zeolite-bearing lithologies was not realized until 1975, when a more thorough investigation was conducted. Figure 2 shows sample locations and general outcrop limits of the more extensively zeolitized rocks.

The most promising of several volcanic tuff and tuffaceous sedimentary units that crop out along Iliamna Lake is a 20-ft-thick, green, fine-grained, altered tuff bed (sample 1) exposed for 150 ft along the lake shore. Favorable analytical results (Madonna, 1975) and

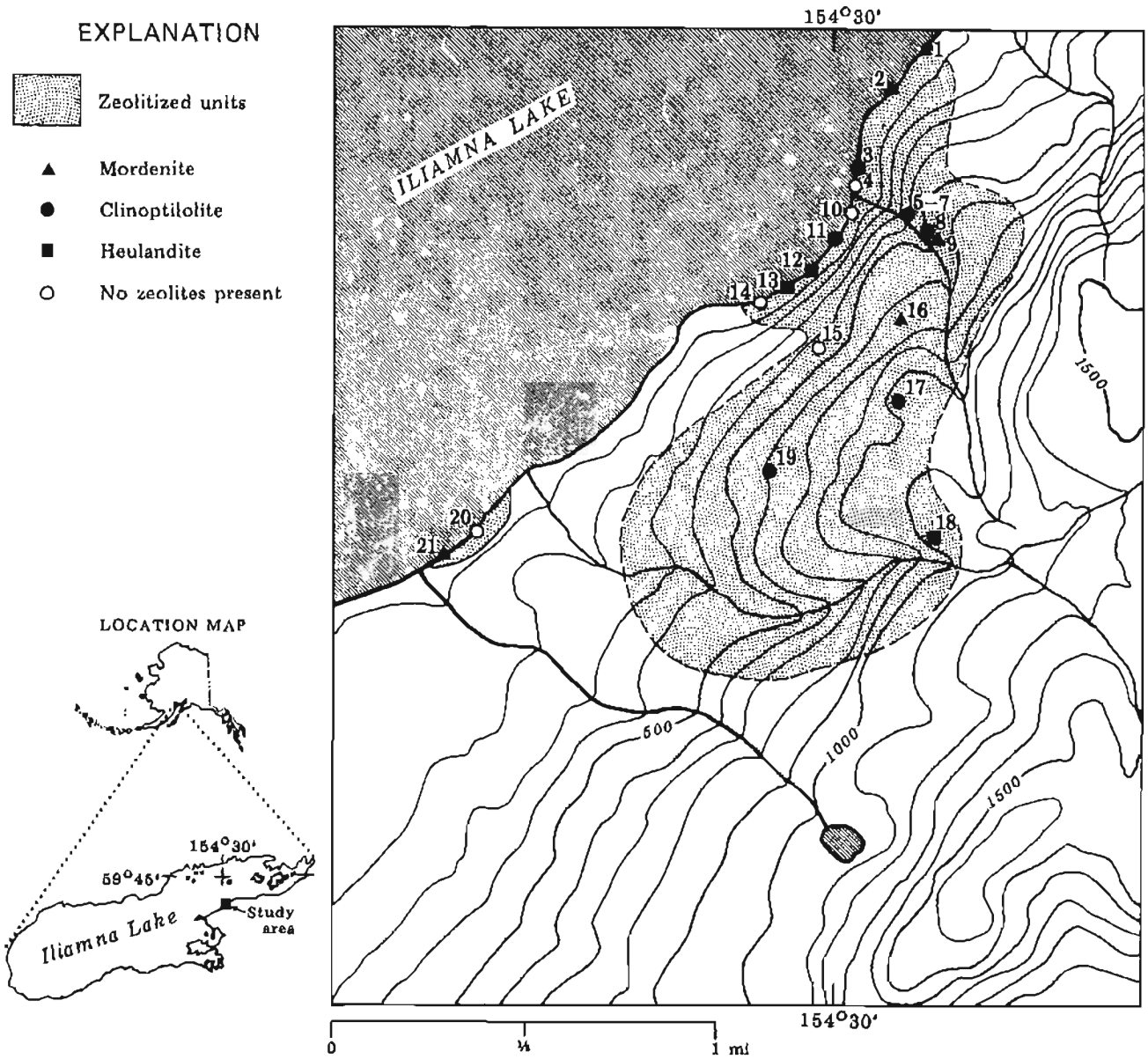

Figure 2. Sample locations and zeolitized units, southern shore of Lake Iliamna, Alaska.

moderate areal extent suggest this deposit may be an economic source of mordenite.

Of almost equal interest are the mordenite-bearing volcanic tuffs that crop out at sample points 2 and 21. Similar physical and mineralogical characteristics, including their light-green color, the presence of abundant spherical structures that indicate agitation in an aqueous environment, and the high concentration of mordenite (Madonna, 1975), suggest these outcrops are part of the same tuff bed. In addition, strike and dip measurements indicate the beds are on the respective east and west limbs of a gently folded north-south-trending anticline. This interpretation is further supported by the presence of anticlinally folded Tertiary sediments along the lakeshore between the two mordenite-bearing units (samples 3-14). Both units are approximately 15 ft thick and are exposed for about 100 ft along the lake shore. The high zeolite concentration and apparent large areal extent suggest that these units may also be of economic interest.

Other zeolitized tuffaceous sediments are exposed along the lake shore and in a small, southeast-trending tributary (samples 5-9). The sediments vary from fine-grained tuffaceous siltstone to reworked volcaniclastics and rough, bouldery, tuffaceous conglomerates. As indicated above, the sediments are exposed in a gently folded, north-south-trending anticline.

The most important zeolitization is found in three clinoptilolite-bearing tuffaceous sandstones and reworked volcaniclastic units (samples 5-7) exposed as a combined 60-ft-thick sequence in a small southeast-trending drainage. Although clearly exposed within the limits of the drainage and to a somewhat lesser extent along the lakeshore, extensive vegetation prevented accurate measurement of the length and width of the units. However, a conservative estimate from the observed outcrops suggests a 1/2-mi length along the lakeshore and a 1/4-mi width along the drainage. This deposit may be an economic source of clinoptilolite; however, a more extensive evaluation is required.

The foothills adjacent to the lake's southern shore (samples 15-19) and near the zeolitized units described above consist of green clinoptilolite- and mordenite-bearing vitric and welded tuffs. These units are easily measured because of their position above tree line and the general lack of vegetation. Observed dimensions include an overall length of 3/4 mi, a width of about 1/3 mi and an average thickness of 400 ft. The comparatively high concentrations of clinoptilolite and mordenite determined by mineralogical tests (Madonna, 1975) and their respectable outcrop dimensions suggest that these units may be among the more important zeolite-bearing tuffs in the Iliamna area.

GENESIS OF THE DEPOSITS

The clinoptilolite- and mordenite-bearing lithologies exposed along the southern lake shore and in the small southeast-trending drainage consist of nonmarine reworked volcanics and water-laid tuffs. However, the zeolite-bearing vitric tuffs exposed in the adjacent foothills do not exhibit characteristics typical of an aqueous environment; in fact, their stratigraphic position and high elevation suggest terrestrial deposition.

The clinoptilolite and mordenite deposits were formed by the alteration of this volcanic material. The mineralogy, mode of occurrence, and depositional environment suggest that these zeolites were produced in 'open' systems of fresh-water lakes or ground-water systems (type b, Mumpton's classification). In addition, the presence of the clinoptilolite-mordenite assemblage indicates a low-temperature, low-pressure environment above the zone of significant alteration caused by burial diagenesis.

CONCLUSIONS

Favorable results of mineralogical examinations of selected samples (Madonna, 1975) and the rather large aerial extent of the zeolite-bearing tuffs and tuffaceous sediments suggest they may be of economic interest as a future source of clinoptilolite and mordenite.

ACKNOWLEDGMENTS

I wish to thank D.B. Hawkins, Professor of Geology, University of Alaska, and M.A. Wiltse, Geochemist, DGGS, for their thoughtful reviews of the manuscript.

REFERENCES CITED

Deffeys, K.S., 1959, Zeolites in sedimentary rocks: Journal of Sedimentary Petrology, v. 19, p. 602-609.

Detterman, R.L., and Reed, B.L., 1968, Geology of the Iliamna Quadrangle, Alaska: U.S. Geological Survey Open-file Report 300.

Hay, R.L., 1966, Zeolites and reactions in sedimentary rocks: Geological Society of America Special Paper 85, 130 p.

Hawkins, D.B., 1973, Sedimentary zeolite deposits of the upper Matanuska Valley, Alaska: Alaska Division of Geological and Geophysical Surveys Special Report 6, 17 p.

Madonna, J.A., 1973, Zeolite occurrences in Alaska: Fairbanks, University of Alaska, unpublished M.S. thesis.

_____, 1975, Zeolite deposits of possible economic significance on the northern Alaska Peninsula: Alaska Division of Geological and Geophysical Surveys Open-file Report 87, 27 p.

Mumpton, F.A., 1973, Worldwide deposits and utilization of natural zeolites: Industrial Minerals, no. 73, 11 p.

Sheppard, R.A., 1971, Zeolites in sedimentary deposits of the United States, a review *in* Gould, R.F., *ed.*, Molecular sieve zeolites-1: American Chemical Society, Advances in chemistry, series 101, p. 179-310.

THE KEETE INLET THRUST FAULT, PRINCE OF WALES ISLAND

By Earl Redman[1]

INTRODUCTION

The Keete Inlet thrust fault, located in the Craig A-2 Quadrangle on southern Prince of Wales Island, was originally mapped and described by Herreid (1975). On the basis of outcrops along the west side of Keete Inlet, Herreid and others (1978) concluded that the fault forms the contact between the pre-Ordovician Wales Group greenschist and the overlying Descon Formation and Devonian bedded rocks.

DISCUSSION

Regional geologic mapping during a 1975-76 reconnaissance minerals-exploration program extended the Keete Inlet thrust fault south to lower Klakas Inlet and east to Port Johnson (fig. 1). During mapping, the juxtaposition of Wales Group rocks with Descon Formation and Devonian rocks was observed; the fault plane itself was not identified in outcrop.

The fault plane has a southeast-plunging synclinal form. Dips are shallow, varying from 25° to 40° SE (Herreid and others, 1978). The Niblack area---a window through the Descon Formation into the Wales Group greenschist---may have been created by doming of the Wales Group along the Dolomi-Sulzer arch (Peek, 1975). The plane of the fault is moderately contorted, as shown by the abrupt change in direction near Port Johnson and the presence of the Niblack window.

Herreid and others (1978) note pervasive shearing of the Wales Group up to 450 m from the fault. In the Ruth Bay/Klakas Inlet area, several hundred meters of the Wales Group adjacent to the fault are strongly silicified, but overlying rocks are unaffected.

To date, the age of the Keete Inlet thrust fault is defined only by the Devonian rocks involved in the thrusting and by the Cretaceous intrusive rocks (Turner and others, 1977) that intrude the fault. However, during my field work, I identified two undated granitic plutons that cut the fault.

ACKNOWLEDGMENTS

The reviewing efforts of John Decker and T.K. Bundtzen are appreciated.

[1]C.C. Hawley and Associates, Juneau, Alaska 99801.

REFERENCES CITED

Herreid, Gordon, 1975, Geologic map of the Craig A-2 Quadrangle, Prince of Wales Island, Alaska: Alaska Division of Geological and Geophysical Surveys Open-file Report 35, 1 pl.

Herreid, Gordon, Bundtzen, T.K., and Turner, D.L., 1978, Geology and mineral deposits of the Craig A-2 Quadrangle and vicinity, Prince of Wales Island, Alaska: Alaska Division of Geological and Geophysical Surveys Geologic Report 48, 49 p.

Peek, B.C., 1975, Geology and mineral deposits of the Niblack Anchorage area, Prince of Wales Island, Alaska: Fairbanks, University of Alaska unpublished M.S. thesis, 50 p.

Turner, D.L., Herreid, Gordon, and Bundtzen, T.K., 1977, Geochronology of southern Prince of Wales Island, Alaska: Alaska Division of Geological and Geophysical Surveys Geologic Report 55, p. 11-16.

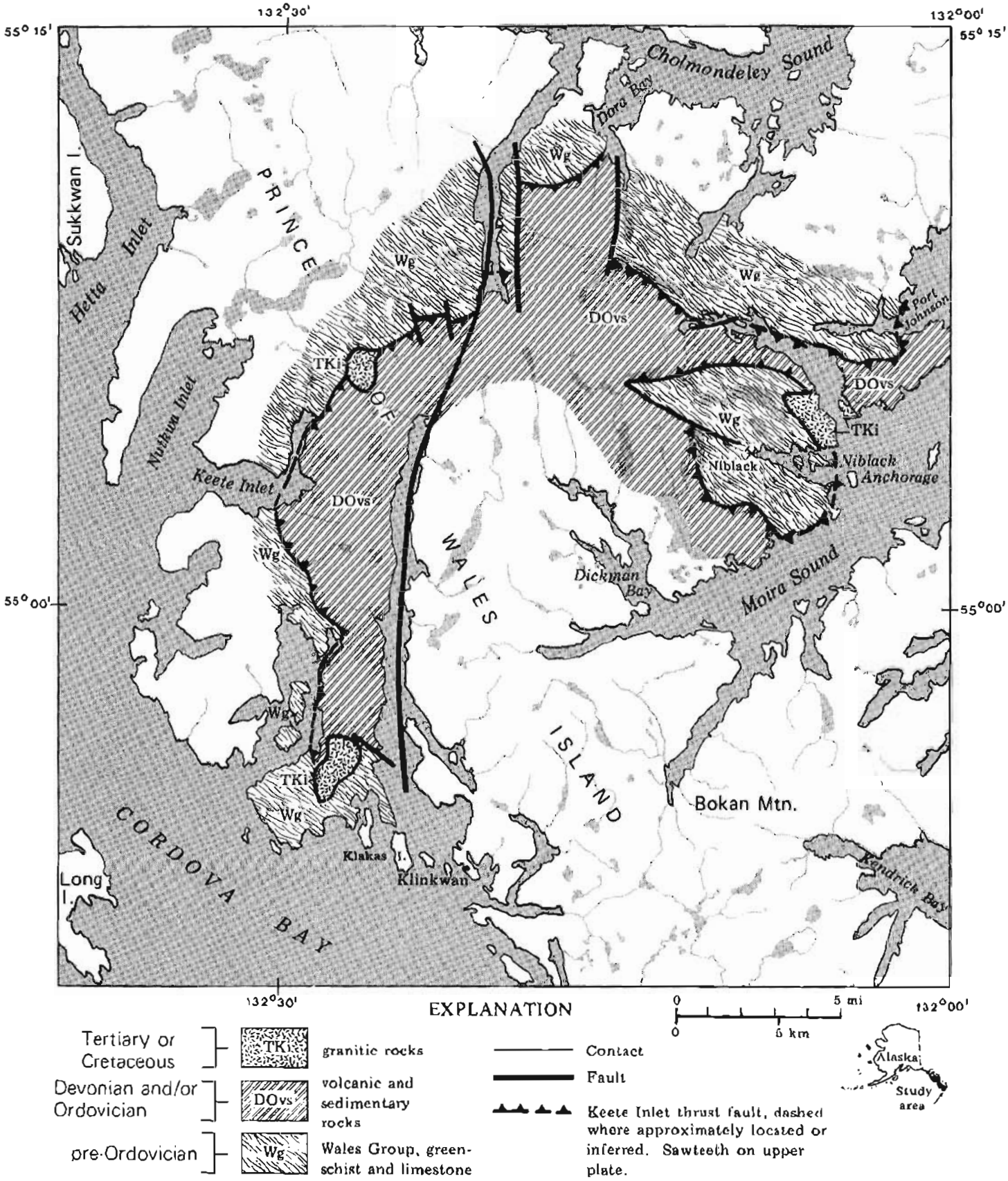

Figure 1. The Keete Inlet thrust fault, Prince of Wales Island, Alaska.

TWO HOLOCENE MAARS IN THE CENTRAL ALASKA RANGE

By Mary D. Albanese[1]

GEOLOGIC SETTING

The study area is underlain by the California Creek Member of the Totatlanika Schist, a quartz-orthoclase-sericite schist and gneiss metarhyolite of Mississippian age. This unit is overlain locally by the Lignite Formation and the Nenana Gravel, both of Tertiary age, and Pleistocene to Recent alluvium.

The study area is situated above a Benioff zone (strike N. 48° W., plunge northwest) near the Denali fault. Holocene maars occur at the northeast corner of this zone, above the 125-km depth contour of the subduction zone (Agnew, 1979).

DESCRIPTION

Two adjacent craters located southwest of Buzzard Creek, a tributary of the Totatlanika River on the north flank of the central Alaska Range (fig. 1), have been identified as maars. The floors of the craters are broad and shallow (fig. 2) and are bounded by a semicircular rim consisting of about 80 percent angular schist fragments and 20 percent subrounded vesicular-basalt ejecta ranging from cinders to blocks. An ejecta blanket can be traced a distance of 1.1 km northeast of the larger crater. Each crater contains a small pond.

The larger crater was previously identified as a cinder cone from a late Pleistocene or Holocene volcanic eruption (Péwé and others, 1966). However, a recent study suggests the craters are probably maars, which are defined as shallow, broad, low-rimmed explosion craters formed by phreatic and phreatomagmatic eruption (Ollier, 1967; Lorenz, 1973).

ORIGIN

The semicircular shape of the craters and rims and the presence of basaltic ejecta suggest that the craters are volcanic features. During the eruption of a maar or tuff ring, large volumes of steam and water vapor are released and spread ejecta away from the vent. The craters produced under these conditions are broad, shallow features with characteristic height-to-width ratios of 1:10 to 1:30 (Heiken, 1971). This ratio apparently does not apply to extremely young or currently active maars, such as the Ukinrek Maars, which erupted in 1977 and resulted in a height-to-width ratio of 1:4 (Kienle and others, 1980). Purely magmatic eruptions containing little or no water for steam generation often produce cinder cones during lava fountaining. The resultant craters are steeply sloping depressions in large mounds of volcanic ejecta; height-to-width ratios vary from 1:5 to 1:16. The ratio of 1:22 for the larger crater at Buzzard Creek suggests that the crater is a maar or tuff ring.

The primary distinction between maars and tuff rings is that maars form below the preeruption surface as negative features, whereas tuff rings form above the preeruption surface as positive features. According to Lorenz (1973), this difference is a function of the depth of the eruption source. The preeruption surface of the larger crater at Buzzard Creek can be inferred from the slope of the surrounding terrain (fig. 3). Superposition of profiles B and C onto profile A, which bisects the crater, shows the height of the crater relative to the land surface on either side. The preeruption surface can be inferred along profile A by removing the ejecta blanket and extending this surface upslope, using a slope similar to profiles B and C. This inferred preeruption surface suggests that the larger crater is a negative feature.

Because the eruption source for maars is deeper than that of tuff rings, a greater percentage of country rock participates in the eruption. According to Lorenz (1973), maar ejecta may contain more than 60 percent country rock, whereas tuff-ring ejecta often consist of less than 10 percent country rock. As stated earlier, the rim material at the Buzzard Creek craters consists of about 80 percent country rock and 20 percent vesicular-basalt ejecta, suggesting a maar-eruption origin.

Lorenz (1973) also inferred that tuff rings generally form above the water table, whereas maars form near or below the water table and frequently contain small lakes. The fact that both craters at Buzzard Creek contain ponds also supports a maar-eruption origin.

AGE OF BASALTIC EJECTA

Three samples of charcoal from above and below basaltic ejecta from the larger crater were radiocarbon dated at Krueger Enterprises, Inc., Geochron Laboratories Division, Cambridge, Massachusetts (fig. 1, table 1). The samples from below the basaltic ejecta yield a mean age of 3,140 ± 230 yr B.P.; a sample from directly above the ejecta yields a radiocarbon age of 2,910 ± 230 yr B.P. These dates indicate that the

[1]DGGS, College, AK 99708.

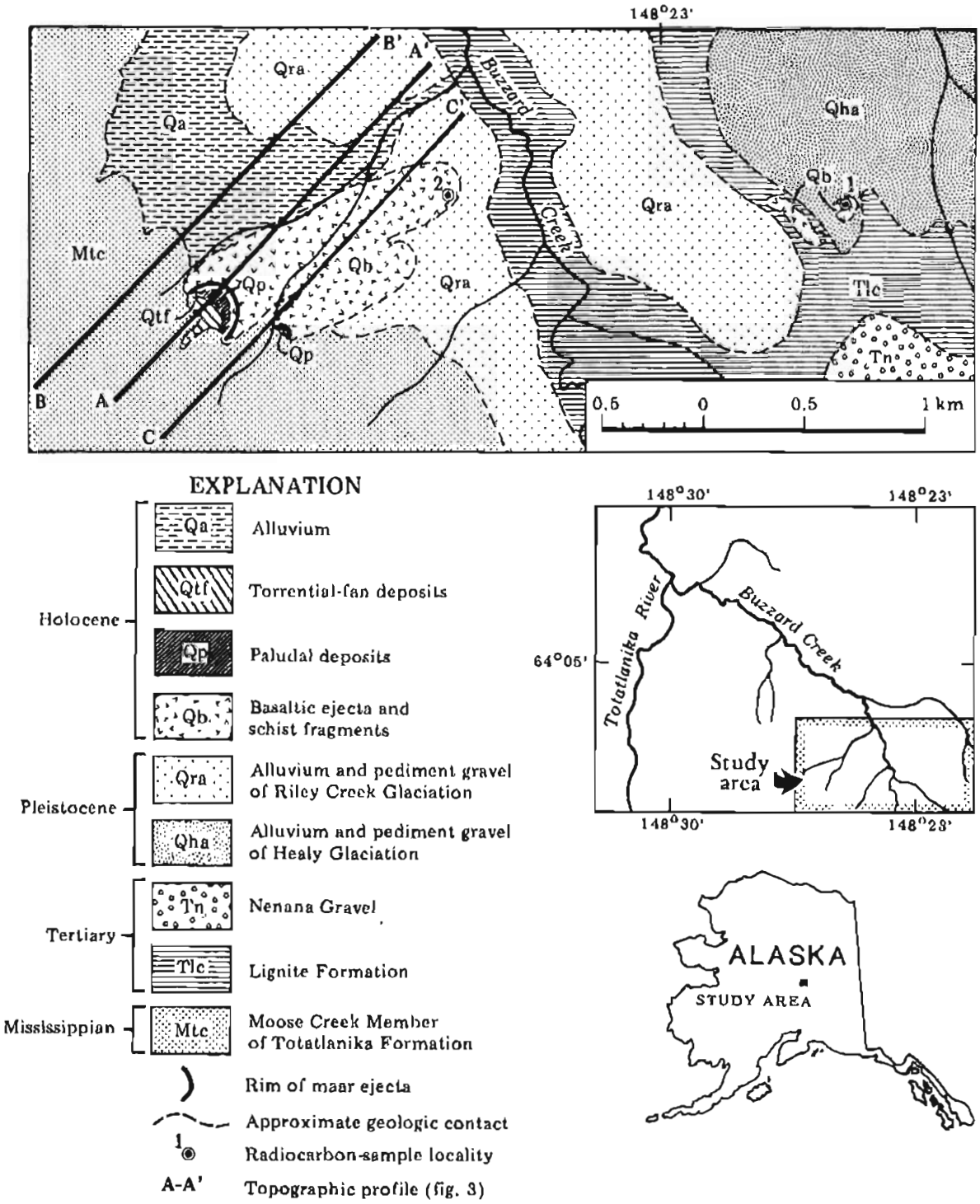

Figure 1. Geologic map of the Buzzard Creek area, Fairbanks A-3 Quadrangle, Alaska.

Table 1. *Ages of basaltic ejecta in the Buzzard Creek area, central Alaska Range, Alaska*

Sample no.	Description	Age* (^{14}C yr)	Sample weight (mg)	Stratigraphic position
1	Charcoal	2910 ± 230	50	Dark humus layer at base of 1.6-cm-thick layer of modern organic material that overlies 2 cm of basaltic ejecta
2	Charcoal	3585 ± 235	110	Discontinuous, organic layer up to 1 2 cm thick overlain by a 41-cm-thick layer of basaltic ejecta.
3	Charcoal	2695 ± 220	50	Duplicate sample from same unit as above.

*Dates based on Libby half-life (5,570 yr) for radiocarbon. Error stated is ± 1σ as judged by analytical data. Age is referenced to A.D. 1950.

Figure 2. Aerial view of craters at Buzzard Creek, looking west. Photo by R.D. Reger, September 1978.

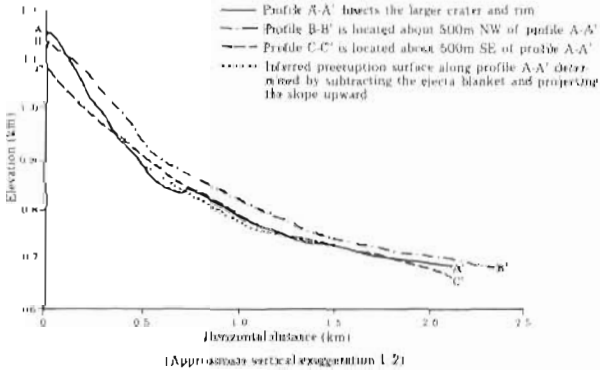

Figure 3. Topographic profiles and inferred preeruption surface in Buzzard Creek area, Fairbanks A-3 Quadrangle, Alaska.

basalt was erupted about 3,000 ± 230 radiocarbon yr B.P.

CONCLUSIONS

Evidence that the larger crater formed below the preeruption surface, the high percentage of country rock within the crater-rim material, and the proximity of both craters to the water table suggest that the two craters at Buzzard Creek are maars. Radiocarbon dates indicate that the larger maar was formed about 3,000 ± 230 yr B.P. The smaller maar was probably formed at about the same time.

ACKNOWLEDGMENTS

This paper was condensed from the author's Master of Science thesis (Albanese, 1980). Funding for the project was provided by U.S. Department of Energy contract EW-78-5-07-1720. Field assistance was provided by Edward Ross. The manuscript was reviewed by D.L. Turner, W.G. Gilbert, R.D. Reger, and J.R. Riehle. Early drafts were reviewed by Juergen Kienle and S.E. Swanson. Reger also provided valuable assistance in the field.

REFERENCES

Agnew J.D., 1979, Seismicity of the central Alaska Range: Alaska Science Conference, 30th, Fairbanks, 1979, Proceedings, p. 73.

Albanese, M.D., 1980, The geology of three extrusive bodies in the central Alaska Range. Fairbanks, University of Alaska, unpublished M.S. thesis, 101 p.

Heiken, G.W., 1971, Tuff rings, examples from south-central Oregon. Journal of Geophysical Research, v. 76, no. 27, p. 6516-6526.

Kienle, Juergen, Kyle, P.R., Self, Stephen, Motyka, R.J., and Lorenz, Volker, 1980, Ukinrek Maars, Alaska, April 1977 eruption sequence, petrology, and tectonic setting: Journal of Volcanology and Geothermal Research, v. 7, no. 1, p. 11-37.

Lorenz, Volker, 1973, On the formation of maars: Bulletin Volcanologique, v. 37, no. 1, p. 183-204.

Ollier, C.D., 1967, Maars: their characteristics, varieties, and definition: Bulletin Volcanologique, v. 31, no. 1, p. 45-73.

Péwé, T.L. Wahrhaftig, Clyde, and Weber, F.R., 1966, Geologic map of the Fairbanks Quadrangle, Alaska: U.S. Geological Survey Miscellaneous Geological Investigations Map I-455, scale 1:250,000.

Wahrhaftig, Clyde, 1970, Geologic map of the Fairbanks A-3 Quadrangle, Alaska: U.S. Geological Survey Geological Quadrangle Map GQ-809, scale 1:63,360.

RADIOMETRIC-AGE DETERMINATIONS FROM KISKA ISLAND, ALEUTIAN ISLANDS, ALASKA

By Bruce C. Panuska[1]

INTRODUCTION

Kiska Island, located 320 km west of Adak Island in the central Aleutian Island Arc, is the largest island transected by the Near Island-Amchitka Lineament (fig. 1). Six whole-rock potassium-argon age determinations were obtained from samples of andesitic flows and hypabyssal intrusives of the Kiska Harbor Formation collected in 1977.

[1]Geophysical Institute, University of Alaska, Fairbanks 99701.

LOCAL GEOLOGY

The oldest rocks on Kiska Island belong to the Vega Bay Formation (fig. 2), which consists of at least 600 m of late Oligocene to early Miocene volcanic and volcaniclastic rocks (Coats and others, 1961). The Vega Bay Formation is overlain with angular unconformity by the Kiska Harbor Formation, which consists of coarse-grained sandstone, conglomerate, and breccia that represent braided-stream deposits (Panuska, 1980) interbedded with andesite flows. Panuska (1980) in-

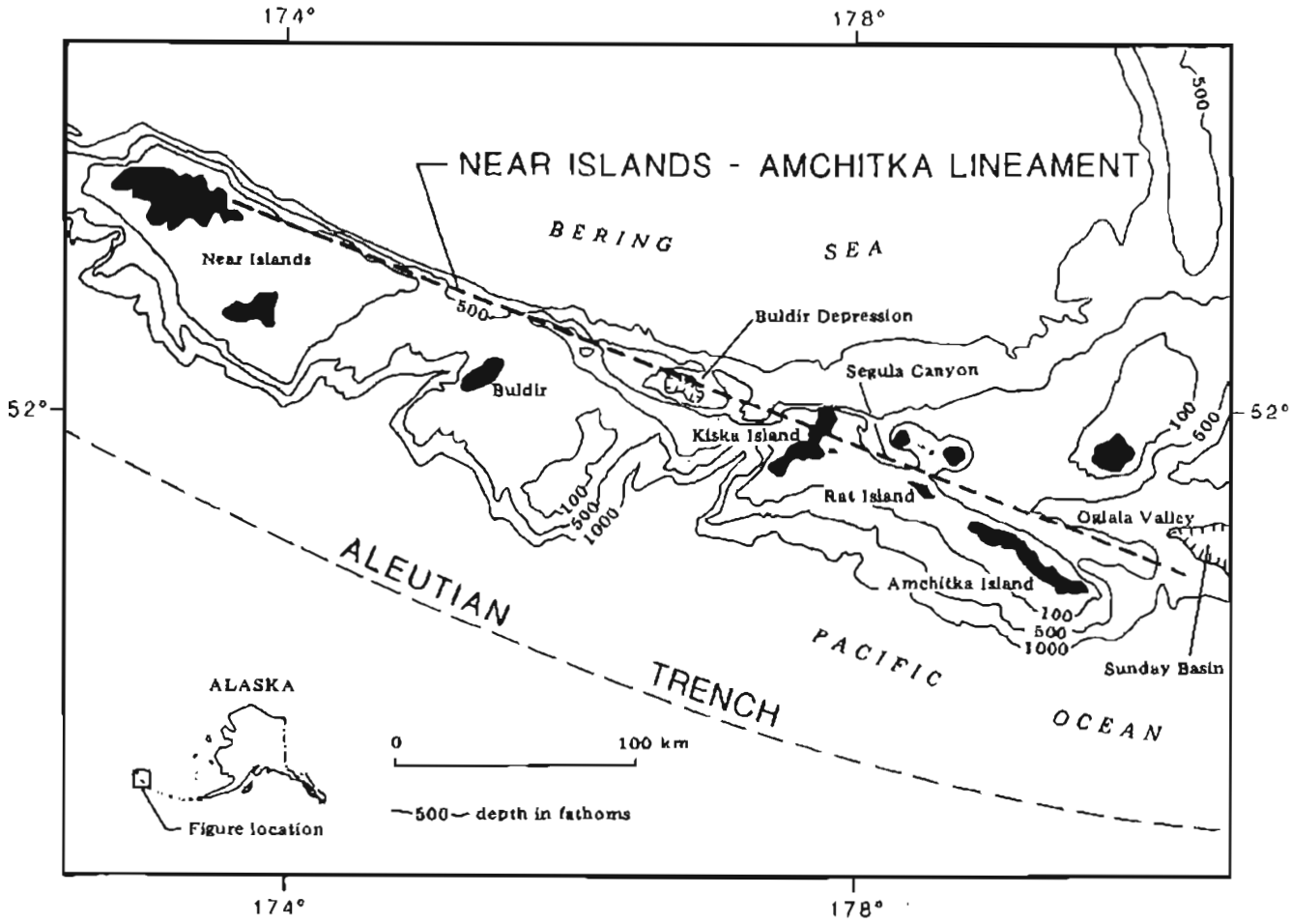

Figure 1. Location of Kiska Island and the Near Island-Amchitka Lineament, central Aleutian Island arc, Alaska.

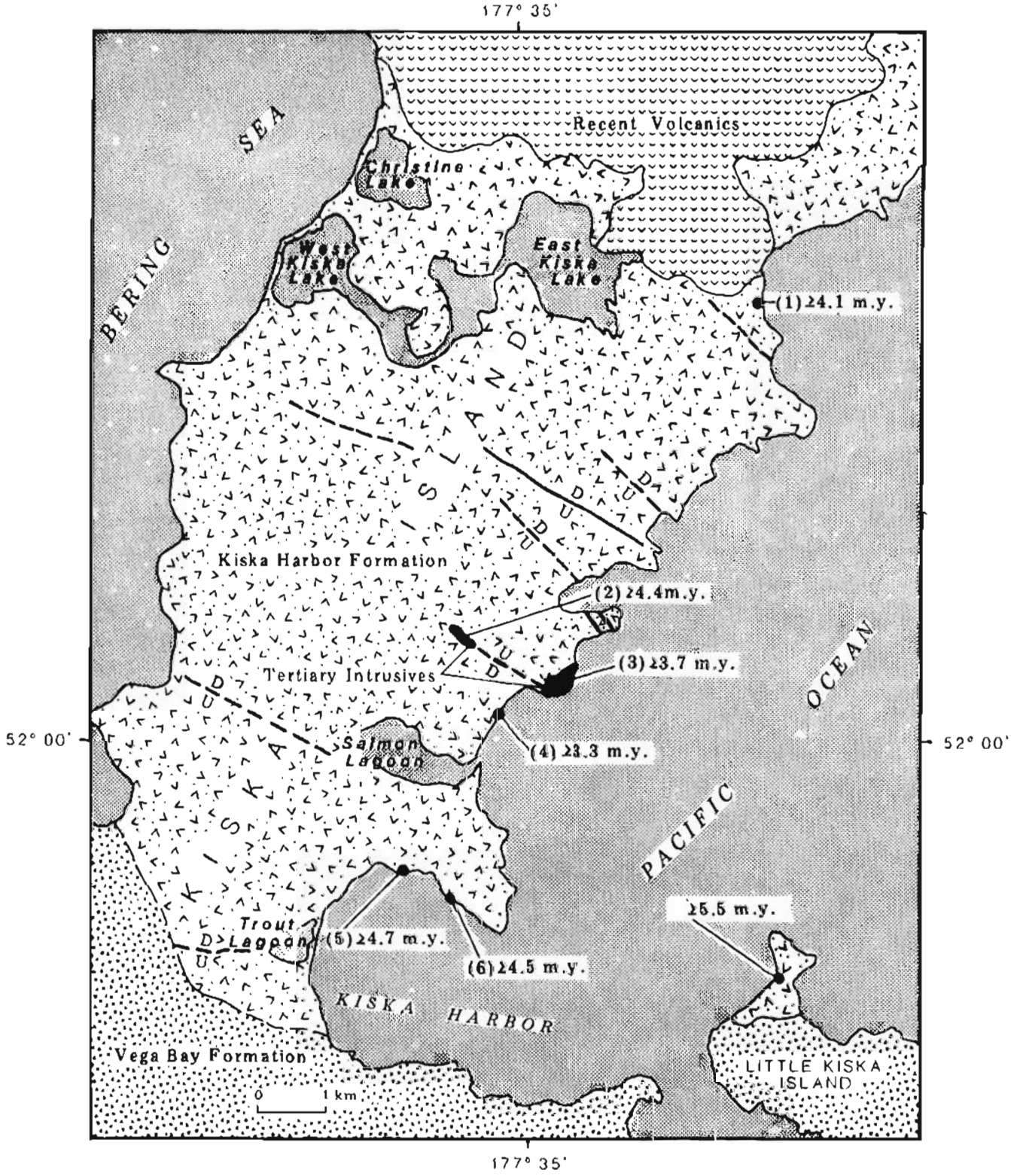

Figure 2. Map of Kiska Island showing sample locations and radiometric ages in millions of years (m.y.). The Little Kiska Island sample, reported in Von Huene and others (1971) and incorrectly located by DeLong and others (1978), is correctly located.

formally subdivided the formation into a lower and upper unit on the basis of paleocurrent direction, depositional environment, and sedimentary petrology. The northern end of the island is capped by recent flows of the active Kiska Volcano.

RADIOMETRIC AGE DATA

Figure 2 shows the location and age of the dated samples (table 1). Except for sample 1 and the Little Kiska Island sample collected by W.J. Carr and Leonard Gard of the U.S. Geological Survey and determined to be 5.5 m.y. by Richard Marvin (also with the USGS), all reported ages are minimum because alteration may have released argon.

Sample 1 was collected from an andesite lava flow in the upper Kiska Harbor Formation and provides a reliable age of 4.1 m.y. Sample 2 was collected from a dike intruded along a fault that cuts the hypabyssal intrusive from which sample 3 was collected. The 4.4-m.y.-minimum age of sample 2 and geological relationships (fig. 3) require that the 3.7-m.y.-minimum age for sample 3 is at least 0.7 m.y. too young.

The same fault-dike relationship that limits the age of sample 3 appears to limit the age of sample 4, which was collected from a lava flow in the upper Kiska Harbor Formation that appears to be cut by the same fault. The age determination for sample 4 (3.3-m.y. minimum) thereby appears to be at least 1.1 m.y. too young. Alternatively, if the material adjacent to the fault breccia is interpreted as talus breccia (fig. 3), the intrusive may have been faulted and uplifted, exposing the intrusion to mechanical weathering that resulted in the accumulation of slide rock as a talus-breccia apron. If these events were followed by sedimentation and eruption of the lava flow, the 3.3-m.y.-minimum age of sample 4 could be correct.

Samples 5 (4.7-m.y.-minimum age) and 6 (4.5-m.y.-minimum age) were collected from an andesite flow near the base of the upper Kiska Harbor Formation. These samples date the minimum age of the onset of upper Kiska Harbor Formation deposition at 4.7 m.y.

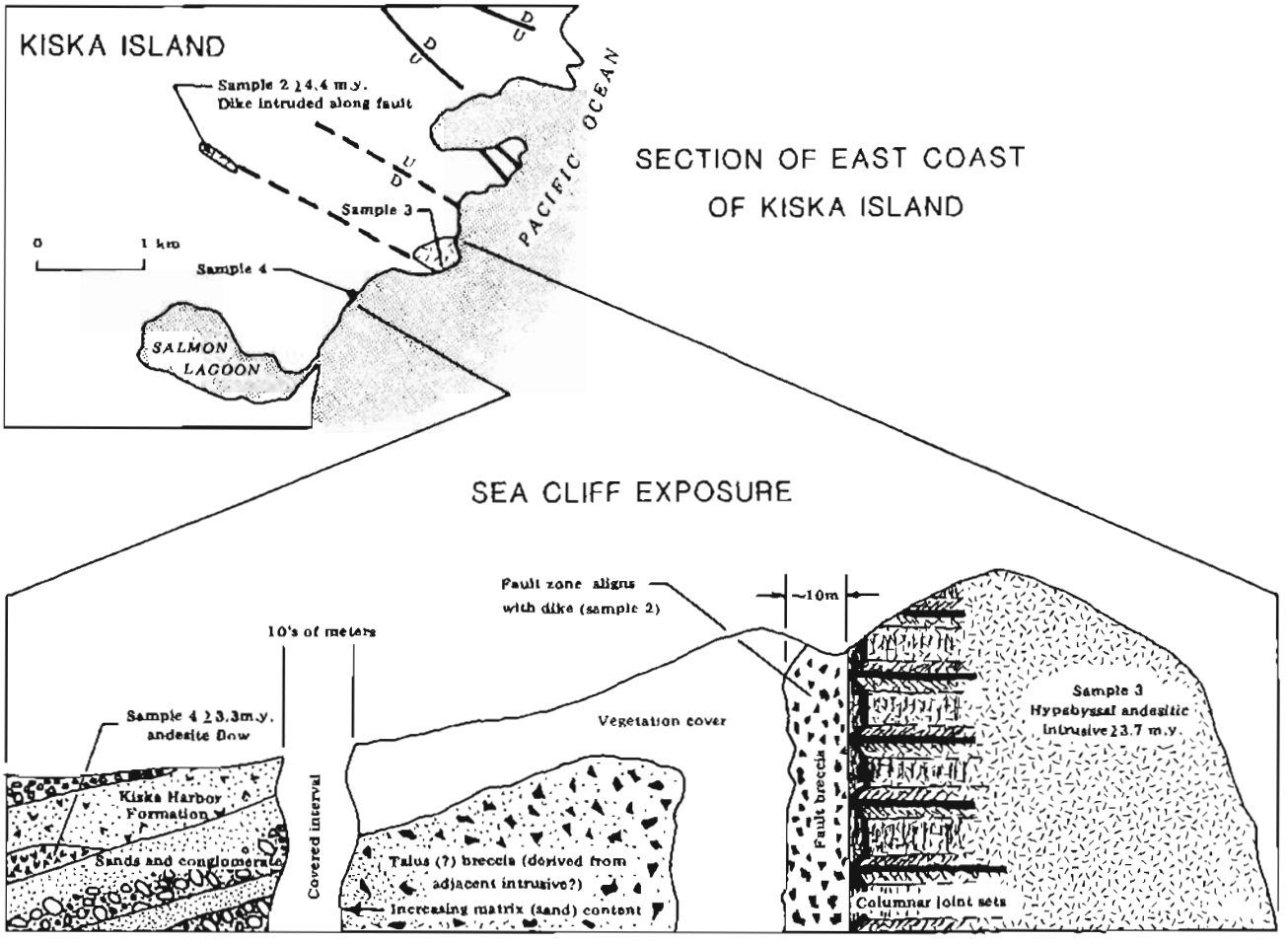

Figure 3. Sea-cliff exposure near hypabyssal intrusive on Kiska Island, central Aleutian Island arc, Alaska.

Table 1. *Whole-rock ^{40}K-^{40}Ar ages of andesitic flows and hypabyssal intrusives*

Sample	K_2O (wt %)	Sample wt (g)	^{40}Ar (rad) (moles/gm) x 10^{-11}	$\frac{^{40}Ar\ (rad)}{^{40}K \times 10^{-3}}$	$\frac{^{40}Ar\ (rad)}{^{40}Ar\ total}$	Age ± 1σ (m.y.)
1	0.690 0.693 0.700 0.710 $\bar{x}$ = 0.698	13.7069	0.414	0.239	0.474	4.1 ± 0.1
2	0.830 0.830 0.830 0.830 $\bar{x}$ = 0.830	12.0710	0.531	0.258	0.415	4.4 ± 0.1 minimum age
3	1.630 1.620 1.610 1.623 $\bar{x}$ = 1.621	12.1383	0.863	0.215	0.664	3.7 ± 0.1 minimum age
4	1.627 1.640 1.637 1.647 $\bar{x}$ = 1.638	13.5726	0.785	0.193	0.690	3.8 ± 0.1 minimum age
5	0.947 0.940 0.940 0.950 $\bar{x}$ = 0.944	11.4662	0.643	0.275	0.145	4.7 ± 0.1 minimum age
6	1.200 1.200 1.180 1.177 $\bar{x}$ = 1.189	12.8473	0.772	0.262	0.582	4.5 ± 0.1 minimum age

*Analytical error corresponds to uncertainty of ± 0.1 m.y.

The 5.5 (± 0.7)-m.y. age from Little Kiska Island was obtained from a lava flow at the base of the Kiska Harbor Formation. This age was originally reported by Von Huene and others (1971) and incorrectly located by DeLong and others (1978). The location is correctly reported here (Leonard Gard, written commun., 1978).

CONCLUSIONS

These radiometric-age data and the previously reported 5.5-m.y. date on Little Kiska Island indicate that the Kiska Harbor Formation is late Miocene to early Pliocene in age. The lower Kiska Harbor Formation braided-stream sediments were deposited 5.5 to 4.7 m.y. ago, and normal faulting of the Kiska Harbor Formation began at least 4.4 m.y. ago. Ground breaks along the same trend have been observed; in fact, a probable fault scarp that cuts a 1962 lava flow suggests current activity.

ACKNOWLEDGMENTS

This paper was reviewed by D.L. Turner and John Decker. Their constructive criticism and valuable suggestions are gratefully acknowledged. The radiometric-age determinations were provided by Turner. Without these data this paper would not have been possible.

REFERENCES CITED

Coats, R.R., Nelson, W.H., Lewis, R.Q., and Powers, H.A., 1961, Geologic reconnaissance of Kiska Island, Aleutian Islands, Alaska: U.S. Geological Survey Bulletin 1028-R, p. 563-581.

DeLong S.E., Fox, P.J., and McDowell, F.W., 1978, Subduction of the Kula Ridge at the Aleutian Trench: Geological Society of America Bulletin, v. 89, no. 1, p. 83-95.

Panuska, B.C., 1980, Stratigraphy and sedimentary petrology of the Kiska Harbor Formation and its relationship to the Near Island-Amchitka Lineament, Aleutian Islands: Fairbanks, University of Alaska, unpublished M.S. thesis, 90 p.

Von Huene, Roland, Carr, W.J., Mcmanus, Dean, and Holmes, Mark, 1971, Marine geophysical study around Amchitka Island, western Aleutian Islands, Alaska, Amchitka-22: U.S. Department of Commerce, National Technical Information Service AT(29-2)-474-74, 35 p.

GEOCHEMICAL SIGNATURE OF THE GOON DIP GREENSTONE ON CHICHAGOF ISLAND, SOUTHEASTERN ALASKA

By John Decker[1]

INTRODUCTION

Many geologists believe that Alaska and western Canada are composed of a mosaic of discrete tectonostratigraphic terranes, each with a characteristic stratigraphic sequence and unique geologic history (Berg and others, 1978; Tipper, 1978; Jones and others, 1981). One of the most extensive terranes is Wrangellia (Jones and others, 1977), which consists predominantly of a distinctive Middle and Upper Triassic sequence of tholeiitic basalt overlain by inner-platform carbonate (fig. 1). Alternate models for the distribution of Wrangellia in southeastern Alaska have been proposed by Brew and Morrell (1979), Plafker and Hudson (1980), and Decker and Plafker (1981a,b). This report summarizes geologic data and presents new geochemical data on the Wrangellia section on Chichagof Island. This information supports the correlation of the Chichagof Island section with similar strata in the type area of Wrangellia.

STRATIGRAPHY

In its type area in the Wrangell Mountains, the Triassic sequence of Wrangellia consists of four formations, the Nikolai Greenstone, the Chitistone Limestone, the Nizina Limestone, and the McCarthy Shale. The Nikolai Greenstone is a thick, weakly deformed sequence of predominantly subaerial, but locally pillowed basalt of Middle and/or Late Triassic age. It generally unconformably overlies late Paleozoic volcaniclastic rocks and limestone, but locally overlies grayish-black chert, siltstone, and shale of Middle Triassic (Ladinian) age. The Chitistone Limestone disconformably overlies the Nikolai Greenstone and consists of inner-platform carbonate rocks that grade upward into open-platform and basinal carbonate rocks of the Nizina Limestone; both limestone units are of Late Triassic age. The Nizina Limestone is conformably overlain by the McCarthy Shale, a sequence of calcareous shale, chert, and limestone of Late Triassic and Early Jurassic age (Jones and others, 1977, 1981).

On the basis of a striking lithologic similarity, Plafker and others (1976) first suggested that the Goon Dip Greenstone and Whitestripe Marble on western Chichagof Island are correlative with the Nikolai Greenstone and Chitistone Limestone, respectively (fig. 2).

The Goon Dip Greenstone is generally massive, medium-gray-weathering, medium- to dark-gray and greenish-gray, very fine grained, plagioclase- (or rarely pyroxene-) porphyritic basalt and metabasalt. The rocks are dominantly holocrystalline, commonly amygdaloidal, and locally pillowed. Flow breccia, pillow breccia, and crystal-lithic lapilli tuff are less common; diabase dikes are rare. Locally, the rocks have a very weakly developed metamorphic foliation. One particularly well-preserved exposure of the Goon Dip Greenstone (near the top of Whitestripe Mountain) consists of thick-bedded to massive (1 to 2 m thick), shallow, westward-dipping flow units. The amygdaloidal tops, vertical pipe amygdules near the base of flows, and red tuffaceous interbeds together consistently indicate tops to the west, toward the Whitestripe Marble. The lack of pillows, presence of red beds, and amygdaloidal character suggest subaerial volcanism.

The Goon Dip Greenstone has been affected by two periods of metamorphism. The first period produced a regional low-temperature-facies series characterized by mineral assemblages that indicate recrystallization during conditions of the prehnite-pumpellyite and lower greenschist facies. The second period of metamorphism was a thermal overprint that was localized in contact aureoles around Upper Jurassic and Lower Cretaceous plutons, and produced predominantly hornblende hornfels and rarely pyroxene hornfels facies mineral assemblages.

The Whitestripe Marble is generally massive to weakly foliated, white to medium-gray, fine-grained marble. Recrystallization of the Whitestripe Marble produced a peculiar neomorphic texture and color that Augustus K. Armstrong (oral commun., 1979) of the U.S. Geological Survey has seen only in the lower part of the Chitistone Limestone. The neomorphic similarities between the Whitestripe Marble and the Chitistone Limestone are probably due to similar thermal metamorphic histories and not necessarily to similar depositional environments. Locally, the marble includes diorite dikes and greenstone interbeds, lenses, and clasts. Where observable, crude layering within the marble also has a shallow westward dip.

The contact between the Whitestripe Marble and the Goon Dip Greenstone is a steep westward-dipping fault

[1]DGGS, College, Alaska 99708.

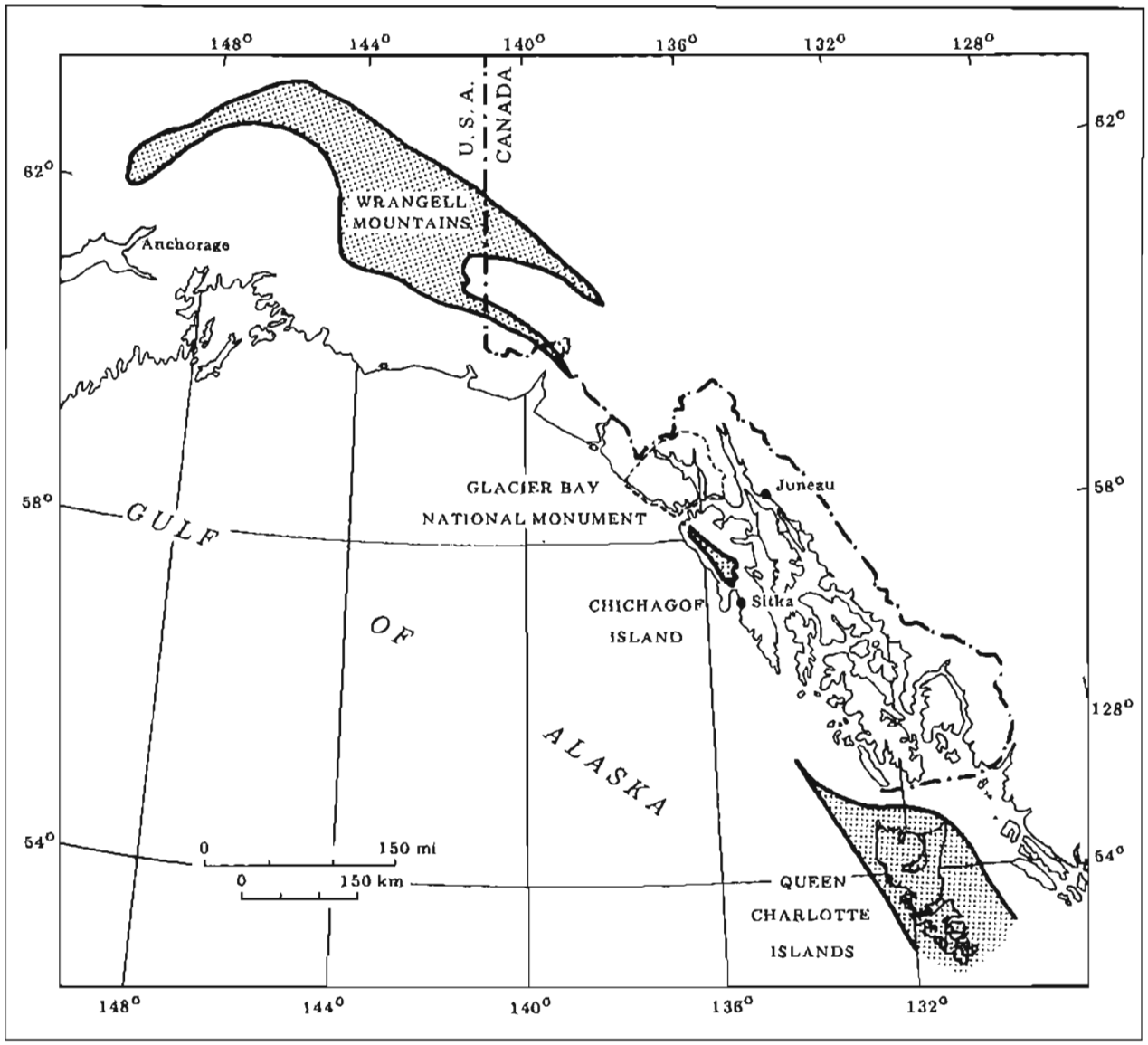

Figure 1. Map showing the distribution of Wrangellia in southern Alaska (modified from Jones and others, 1977, and Decker and Plafker, 1981b).

of unknown but possibly minor displacement that truncates layering in the marble and greenstone units. The fault zone is generally sharp and less than 1 m thick. Locally it contains foliated greenstone with marble clasts.

No age-diagnostic fossils are known from the Whitestripe Marble or Goon Dip Greenstone. However, an isotopically dated tonalite of Late Jurassic (150-164 m.y.) age is probably intrusive into the Goon Dip Greenstone (Loney and others, 1975). On their geologic map, Loney and others (1975) show two migmatite zones at the tonalite-Goon Dip Greenstone contact. Where I have observed this contact, the relationships are generally ambiguous, but at one location it is probably an intrusive contact (Bruce R. Johnson, oral commun., 1979).

DISTRIBUTION AND CORRELATION

Jones and others (1977), Berg and others (1978), and Brew and Morrell (1979) suggest that Wrangellia can be mapped almost continuously between the Wrangell Mountains and Chichagof Island. Recent mapping on northern Chichagof Island and in Glacier Bay National Monument (Decker and Plafker, 1981a,b; Decker and Johnson, 1981) shows that the Goon Dip Greenstone - Whitestripe Marble section is truncated by the Peril Strait fault and does not extend into the monument. Rocks of the Tarr Inlet suture zone---previously thought to represent Wrangellia in Glacier Bay National Monument---are continuous with rocks of the Kelp Bay Group on Chichagof Island, and are now believed to be part of the melange facies of the Chugach terrane (Plafker and others, 1977).

Table 1. *Chemical data from metavolcanic rocks of the Goon Dip Greenstone, Chichagof Island, and the Nikolai Greenstone, Wrangell Mountains (major oxides in percent, trace elements in ppm).*

	Goon Dip Greenstone						Goon Dip sample	Nikolai Greenstone
Sample	764[1]	609[2]	604[2]	245c[3]	240d[3]	253[3]	Average, 6 samples	Average, 39 samples[4]
SiO_2	47.56	47.5	49.4	52.50	50.10	45.47	48.76	47.9
Al_2O_3	14.82	12.5	14.3	14.43	13.26	16.19	14.25	14.5
Fe_2O_3	10.84	6.2	1.2	3.71	3.52	7.36	4.47	5.2
FeO	--	10.4	10.9	7.44	11.08	9.34	9.83	6.4
MgO	6.14	5.1	6.1	5.6	5.5	4.5	5.49	6.9
CaO	10.65	7.8	8.0	9.48	10.20	6.68	8.80	9.4
Na_2O	3.55	3.1	2.7	4.26	2.75	3.58	3.32	3.1
K_2O	0.02	0.30	1.7	0.24	0.73	1.20	0.70	0.48
TiO_2	1.39	3.4	1.3	1.63	2.00	2.68	2.07	1.4
P_2O_5	0.10	0.34	0.18	0.27	0.31	0.62	0.30	0.16
MnO	0.18	0.27	0.22	0.15	0.17	0.16	0.18	0.18
CO_2	--	0.02	0.06	--	--	--	0.04	0.54
H_2O+	--	2.7	2.70	--	--	--	2.70	0.56
H_2O^-	--	0.12	0.14	--	--	--	0.13	3.2
LOI	4.12	1.69[5]	1.98[5]	1.6	2.0	3.1	4.08	--
Total	99.37	99.75	98.90	101.31	101.62	100.88	--	--
Ni	--	--	--	50	50	20	40	--
Zr	126	230	95	104	126	252	155	--
Cr	230	35.8	70.2	157	137	<13	--	--
Y	--	41	28	20	32	33	31	--
Rb	<5	11	50	--	--	--	--	--
Sr	60	228	254	279	194	626	274	--
Ba	--	240	2215	< 9	152	170	--	--
Co	--	46.5	45.2	--	--	--	45.8	--
Cs	--	0.3	1.2	--	--	--	0.8	--
Hf	--	5.6	2.2	--	--	--	3.9	--
Sb	--	1.1	0.3	--	--	--	0.7	--
Ta	--	1.4	0.4	--	--	--	0.9	--
Th	--	1.8	0.6	--	--	--	1.2	--
U	--	0.6	1.0	--	--	--	0.8	--
Zn	--	154	122.5	--	--	--	138.2	--
Sc	--	39.4	44.0	--	--	--	41.7	--
La	--	17.5	6.5	--	--	--	12.0	--
Ce	--	33.5	14	--	--	--	23.8	--
Nd	--	29.5	14.5	--	--	--	22.0	--
Sm	--	8.4	3.6	--	--	--	6.0	--
Eu	--	2.2	1.1	--	--	--	1.6	--
Gd	--	8.0	4.0	--	--	--	6.0	--
Tb	--	1.8	0.8	--	--	--	1.3	--
Ho	--	1.1	<0.6	--	--	--	--	--
Tm	--	0.6	0.4	--	--	--	0.5	--
Yb	--	4.4	3.1	--	--	--	3.8	--
Lu	--	1.2	0.7	--	--	--	1.0	--

[1]Major element analyses by XRF; Zr, Cr, Rb, Sr by AA.
[2]Major element analyses by rapid rock; Y, Rb, Sr by XRF; remaining trace elements by INAA.
[3]FeO by AA, Ni by emission spectroscopy, remaining elements by XRF.
[4]MacKevett and Richter (1974).
[5]LOI not calculated in total.

GEOCHEMISTRY

Major, minor, and trace-element geochemical analyses using X-ray-diffraction, rapid-rock, atomic-absorption, and neutron-activation (INAA) techniques were performed on six metavolcanic rocks from the Goon Dip Greenstone. All samples were crushed with metallic machinery to approximately 1-cm-diameter pieces that were hand picked, ultrasonically washed for 5 min, and scrubbed with a stiff-bristle nylon brush. After each piece was examined to ensure that all visible metallic-looking residue was removed, the pieces were ground to a fine powder using ceramic crushing equipment. A minimum of 1 kg was homogenized from each sample, and sample splits were made for the different types of analyses.

Chemical data listed in table 1 include results of analyses from the Nikolai Greenstone (MacKevett and Richter, 1974) for comparison. Sample descriptions are given in table 2. The range in composition for the Goon Dip Greenstone suggests it was initially basalt with a mean SiO_2 content of 48.77 percent and range of 45.47 to 52.50 percent. Most samples are classified as subalkaline (fig. 3a) and tholeiitic (fig. 3b) according to Irvine and Baragar (1971), but generally plot near the dividing line between fields. The average composition of the Nikolai Greenstone also plots in the subalkaline and tholeiitic fields.

Several authors (Pearce and Cann, 1973; Garcia, 1978; Wood and others, 1979) have attempted to discriminate metabasalts from different environments using stable (and questionably stable) minor and trace elements such as titanium, yttrium, zirconium, chromium, phosphorus, strontium, thorium, tantalum, hafnium, and rare-earth elements. When metabasalts from the Goon Dip Greenstone are plotted on various discriminant diagrams (figs. 4a,b), they consistently fall in or near the ocean-floor-basalt field. Wood and others (1979) have further subdivided ocean-floor basalts into normal mid-ocean-ridge basalts (MORB-N type) and rift-related basalts forming within plates or associated with hot spots (MORB-E type) based on a hafnium-thorium-tantalum discriminant (fig. 4c). Two samples from the Goon Dip Greenstone fall within the hot spot-MORB field on the hafnium-thorium-tantalum diagram. Similarly, basalts from the Red Sea and Afar rift systems plot in the hot spot-MORB field and thus support the suggestion of Jones and others (1977) that the Wrangellia basalts formed by rift volcanism. Similar trace-element data are not yet available from the Nikolai Greenstone.

SUMMARY

The Goon Dip Greenstone is lithologically and chemically similar to the Nikolai Greenstone in the Wrangell Mountains, and together with the Whitestrip Marble probably represents an isolated segment of Wrangellia on western Chichagof Island. The trace-element signature of the Goon Dip Greenstone supports the interpretation of Jones and others (1977), based on geologic data, that the Wrangellia basalts formed by rift volcanism.

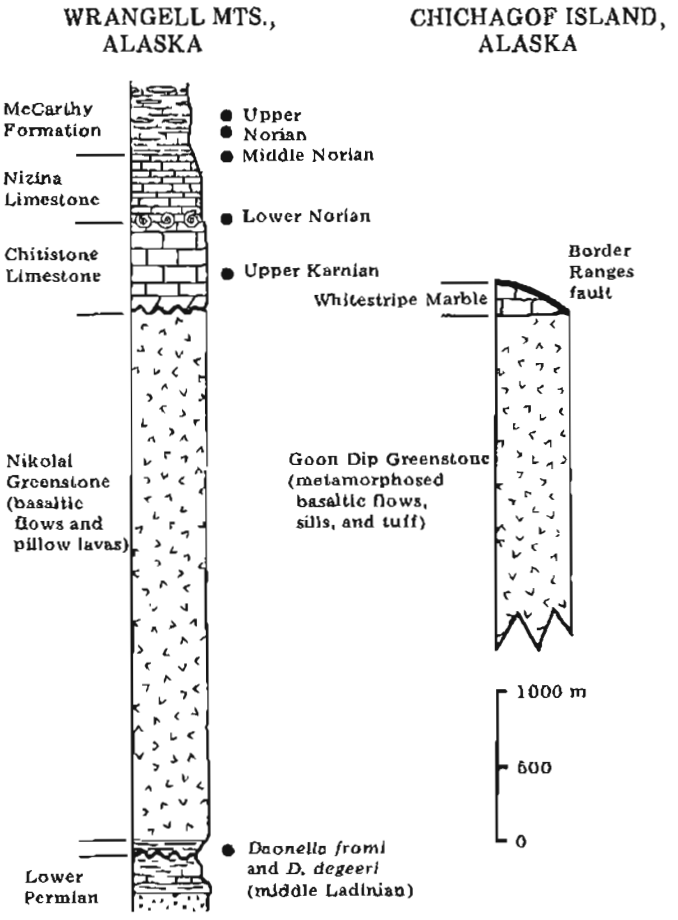

Figure 2. Diagrammatic stratigraphic columns of Triassic rocks from the type area of Wrangellia in the Wrangell Mountains, and suggested correlative rocks from Chichagof Island (modified from Jones and others, 1977).

ACKNOWLEDGMENTS

Thoughtful reviews by Wyatt G. Gilbert and Edward M. MacKevett, Jr. are greatly appreciated. This research was funded by the Alaska Branch of the U.S. Geological Survey.

REFERENCES CITED

Berg, H.C., Jones, D.L., and Coney, P.J., 1978, Map showing pre-Cenozoic tectonostratigraphic terranes of southeastern Alaska and adjacent areas: U.S. Geological Survey Open-file Report 78-1085, scale 1:1,000,000, 2 sheets.

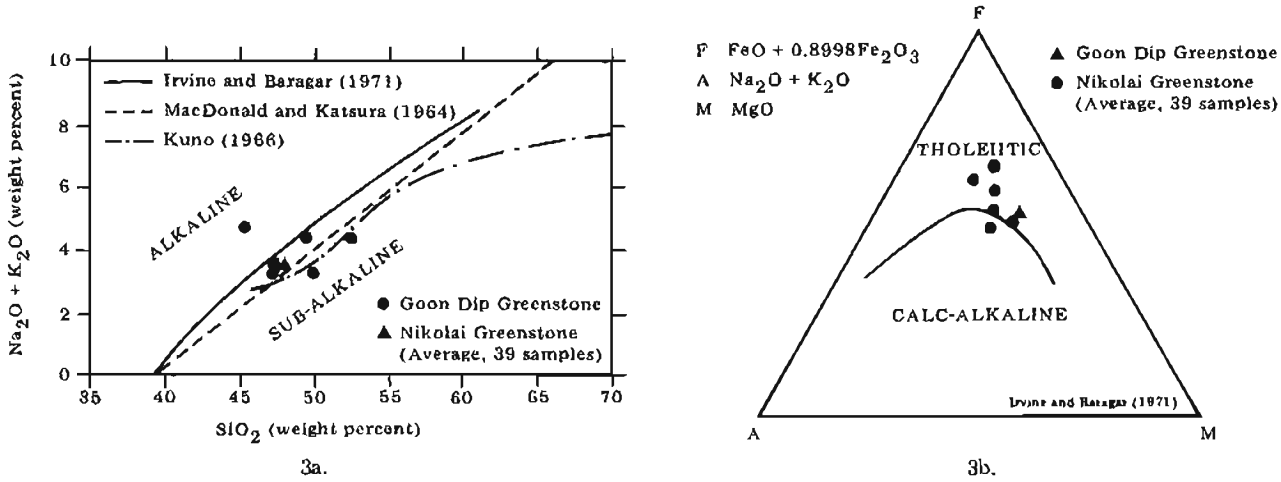

3a. 3b.

Figure 3. Classification of basalts. Metabasaltic rocks from the Goon Dip Greenstone are subalkaline (fig. 3a) when plotted on an SiO_2 versus total alkalies (K_2O + Na_2O) diagram, and tholeiitic (fig. 3b) when plotted on an F-A-M diagram using the discriminant lines by Irvine and Baragar (1971).

Table 2. *Description of metavolcanic rocks analyzed from the Goon Dip Greenstone*

Sample number	FIELD DESCRIPTION	THIN-SECTION DESCRIPTION	
		Metamorphic minerals	Relict features
245c	massive, fine-grained, highly fractured greenstone	calcite, epidote, actinolite, chlorite	holocrystalline, very fine-grained; aphyric, no relict minerals
245d	thick-bedded, fine-grained greenstone	calcite, epidote, chlorite	holocrystalline, fine-grained; aphyric, no relict minerals
253c	fine-grained greenstone interlayered with marble; pillow basalt nearby	no thin section	no thin section
604	massive, fine- to medium-grained basalt(?)	prehnite, actinolite	holocrystalline, fine-grained; altered plagioclase
609	massive, fine-grained, altered basalt	epidote, actinolite, chlorite, quartz	holocrystalline, fine-grained; plagioclase, highly altered clinopyroxene, magnetite
764	amygdaloidal, porphyritic basalt	calcite, epidote; with chlorite, pumpellyite amygdules	holocrystalline, fine-grained; plagioclase, clinopyroxene, magnetite

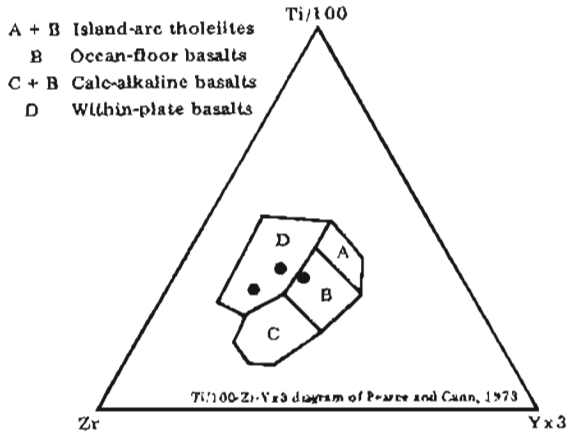

4a.

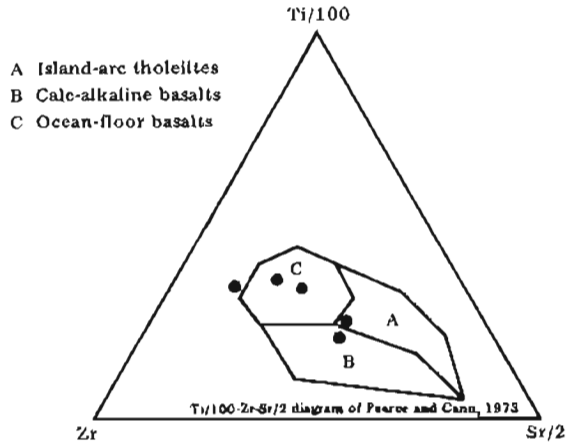

4b.

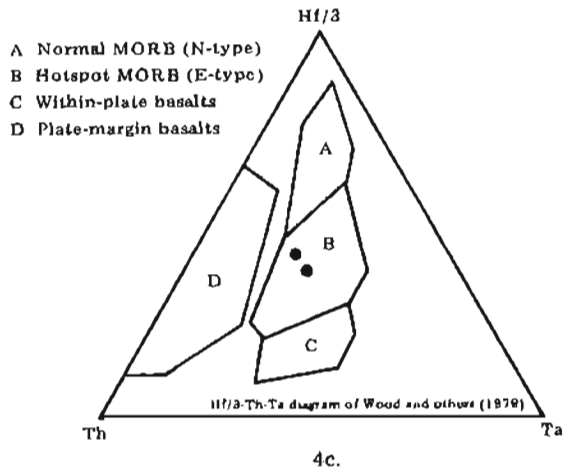

4c.

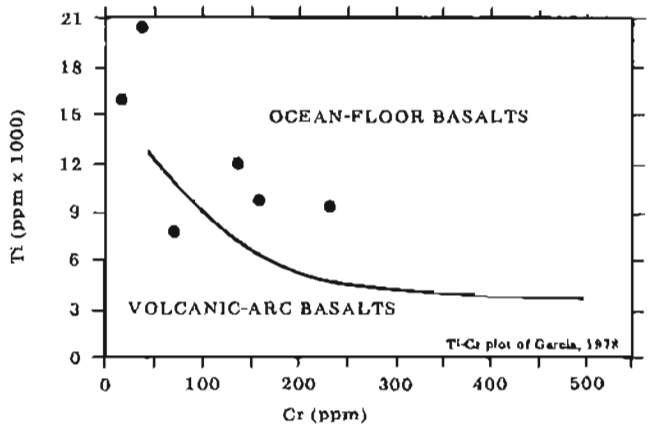

4d.

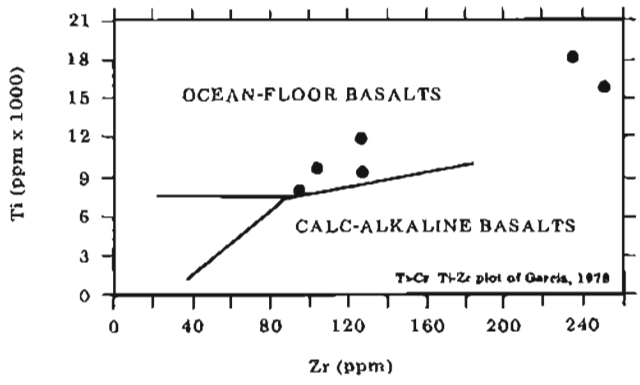

4e.

Figure 4(a-e). Classification of basaltic rocks according to tectonic environment based on minor and trace-element geochemistry. See Hill (1979) or Garcia (1978) for a discussion of confidence and validity of using these diagrams for altered rocks.

Brew, D.A., and Morrell, R.P., 1979, The Wrangell terrane ('Wrangellia') in southeastern Alaska: The Tarr Inlet suture zone with its northern and southern extensions, *in* Johnson, K.M., and Williams, J.R., eds., United States Geological Survey in Alaska: Accomplishments during 1978: U.S. Geological Survey Circular 804-B, p. B121-B123.

Decker, John, and Johnson, B.R., 1981, The nature and position of the Border Ranges fault on Chichagof Island, *in* Albert, Nairn, and Hudson, Travis, eds., United States Geological Survey in Alaska: Accomplishments during 1979: U.S. Geological Survey Circular 823-B, p. 102-104.

Decker, John, and Plafker, George, 1981a, Correlation of the Tarr Inlet suture zone, southeastern Alaska: Geological Association of Canada Abstracts, v. 6, p. A-14.

_____, 1981b, Correlation of rocks in the Tarr Inlet suture zone with the Kelp Bay Group, *in* Coonrad, W.L., ed., United States Geological Survey in Alaska: Accomplishments during 1980: U.S. Geological Survey Circular 844, p. 119-122.

Garcia, M.O., 1978, Criteria for the identification of ancient volcanic arcs: Earth Science Reviews, v. 14, p. 147-165.

Hill, M.D., 1979, Volcanic and plutonic rocks on the Kodiak-Shumagin shelf, Alaska: Subduction deposits and near-trench magmatism: Santa Cruz, University of California, unpublished Ph.D. thesis, 259 p.

Irvine, T.N., and Baragar, W.R.A., 1971, A guide to the chemical classification of the igneous rocks: Canadian Journal of Earth Science, v. 8, p. 523-548.

Jones, D.L., Silberling, N.J., Berg, H.C., and Plafker, George, 1981, Tectonostratigraphic terrane map of Alaska: U.S. Geological Survey Open-file Report 81-792, 20 p.

Jones, D.L., Silberling, N.J., and Hillhouse, J.W., 1977, Wrangellia–a displaced terrane in northwestern North America: Canadian Journal of Earth Sciences, v. 14, no. 11, p. 2565-2577.

Kuno, H., 1966, Lateral variation of basalt magma across continental margins and island arcs: Geological Survey of Canada Paper 66-15, p. 317-336.

Loney, R.A., Brew, D.A., Muffler, L.J.P., and Pomeroy, J.S., 1975, Reconnaissance geology of Chichagof, Baranof, and Kruzof Islands, southeastern Alaska: U.S. Geological Survey Professional Paper 792, 105 p.

MacDonald, G.A., and Katsura, T., 1964, Chemical composition of Hawaiian lavas: Journal of Petrology, v. 5, p. 82-133.

MacKevett, E.M., Jr., and Richter, D.H., 1974, The Nikolai Greenstone in the Wrangell Mountains, Alaska and nearby areas: Geological Association of Canada, Cordilleran Section, Program and Abstracts, p. 13-14.

Pearce, J.A., and Cann, J.R., 1973, Tectonic setting of basic volcanic rocks determined using trace element analyses: Earth and Planetary Science Letters, v. 19, p. 290-300.

Plafker, George, and Hudson, Travis, 1980, Regional implications of Upper Triassic metavolcanic and metasedimentary rocks on the Chilkat Peninsula, southeastern Alaska: Canadian Journal of Earth Sciences, v. 17, p. 681-689.

Plafker, George, Jones, D.L., Hudson, Travis, Berg, H.C., 1976, The Border Ranges fault system in the Saint Elias Mountains and Alexander Archipelago, *in* Cobb, E.H., ed., United States Geological Survey in Alaska: Accomplishments during 1975: U.S. Geological Survey Circular 733, p. 14-16.

Plafker, George, Jones, D.L., and Pessagno, E.A., Jr., 1977, A Cretaceous accretionary flysch and melange terrane along the Gulf of Alaska margin, *in* Blean, K.M., ed., United States Geological Survey in Alaska: Accomplishments during 1976: U.S. Geological Survey Circular 751-B, p. B41-B43.

Tipper, H.W., 1978, Tectonic assemblage map of the Canadian Cordillera: Geological Survey of Canada Open-file Report 572, scale 1:2,000,000.

Wood, D.A., Joron, Jean-Louis, and Treuil, Michel, 1979, A reappraisal of the use of trace elements to classify and discriminate between magma series erupted in different tectonic settings: Earth and Planetary Science Letters, v. 45, p. 326-336.

URANIUM MINERALIZATION IN THE NENANA COAL FIELD, ALASKA

By Robert K. Dickson [1]

INTRODUCTION

The Tertiary coal-bearing group in the Nenana Coal Field was intensively prospected for uranium between 1974 and 1979. Although mineralization was discovered, the potential for economic deposits is considered quite low.

Three types of uranium mineralization were discovered: a) a small roll-front system near Jumbo Dome, b) a fracture coating in micaceous schist, and c) an epigenetic, tabular deposit in conglomeratic sands at Dexter Creek (fig. 1). The tabular deposit is of greatest interest because of its high grade, more favorable accessibility, and potential value in interpretation of the depositional environment.

GEOLOGIC SETTING

The geology of the Nenana Coal Field has been described in detail by Wahrhaftig (1958, 1970a-b, 1973), Wahrhaftig and others (1969), and Triplehorn (1976). Figure 1 is a generalized geologic map of the study area and figure 2 is a stratigraphic column.

The Tertiary coal-bearing group unconformably overlies Paleozoic metasediments and metavolcanics that are assigned to the Birch Creek Schist, Totatlanika Schist, and Keevy Peak Formations. The basal unit of the coal-bearing group is the upper Oligocene - lower Miocene Healy Creek Formation, a sequence of fluvial conglomeratic sandstones interbedded with claystones and subbituminous coal. The Healy Creek Formation is conformably overlain by the Sanctuary Formation, a locally thick lacustrine claystone that is overlain---in places unconformably---by the middle Miocene Suntrana Formation, which is lithologically similar to the Healy Creek Formation. The Lignite Creek Formation, a fluvial sequence of arkosic conglomerates, claystones, and coal, conformably overlies the Suntrana Formation in most places, but local unconformities are present. The most recently deposited unit of the coal-bearing group is the upper Miocene Grubstake Formation, which consists of siltstone and claystone with interbedded sands and locally reworked ash beds. The coal-bearing group is unconformably overlain by the Pliocene Nenana Gravel.

A northern provenance is inferred for the coal-bearing group, primarily because of the presence of abundant black chert. No chert is reported locally and the most likely source is the Yukon-Tanana Upland. Garnet in the Suntrana Formation also suggests a northern source.

Two lithologic changes are indicative of climatic cooling and a decrease in chemical weathering from older to younger formations. First, clay mineralogy changes from dominantly kaolinite in the Healy Creek Formation to dominantly montmorillonite in the Suntrana Formation and above. Second, pebbles in the Healy Creek and Suntrana Formations are more resistant than those of the arkosic Lignite Creek Formation.

URANIUM MINERALIZATION

Three types of uranium mineralization were discovered: a) a roll-front system, b) a fracture coating or filling in micaceous schist, and c) a tabular occurrence in conglomeratic sands.

The roll-front system was discovered during drilling in Suntrana and Healy Creek Formation sediments north of Jumbo Dome (fig. 1). Altered tongues extend from a canyon that was incised in these formations (fig. 3) and later filled with very permeable Lignite Creek Formation conglomerates. Probable sources of uranium are the ash beds in the Grubstake Formation or intraformational tuffaceous material. The Lignite Creek Formation is an excellent conduit for oxidizing ground waters. These waters invaded the canyon walls and deposited uranium along the reduction-oxidation boundary of the geochemical cells. The highest grade mineralization included 3 ft of 0.016 percent eU_3O_8[2]. The extreme depth of the anomalies (400-700 ft) and difficult drilling conditions complicated their evaluation.

The second type of mineralization is located in the Lignite Creek drainage and occurs in fractured and oxidized micaceous Birch Creek Schist. The first indication of mineralization was a strong anomaly in stream-sediment and water samples. A fractured and oxidized schist outcrop with 79 ppm U_3O_8---about 10 times the observed background value---was located. The most probable origin for this occurrence is percolation of mineralized ground water from overlying Healy Creek Formation sediments that have since been removed by

[1] Urangesellschaft U.S.A., Inc., Denver, Colorado 80222.

[2] Equivalent uranium, defined as the apparent amount of uranium as calculated from the gamma-ray emission of ^{214}B, according to Levinson (1980, p. 696).

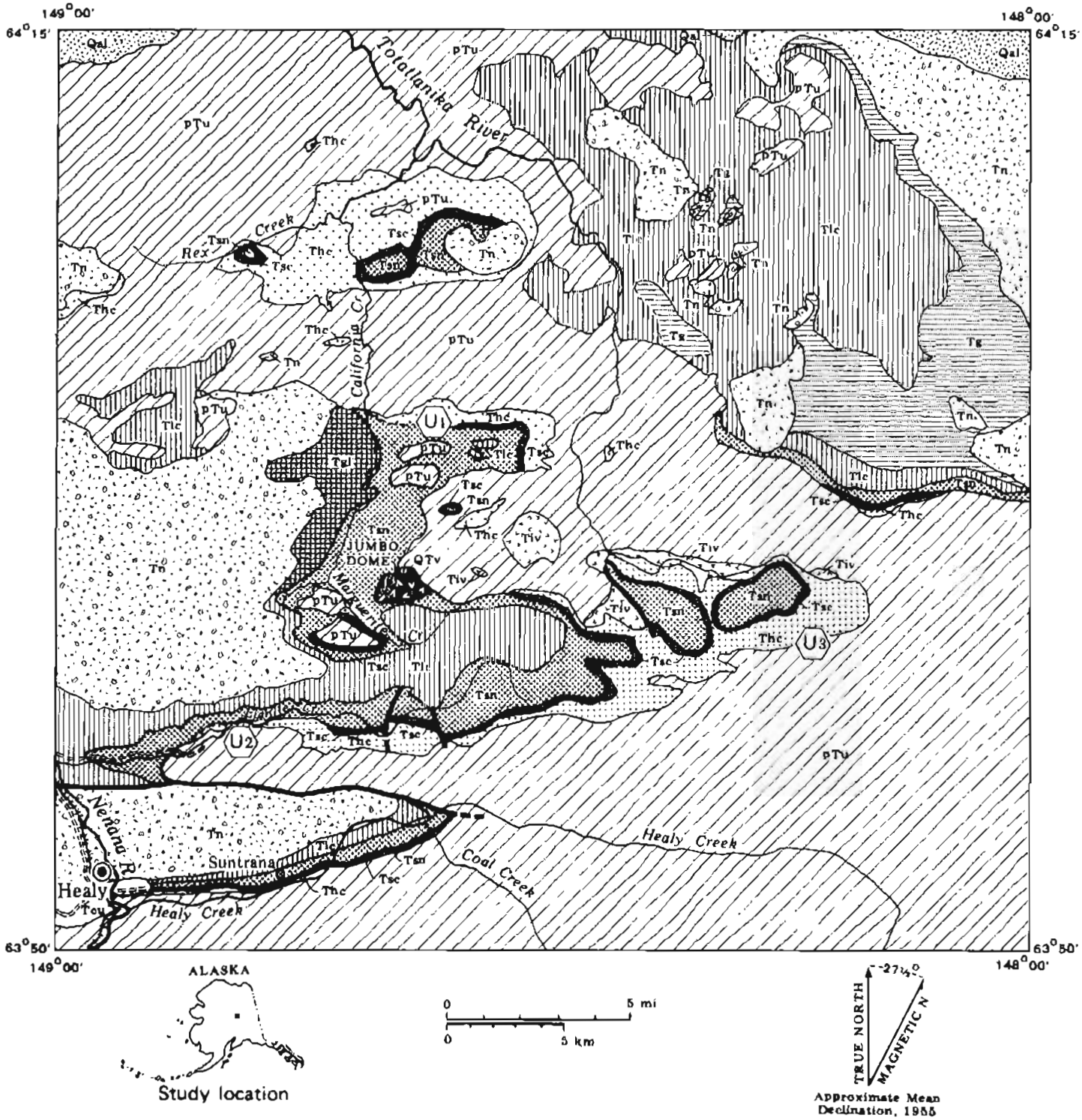

Figure 1. Geologic map of the study area, after Wahrhaftig (1970a,b).

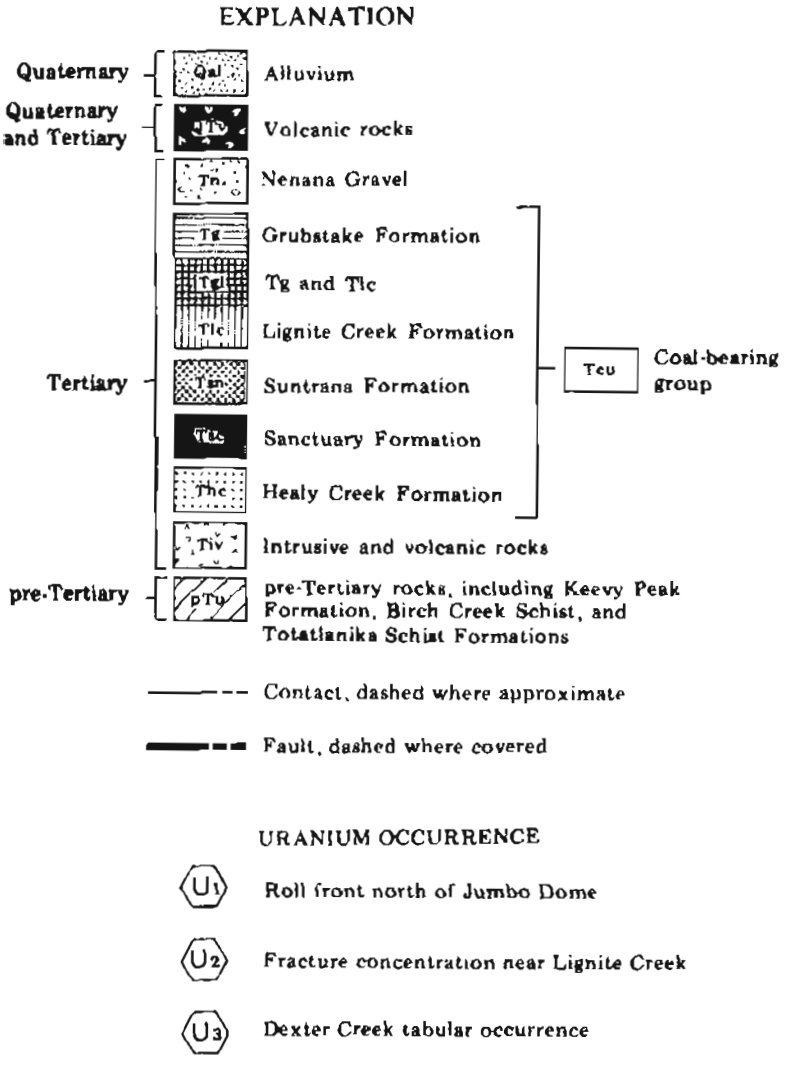
EXPLANATION
Quaternary
Qal
Alluvium
Quaternary and Tertiary
Volcanic rocks
Tn
Nenana Gravel
Tg
Grubstake Formation
Tgl
Tg and Tlc
Tlc
Lignite Creek Formation
Tertiary
Tsn
Suntrana Formation
Teu
Coal-bearing group
Tsc
Sanctuary Formation
Thc
Healy Creek Formation
Tiv
Intrusive and volcanic rocks
pre-Tertiary
pTu
pre-Tertiary rocks, including Keevy Peak Formation, Birch Creek Schist, and Totatlanika Schist Formations
Contact, dashed where approximate
Fault, dashed where covered
URANIUM OCCURRENCE
U1
Roll front north of Jumbo Dome
U2
Fracture concentration near Lignite Creek
U3
Dexter Creek tabular occurrence

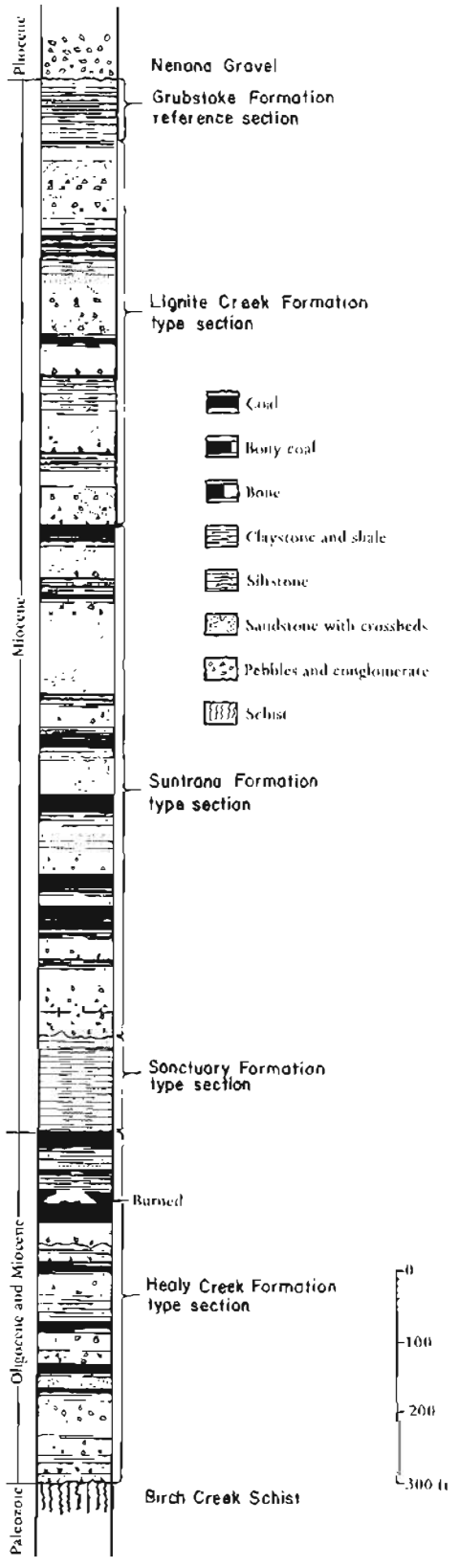

Figure 2. Stratigraphic section of the coal-bearing group at Suntrana, after Wahrhaftig (1970b).

erosion. The uranium mineralogy and exact mode of occurrence were not determined.

The third and most significant type of uranium mineralization is a tabular deposit that crops out along Dexter Creek in the headwaters of the Totatlanika River (fig. 1). Airborne radiometry and stream-geochemistry reconnaissance detected anomalies that led to the discovery of a 2-ft-thick mineralized zone in the basal Healy Creek Formation; values ranged up to 0.17 percent U_3O_8 in 'high-graded' samples. Host rock for the mineralization is a silty to shaly sandstone interbedded with a coarse-grained, conglomeratic, tuffaceous sandstone. The mineralized zone is iron stained from oxidation of siderite cement and contains siderite nodules and organic debris. Dickinson (1978) described uraninite-bearing siderite nodules from this outcrop. Adjacent iron- and organic-rich zones are barren. Megascopically, the zones are very similar; the reason only one is mineralized is unclear. The mineralized zone can be traced for about 100 ft along the outcrop, which runs oblique to strike. A polished slab and autoradiograph of the silty, mineralized rock shows distinct banding of uranium mineralization along bedding laminae.

The uranium mineralogy at Dexter Creek probably includes a urano-organic compound as well as the uraninite reported by Dickinson (1978). Channel sampling across a trenched face 12 ft long and 7 ft deep yielded up to 495 ppm U_3O_8 and averaged 73 ppm U_3O_8 for the upper 6 to 12 in. of the mineralized zone. Unfortunately the trench did not intersect the entire mineralized zone and could not be extended because the outcrop is used as a mineral lick by Dall sheep. A correlation between sheep licks and uranium mineralization was considered, but other licks in the area are barren of uranium. The basal Healy Creek Formation interval characteristically produced stream-sediment geochemical anomalies and occasional low-grade radiometric anomalies, especially in the headwaters of the Totatlanika River.

Drilling about 400 ft downdip from the outcrop intersected a 2-ft-thick mineralized zone of 0.068 percent eU_3O_8, and in an offset core hole a 2-ft-thick interval of 0.0175 percent U_3O_8 was encountered. Multielement analysis showed that the uranium is associated with organic carbon, maganese, magnesium, and iron. The uranium is slightly out of equilibrium with its daughter products, which causes higher radiometric than chemical assays.

The mineralized core from the offset hole is a very coarse grained, quartz-pebble conglomerate with a kaolinite and siderite matrix. Rare montmorillonite and sericite have also been noted in the matrix. Some kaolinite occurs as clasts that display relict volcanic-ash textures. These lithologic characteristics and the stratigraphic position of the Dexter Creek mineralization are critical to an explanation of the origin of the mineralization.

DISCUSSION OF THE DEXTER CREEK OCCURRENCE

The nature of the basal Healy Creek Formation is considered critical to interpreting the environmental conditions leading to the mineralization observed at Dexter Creek. The following discussion is based on work by Wahrhaftig (1958, 1973), Triplehorn (1976), and Abbott and Dickson (1978), and on internal Urangesellschaft U.S.A., Inc. reports.

In many locations, the Healy Creek Formation contains a basal quartz-pebble conglomerate, as it does

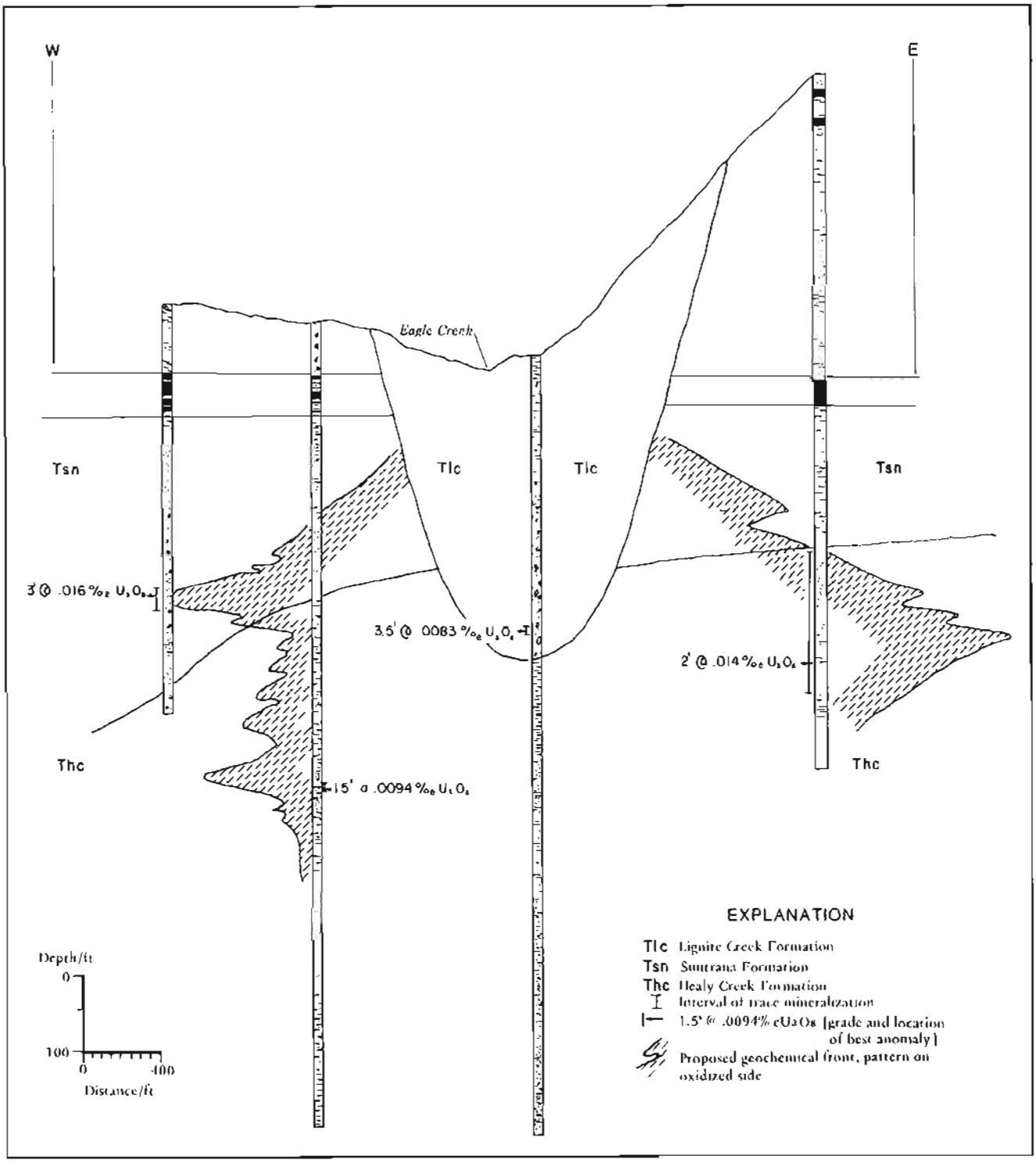

Figure 3. Roll-front system north of Jumbo Dome. Cross section across Eagle Creek compiled from drill-hole data.

at Dexter Creek. The characteristics of this conglomerate are indicative of a high-energy fluvial environment. The conglomerate contains a sand and clay matrix but is generally not well consolidated. The quartz pebbles are poorly rounded and are apparently derived from quartz veins in nearby metavolcanics. In areas where the conglomerate is absent, a deeply weathered erosional surface on the underlying schists is preserved and the schist is altered to quartz and kaolinite, which suggests intense chemical weathering in a warm, humid climate. Fragments of this weathered material, which represent initial fluvial deposition of reworked, weathered schist with locally derived sand and pebbles, are present in the basal Healy Creek conglomerate. The recognition of a warm, humid paleoclimate is critical to the epigenetic uranium potential of interior Alaska.

Volcanic ash in the basal Healy Creek Formation is indicated by relict textures observed in thin section and by a doubly terminated beta-quartz crystal identified in drill cuttings from Healy Creek strata in the California Creek basin, 10 miles north of Jumbo Dome. Volcanic ash has been noted elsewhere in the coal-bearing group (Triplehorn, 1976).

At the Dexter Creek location, several feet of weathered schist are preserved below a thin basal conglomerate. The exact position of the contact is difficult to define. In the drill holes, the mineralization is only 2 to 3 ft above the weathered schist, which is about 3.5 ft thick. In outcrop, the interval between the mineralized zone and the underlying schist is between 10 and 30 ft.

On the basis of these observations, the mineralized horizon was probably deposited in a relatively high-energy fluvial system and later isolated, producing the stagnant conditions indicated by the abundant organic carbon and manganese. After burial, uranium was leached from the ash and precipitated by the reducing action of the organic material. Evidently, enough ash was present to account for the amount of uranium encountered. The conditions that restricted the mineralization to a single horizon within a sequence of apparently similar beds are unknown. At Dexter Creek, seepage into fractures in the underlying schist produced minor anomalies similar to the mineralization previously noted in the Lignite Creek drainage.

Additional drilling indicated a limited extent of the Dexter Creek occurrence. To determine the potential for further 'Dexter Creek type' mineralization, a series of radon surveys was conducted across Healy Creek Formation sediments. Although several anomalies were located, they were usually quite small or were easily explained by proximity to high-uranium-background metavolcanics. A single drill hole in the largest anomaly failed to intersect any mineralization. The 'Dexter Creek type' mineralization seems limited to very small, low-grade occurrences.

CONCLUSION

The recognition of epigenetic-uranium mineralization in Tertiary sediments of interior Alaska is significant for paleoenvironmental and exploration considerations. The uranium occurrences were located by intensive geochemical prospecting, airborne radiometry, widespread radon surveys, and over 21,000 ft of drilling at 43 locations. Although the potential for undiscovered, economic uranium deposits in this area is now judged to be quite low, future workers should benefit from a review of geologic processes that occurred within the Tertiary coal-bearing group in the Nenana Coal Field.

ACKNOWLEDGMENTS

I thank the management of Urangesellschaft U.S.A., Inc. for their support and permission to release proprietary information. I also thank Dr. Volkmar Janicke, William Schneider, Jane Dickson, and Barbara Magg for their assistance and criticism. I am especially indebted to Dr. Earl Abbott for his contribution of ideas, criticism, and encouragement. I also wish to acknowledge Gilbert R. Eakins and Daniel B. Hawkins for their reviews of the manuscript and helpful suggestions.

REFERENCES

Abbott, E.W., and Dickson, R.K., 1978, Sedimentary uranium in Alaska: Northwest Mining Association Convention, 84th, Spokane, Washington, November 30-December 2, 1978, unpublished.

Dickinson, K.A., 1978, Uraninite in sideritic nodules from Tertiary continental sedimentary rocks in the Healy Creek basin area, central Alaska: U.S. Geological Survey Circular 804-B, p. B98-B99.

Levinson, A.A., 1980, Introduction to exploration geochemistry (2d ed.): Wilmette, Illinois, Applied Publishing Ltd., 924 p.

Triplehorn, D.M., 1976, Clay mineralogy and petrology of the coal-bearing group near Healy, Alaska: Alaska Geological and Geophysical Surveys Geologic Report 52, 14 p.

Wahrhaftig, Clyde, 1958, Lithology and conditions of deposition of the formations of the coal-bearing group in the Nenana Coal Field, Alaska: unpublished, 93 p.

_____, 1970a, Geologic map of the Healy D-3 Quadrangle, Alaska: U.S. Geological Survey Quadrangle Map GQ-805, scale 1:63,360.

_____, 1970b, Geologic map of the Healy D-4 Quadrangle, Alaska: U.S. Geological Survey Quadrangle Map GQ-806, scale 1:63,360.

_____, 1973, Coal reserves of the Healy Creek and Lignite Creek coal basins, Nenana Coal Field, Alaska: U.S. Geological Survey Open-file Report 568, 6 p., 28 pl.

Wahrhaftig, Clyde, Wolfe, J.A., Leopold, E.B., and Lanphere, M.A., 1969, The coal-bearing group in the Nenana Coal Field, Alaska: U.S. Geological Survey Bulletin 1274-D, 30 p.

RECONNAISSANCE OF RARE-METAL OCCURRENCES ASSOCIATED WITH THE OLD CROW BATHOLITH, EASTERN ALASKA-NORTHWESTERN CANADA

By James C. Barker[1]

INTRODUCTION

Evidence suggests that the emplacement, tectonics, and chemical composition of the Old Crow batholith, located in eastern Alaska and western Yukon Territory, Canada, are favorable for the occurrence of tin, tungsten, uranium, tantalum, niobium, and other rare metals. This evidence was reinforced by findings of uranium, tin, rare-earth oxides, and base metals during the 1976-80 field seasons.

REGIONAL GEOLOGY

The Old Crow batholith (fig. 1) forms the structural core of the Porcupine Plateau, a discrete physiographic province characterized by an unglaciated, gently rolling terrain (Wahrhaftig, 1965). Vegetation is nearly continuous and there is very little outcrop.

Reconnaissance geologic mapping of the Old Crow area, adapted from Brosgé (1969), is shown in figure 2. The Old Crow batholith intrudes and is bordered on the north by quartz-mica schist to semischist, phyllite, quartzite, and a greenstone substrata, all of Precambrian(?) to early Paleozoic age. These metamorphic rocks may correlate with the Neruokpuk Formation described by Sable (1977).

The batholith is bounded on the south by a succession of prominent allochthonous blocks. Lower Paleozoic (possibly Precambrian) quartzite and phyllite units are overthrusted by Mississippian to Jurassic sandstone and chert strata. Thrusting is apparently from the southwest, possibly associated with past movement along the very poorly defined Kaltag-Porcupine fault system. Within the batholith, extensive fracturing, faulting, and offsets, frequently with an east-to-north-orientation, are readily apparent.

West of the Old Crow batholith is a structural basin that contains an ophiolite sequence of uncertain age. Sheet dikes of diorite and gabbro are common in the cherts, argillites, basalts, and greenstones of the sequence.

AGE CORRELATION AND STRUCTURAL SETTING

Potassium-argon mica ages from intrusive rocks of the Old Crow batholith range from 220 to 345 ± 10 m.y. (table 1).

The oldest date correlates closely with those recently reported for Brooks Range (Dillon and others, 1979) and northern Yukon granites (Baadsgaard and others, 1961). The younger dates probably indicate recrystallization ages within the batholith, and suggest repeated postintrusive tectonic and thermal-alteration events. The initial intrusion would then correlate with the regional Late Devonian orogeny of northern Alaska (Sable, 1977). A major regional unconformity between Upper Devonian or Mississippian and older rocks, referred to by Baadsgaard and others (1961) and other more recent investigators, lends credence to this hypothesis. Thus, the age of the Old Crow batholith is inferred to be Carboniferous or Devonian. Sable (1977)

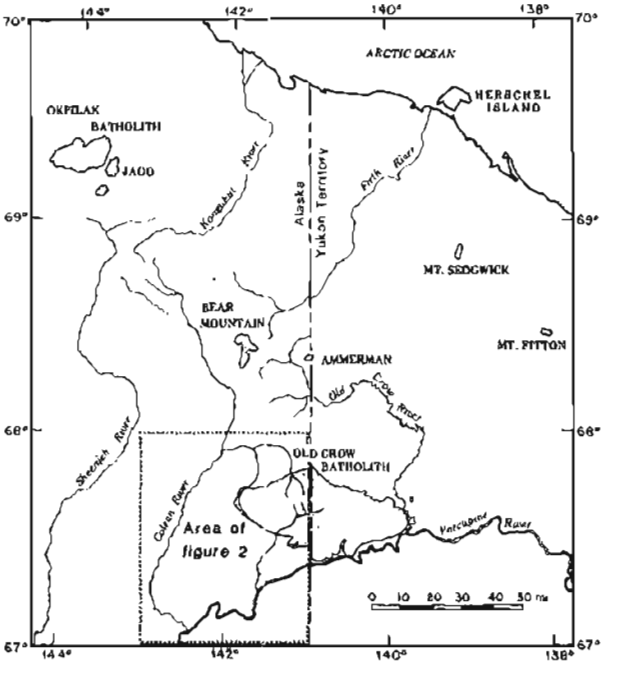

Figure 1. Location of study area, Porcupine Plateau, Alaska.

[1]U.S. Bureau of Mines, Fairbanks, Alaska 99701.

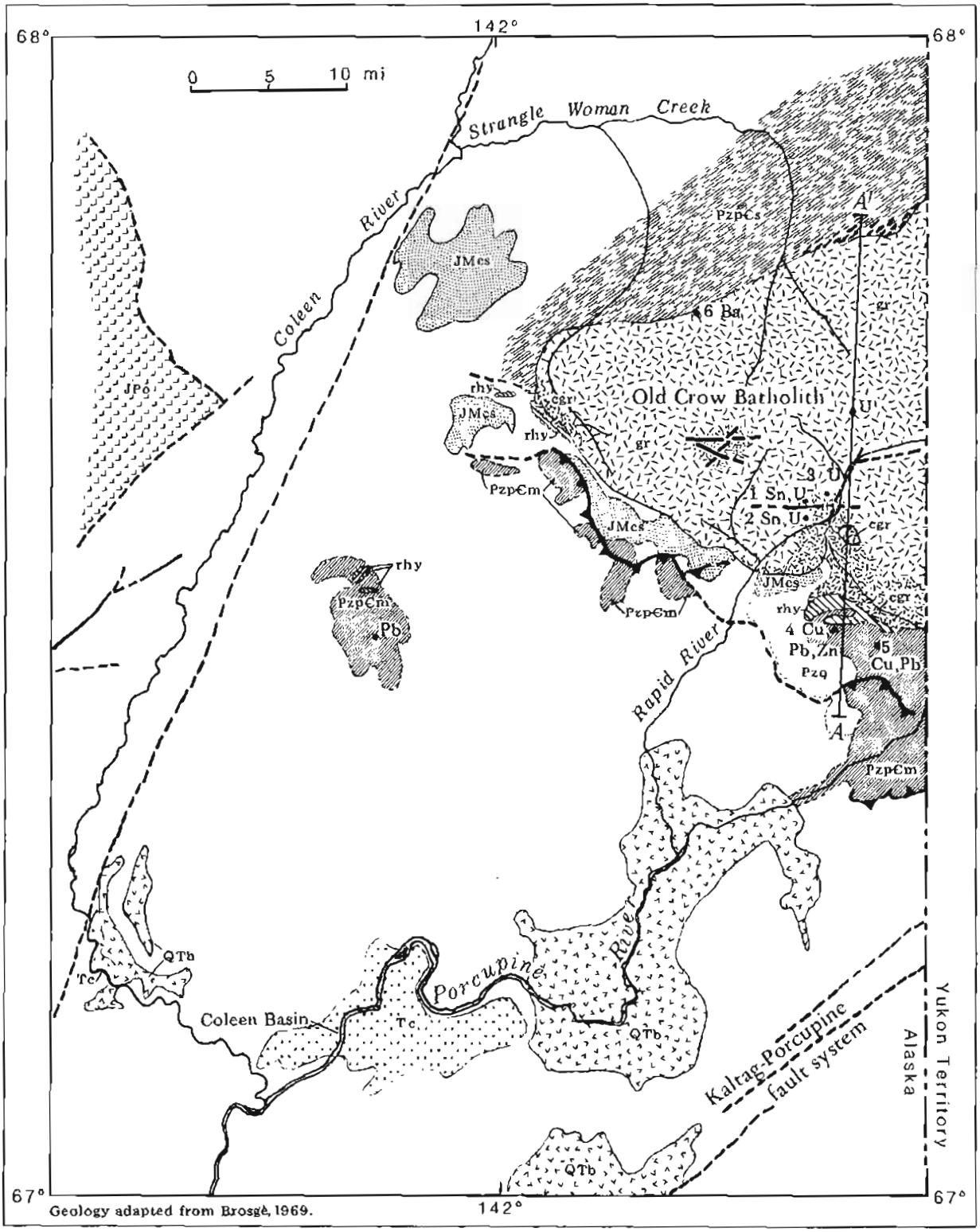

Geology adapted from Brosgé, 1969.

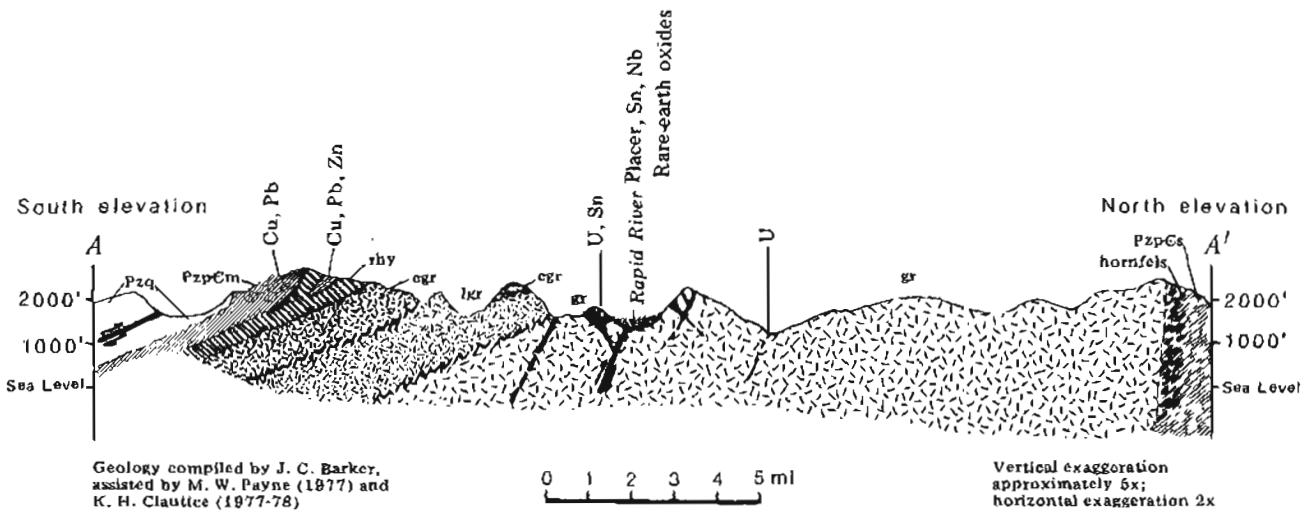

EXPLANATION

- Contact, dashed where approximate
- Gradational contact
- High-angle fault, dashed where approximate
- Thrust fault, dashed where approximate
- Quartz vein
- • 6 Ba — Mineral occurrence; number indicates discussion in text
- QTb — Quaternary or Tertiary basalt
- Tc — Tertiary coal-bearing sandstone, mudstone, and conglomerate
- JPo — Jurassic or Permian Christian Complex ophiolite
- JMcs — Jurassic or Mississippian chert and sandstone
- Pzq — Paleozoic quartzite
- rhy — Rhyolite-porphyry sills
- gr/lgr/cgr — Carboniferous Old Crow Batholith; includes locally porphyritic biotite granite and quartz monzonite (gr), typically altered leucocratic zone (lgr), and dark-colored, granitized intrusive border zone (cgr)
- PzpCs — Paleozoic or Precambrian schist and quartzite
- PzpCm — Paleozoic or Precambrian metasediments

suggests the potassium-argon age dates indicate an intermediate thermal event 220 to 280 m.y. ago.

Uplift of the batholith during Tertiary time resulted in deposition of terrigenous sediments in adjacent areas. Evidence of more recent uplift exists along the Porcupine River, where canyon walls 500 ft high are capped by Quaternary basalt and thick Quaternary(?) gravel terraces. Also, well-preserved and obviously recently abandoned channels of the Porcupine River are present at elevations up to 300 ft above the existent water course. This recent uplift and subsequent erosion and reworking of the granitic material have played an important role in the formation of heavy-mineral placer deposits in the area.

INTRUSIVE GEOLOGY

The Old Crow batholith is a broadly domed, multiphased, partially contaminated granitic body of apparent crustal derivation. Locally, it is a porphyritic quartz monzonite to biotite granite containing large microcline phenocrysts. By modal mineralogy it is an equigranular biotite granite. Biotite is partially altered to chlorite. Hematization and intense alteration of chlorite, silica, and sericite are present.

In cross section, the southern and western parts of the batholith show a gently dipping, granitized contact with the host rock. Aeromagnetic evidence indicates that the intrusion extends at a shallow depth as far south as the Porcupine River (Brosgé and others, 1970). Contaminated black sericite granite with traces of carbonaceous material is typical of the contact region. Abundant replacement tourmaline as rosettes and as a black groundmass suggests boron enrichment in the upper cupola zone. Underlying this contaminated zone is a leucocratic intermediate zone of coarse- to fine-grained quartz monzonite, aplite dikes, and two-mica granite. Within this variable zone, and in conjunction with postintrusive structural features, is much of the mineralization and alteration. The inner core consists of a coarse equigranular to porphyritic quartz monzonite.

Rhyolite-porphyry sills intrude phyllite, argillite, calc-argillite, siltstone, and quartzite on the southern and western edges of the contaminated border zone. The sharp northern contact between the batholith and the quartz-mica schist and quartzite is locally hornfelsed and is garnet and biotite rich.

CHEMICAL CHARACTERISTICS OF THE OLD CROW BATHOLITH

Detailed 44-element chemical analyses of 133 intrusive and contact rocks were performed by neutron activation and X-ray fluorescence in a joint U.S. Bureau of Mines (USBM) - Department of Energy (DOE) analytical program (Stablein, 1980). The data were examined for trace-element levels that would indicate rare-metal potential. The extensive weathering and varied alteration precluded comparison with typical 'tin granites.' Background tin values of 15 to 40 ppm are common in samples with intense chloritic, silicic, and sericitic alteration. Rhyolite sills south of the intrusion did reflect generally higher background amounts of niobium, tantalum, uranium, beryllium, and several other elements; the arithmetic means in 11 rhyolite samples are 70.1, 6.2, 13.7, and 16.4 ppm, respectively. Tin values in the 11 samples ranged from 0 to 698 ppm; up to 0.08 percent tin was found in nearby copper-lead-zinc tactites.

The extremely weathered and eroded granitic surface of the batholith overlies a frozen, impervious layer of clay and clay-rich silts. The frozen material and lack of subsurface water hindered stream-sediment sampling; thus the results are not correlative with mineralization. Tin values of up to 300 ppm in stream-sediment samples are probably due to 'captured' grains of cassiterite. Uranium values were relatively low even in an area of known secondary uranium mineralization.

Sampling of soils brought to the surface in frost boils was generally the most effective geochemical method for isolating mineralized localities. Pathfinder elements such as lead, arsenic, and yttrium appear to correlate with the occurrences of uranium.

Whole-rock and chemical analyses were also performed on splits of 14 typical granite samples from the Old Crow batholith collected by the U.S. Geological Survey in 1967 (table 2). The SiO_2 content averages 76.2 percent and indicates late-stage differentiation.

Table 1. *Potassium-argon age determinations of intrusive rocks, Old Crow Batholith*

Mineral	Sample location	Age (m.y.)	Reference
Biotite	Alaska	314 ± 9	Brosgé, 1969
Muscovite	Alaska	335 ± 10	Brosgé, 1969
Biotite	Alaska	299 ± 9	Brosgé, 1969
Biotite	Alaska	295 ± 9	Brosgé, 1969
Biotite	Canada	220	Baadsgaard and others, 1961
Biotite	Canada	265 ± 12	Wanless and others, 1967
Biotite	Canada	345 ± 10	Bassett and Stout, 1967

Normative quartz averages 42 percent, which equals or exceeds the range indicative of tin granites (Hesp and Rigby, 1974). The tin content of 14 other typical granite samples (table 2) was close to the detection limit of 10 ppm, although 31 altered or sheared, unmineralized granite samples averaged 24 ppm tin.

MINERALIZATION

Mineralization in the Old Crow batholith might be compared with the European Hercynian Orogeny granites that contain uranium- and tin-bearing veins. Within the intermediate or leucocratic zone of the batholith, uranium, tin, and associated base-metals occur with quartz veins, cataclastic zones, and greisen-like alteration.

An excellent example of this type of mineralization occurs along a prominent linear feature that intersects a small, south-flowing tributary of the Rapid River (loc. 1, fig. 2). Feldspars of a cataclastic granite are extensively altered to sericite and muscovite, and finely disseminated secondary hematite is present. The weathered, vuggy surface samples that were examined contained about 0.01 percent uranium and several hundred ppm each of tin, lead, and zinc. Artesian springs in the area periodically emanate anomalous amounts of radon, depending on the season and recent precipitation level.

At the second location (loc. 2, fig. 2), secondary uranium minerals and anomalous concentrations of tin, copper, lead, zinc, and arsenic occur in disseminated pods and as vein and fracture coatings in a leached and sheared quartz vein that extends along a ridge top for about 1,000 ft. X-ray-diffraction analysis revealed the presence of xenotime, uranophane, arsenuranylite, and metatorbernite. Abundant disseminated hematite lends a reddish cast to some quartz veins.

Reconnaissance ground radiometrics and soil sampling identified a number of other localities with possible uranium enrichment. The prospects define an approximate east-west trend that extends to the Canadian border. Location 3 (fig. 2) encompasses a 600- by 2,400-ft tundra-covered area.

Thorium is not present in appreciable amounts at these sites, although heavy-mineral concentrates from streams in the area frequently contain 40 to 65 percent monazite. The source of the rare-earth minerals has not been identified. There is an apparent potential for extensive placer deposits of cassiterite, monazite, and resistant uranium-bearing minerals such as allanite and xenotime, with minor amounts of an unidentified niobium-tantalum-bearing mineral and scheelite. Bulk samples of loose, poorly sorted surface gravels from nearly all active streams that drain the batholith indicate the consistent presence of these minerals in aggregate amounts of about 1 lb/yd^3. Concentrates contained 2 to 25 percent tin, with up to 10 percent thorium and about 0.5 percent tungsten. There has been no drilling or trenching.

Many drainage systems in the area have a low gradient and contain enough water to support a large-scale dredge or dragline operation. Recent uplift removed and disintegrated large quantities of granitic rock, causing the heavy minerals to be reworked and concentrated into placer deposits. Broad valleys containing alluvial-gravel deposits are particularly noticeable along the Rapid River and the main channels of Strangle Woman Creek.

Near the southern margin of the batholith, rhyolite-porphyry sills intrude calc-argillites and hornfels phyllites, and small skarn deposits (loc. 4, fig. 2) are present along the contacts. These deposits contain up to 10 percent copper in the form of chalcopyrite and bornite, with associated galena, sphalerite, and magnetite. Tin (up to 0.08 percent), beryllium, and silver are present in anomalous amounts. Heavy manganese-oxide coatings are common. Although the mineralization could be measured only as thin lenses up to 50 ft in strike length, the area is an obvious geochemical target.

East of this locality, a silicified fracture zone in black phyllite and siltstone contains disseminated chalcopyrite and galena (loc. 5, fig. 2). Mineralization, which rarely exceeds several percent of the combined metal content of copper and lead, occurs as rubble along the fracture zone for about 1,200 ft. Zinc is present in negligible amounts. Apparently the mineralization at these two localities along the southern margin of the batholith is intimately related to the rhyolite-porphyry sills and not to the granites. The relationship between the sills and the batholith is unclear.

Several veins of massive barite occur along the northern contact of the batholith (loc. 6, fig. 2). No sulfides are associated with these veins.

ACKNOWLEDGMENTS

Information for this report was primarily derived from reconnaissance-level mineral investigations conducted by the U.S. Bureau of Mines in east-central Alaska from 1976 to 1980. More detailed information is available in USBM Open-file Report 27-81, 'Mineral investigations in the Porcupine River drainage.' The author acknowledges the previous geologic mapping and whole-rock-sample splits provided by W.P. Brosgé of the U.S. Geological Survey and the petrographic assistance of T.C. Mowatt (USBM). N.K. Stablein (1980) of Bendix Engineers provided analytical support through a DOE contract with the Los Alamos Scientific Laboratory, New Mexico.

REFERENCES CITED

Baadsgaard, H., Folinsbee, R.E., and Lipson, J., 1961, Caledonian or Acadian granites of northern Yukon Territory, *in* Raasch, G.O., ed., Geology of the Arctic: Toronto University Press, p. 458-465.

Table 2. *Chemical analyses (wt %) and CIPW norms of 14 granitic rock samples from the Old Crow batholith.*

	512A	512V	512W	512X	512Y	512Z	514	514B	517	519	520	522	525	527
SiO_2	74.80	73.70	75.20	75.20	74.80	73.40	76.00	74.40	73.40	90.00	73.40	81.90	76.10	75.00
TiO_2	0.11	0.05	0.12	0.13	0.09	0.01	0.08	0.17	0.23	0.00	0.35	0.13	0.08	0.16
Al_2O	13.40	14.80	13.30	12.80	13.60	13.80	12.90	13.30	13.00	5.50	14.00	11.20	13.40	12.70
Fe_2O	1.20	5.50	0.55	0.70	0.50	0.25	0.32	0.70	0.70	0.25	0.80	0.61	0.50	1.30
MnO	0.07	0.10	0.07	0.07	0.03	0.03	0.07	0.07	0.03	0.03	0.07	0.00	0.07	0.06
MgO	0.35	0.13	0.19	0.25	0.16	0.13	0.28	0.40	0.50	0.19	0.86	0.42	0.28	0.28
CaO	0.66	0.20	0.86	0.49	0.79	0.20	0.62	0.33	0.92	0.00	1.20	0.10	0.66	0.89
Na_2O	2.50	1.90	2.60	3.00	2.60	2.10	2.80	2.40	2.40	0.73	2.30	0.10	2.80	2.30
K_2O	4.30	0.35	5.10	4.50	6.30	8.70	6.80	5.40	4.80	1.70	4.80	3.70	4.50	4.60
P_2O_5	0.02	0.00	0.01	0.05	0.01	0.03	0.01	0.03	0.03	0.03	0.08	0.04	0.03	0.06
H_2O+	0.97	1.10	0.82	0.92	0.87	0.68	0.80	1.20	1.10	0.57	1.10	1.30	0.73	0.89
H_2O-	0.03	0.10	0.09	0.07	0.08	0.06	0.08	0.14	0.19	0.05	0.18	0.12	0.16	0.21
CO_2	0.03	0.02	0.03	0.02	0.02	0.04	0.04	0.03	0.03	0.02	0.05	0.02	0.04	0.02
FeO	0.88	0.64	0.92	0.96	0.92	0.44	0.52	1.20	2.20	0.24	2.20	0.72	1.00	0.76
Total	99.32	98.59	99.86	99.16	100.77	99.87	101.32	99.77	99.53	99.31	101.39	100.36	100.35	99.23
						Elemental analysis (ppm)								
Ba	-113	-98	-114	-142	-103	-91	-122	-124	-116	-91	304	104	-141	204
Ca	3034	-728	5836	4934	4500	-643	-1032	2446	7570	-431	8450	-434	4541	7889
Fe	7351	18140	6392	6331	5755	2937	7463	6928	13040	2015	11870	6130	5947	7316
K	26980	-2300	38450	30120	40170	59590	33630	35770	30860	16280	32810	23630	32620	29680
Li	58	25	28	83	35	28	65	56	115	28	106	22	46	78
Mg	-3288	-2619	-3365	-4237	-3243	-2864	-3512	-3705	5909	-1821	7402	3141	-4094	-2881
Mn	305	387	240	251	241	98	281	385	389	108	403	18	320	251
Na	15070	9716	16910	18630	16510	13220	17610	18060	16680	2094	15230	345	18230	14900
Nb	-20	-20	-20	-20	-20	-20	-20	-20	-20	23	24	-20	-20	-20
Pb	28	-5	32	16	22	36	33	33	15	-5	37	-5	37	28
Rb	121	-22	115	116	104	165	152	128	112	105	102	120	149	112
Sn	-10	16	-10	-10	-10	-10	-10	-10	-10	-10	11	-10	-10	-10
Sr	-248	-222	-247	-291	-227	-186	-263	-274	-258	-160	-290	-118	-293	-207
Ta	-1	2	-1	-1	-1	-1	1	1	1	-1	-1	-1	-1	-1
Th	16.4	4.5	34.8	18.1	28.0	7.9	31.5	27.5	58.5	4.3	23.9	18.5	19.5	22.4
Ti	-591	-522	-586	-699	-550	-442	-633	1050	1556	-394	2360	514	-708	825
U	3.44	1.99	3.45	5.27	3.62	1.18	6.06	7.48	8.53	1.87	5.78	2.63	4.03	3.59

CIPW norms

qtz	40.14	60.44	36.20	37.20	31.22	25.65	29.70	36.38	35.67	78.33	34.76	64.93	38.17	40.41
or	26.37	2.22	30.98	27.52	37.81	52.40	40.46	33.01	29.47	10.76	28.90	23.14	27.18	28.34
ab	23.30	18.33	24.00	27.88	23.72	19.22	25.32	22.30	22.39	7.02	21.04	0.95	25.70	21.54
an	3.07	0.93	4.13	2.05	3.79	0.55	2.57	1.30	4.34	0.35	5.21	0.11	2.89	4.06
di	0.00	0.00	0.00	0.00	0.00	0.00	0.17	0.00	0.00	0.00	0.00	0.00	0.00	0.00
hy	1.51	0.39	1.55	1.68	1.46	0.92	1.22	2.43	4.25	0.82	4.94	1.77	2.02	0.95
mt	1.30	1.74	0.59	0.76	0.53	0.27	0.34	0.76	0.76	0.28	0.85	0.68	0.53	1.42
il	0.16	0.07	0.17	0.19	0.13	0.01	0.11	0.25	0.33	0.00	0.50	0.19	0.11	0.23
ap	0.04	0.00	0.02	0.11	0.02	0.06	0.02	0.06	0.07	0.07	0.17	0.09	0.06	0.13
cc	0.08	0.05	0.08	0.05	0.05	0.10	0.10	0.08	0.08	0.05	0.13	0.05	0.10	0.05
hm	0.00	2.96	0.00	0.00	0.00	0.00	0.00	0.00	0.00	0.00	0.00	0.00	0.00	0.00

Analyses by Los Alamos Scientific Laboratory, New Mexico. U by delayed neutron counting; Nb, Pb, Sn by X-ray fluorescence; Li by arc-source emission spectrophotometry; all others by neutron activation. (-) indicates value below individual sample-matrix-detection level. Sample splits provided by W.P. Brosgé.

Barker, J.C., 1981, Mineral investigations in the Porcupine River drainage: U.S. Bureau of Mines Open-file Report 27-81, 189 p.

Bassett, H.G., and Stout, J.G., 1967, Devonian of western Canada, *in* Oswald, D.H., ed., International Symposium on the Devonian System, Calgary, 1967: Alberta Society of Petroleum Geologists, v. 1, p. 717-752.

Brosgé, W.P., 1969, Preliminary geologic map of the Coleen Quadrangle, Alaska: U.S. Geological Survey Open-file Map 370.

Brosgé, W.P., Brabb, E.E., and King, E.R., 1970, Geologic interpretation of reconnaissance aeromagnetic survey of northeastern Alaska: U.S. Geological Survey Bulletin 1271-F, p. F1-F14.

Dillon, J.T., Pessel, G.H., Chen, J.H., Veach, N.C., 1979, Tectonic and economic significance of Late Devonian and Late Proterozoic U-Pb zircon ages from the Brooks Range, Alaska, *in* Short Notes on Alaskan Geology - 1978: Alaska Division of Geological and Geophysical Surveys Geologic Report 61, p. 36-41.

Hesp, W.R., and Rigby, D., 1974, Some geochemical aspects of tin mineralization in the Tasman geosyncline: Mineralium Deposita, v. 9, p. 49-60.

Sable, E.G., 1977, Geology of the western Romanzof Mountains, Brooks Range, northeastern Alaska: U.S. Geological Survey Professional Paper 897, p. 81.

Stablein, N.K., 1980, Report on mineral resource investigations in six areas of central and northeastern Alaska: Bendix Field Engineering Corporation for U.S. Department of Energy, DOE Open-file Report GJBX-33(80), 186 p.

Wahrhaftig, Clyde, 1965, Physiographic divisions of Alaska: U.S. Geological Survey Professional Paper 482, 52 p.

Wanless, R.K., Stevens, R.D., Lachance, G.R., and Edmonds, C.M., 1967, Age determinations and geological studies - K-Ar isotopic ages, report 7: Canada Geological Survey Paper 66-17, 120 p.

A RECENT EARTHQUAKE ON THE DENALI FAULT IN THE SOUTHEAST ALASKA RANGE

By Larry Gedney[1] and Steven Estes[1]

INTRODUCTION

Alaska's Denali fault is probably the best documented fault system in the state. Unquestionably, it has the most striking topographic expression of all the large-scale, strike-slip faults in Alaska; its deeply incised fault-line valley can be traced for several hundred kilometers through the Alaska Range and southeast into the Shackwak Valley and Yukon Territory, Canada (Forbes and others, 1976).

On April 2, 1981, an earthquake of magnitude 4.4 occurred in the southeastern Alaska Range on a segment of the fault previously thought to be seismically dormant. Because the earthquake epicenter was located about 50 km from the Alaska Highway---and the proposed natural-gas-pipeline route---modification of current estimates of seismic risk in adjacent areas may be necessary.

SEISMICITY OF THE SOUTHEAST DENALI FAULT DURING HISTORIC TIME

According to Tobin and Sykes (1966), only one earthquake---on August 31, 1958---was recorded in the southeast segment of the Denali fault from 1954 to 1964. A very low level of seismicity has been recorded in the area since 1966, when the University of Alaska Geophysical Institute established the central Alaska seismic network.

In 1967, Boucher and Fitch (1969) conducted a microearthquake survey along portions of the Denali fault from Haines to Mt. McKinley. Although they noted microearthquakes at all sites, the tremors were generally too small to be detected or located by a regional network. Because these authors did not occupy a site within 100 km of the April 2 earthquake, there are no data on background seismic activity for the area.

LATERAL OFFSET ON THE DENALI FAULT

Lateral offset during historic time, whether earthquake-generated or related to fault creep, is not satisfactorily documented along the Denali fault (Page and Lahr, 1971; Page, 1972; Savage, 1975). Estimates of Holocene right-lateral offset range from 50 m near the Delta River (Stout and others, 1973) to 350 m west of Mentasta Pass (Richter and Matson, 1971), and estimates of Pleistocene offset by these authors range from 3 to 6.5 km. On the basis of petrological, structural, and geochronologic evidence, Forbes and others (1974) proposed a 400-km offset along the northeast-central Denali fault since Early Cretaceous time. Richter and Matson (1971) specifically stated that the epicentral area between the Nabesna and Chisana Rivers was one of the few localities in the eastern Alaska Range where they did not observe evidence for Holocene lateral movement on the Denali fault.

THE APRIL 2, 1981 EARTHQUAKE

On April 2, 1981, at 0615 local time, an earthquake of magnitude 4.4 occurred on the southeast Denali fault. The earthquake was felt at Northway, about 65 km from the epicenter, where one resident reported his wood stove rocked back and forth. According to the local store owner, the earthquake was felt by several other persons in the area.

The earthquake was recorded at 83 different seismographic stations in Alaska and Canada. Because scaling difficulties increase with distance, only the 43 stations within a 450-km radius of the epicenter were used to locate the focus at lat. 62.43° N., long. 142.04° W., and 8 km below ground level (fig. 1). The computer solution indicates an uncertainty in epicentral location of 6 km and a possible depth range of from 0 to 20 km.

A 'fault-plane' or 'focal-mechanism' solution of the earthquake is shown in figure 2. Although readings were obtained from more than 80 stations, only 37 had clear enough 'first arrivals' to include in the solution. The stereographic plot indicates the positions where primary longitudinal waves from the earthquake begin their travel to each of the observing stations; refraction of the ray along its path is considered. Most earthquakes generate a quadrant distribution of initial P-wave compressions and dilatations, and these initial impulses are believed to maintain their original sense of motion along their entire travel path (Byerly and Stauder, 1957). For an ideal strike-slip earthquake, the region surrounding the epicenter is divided into four quadrants separated by vertical planes that intersect at right angles and pass through the focus. Stations in adjacent quadrants alternately receive initial compressional or dilatational impulses, depending on whether they are located ahead of or behind the throw of the fault.

[1]Geophysical Institute, University of Alaska, Fairbanks, 99701.

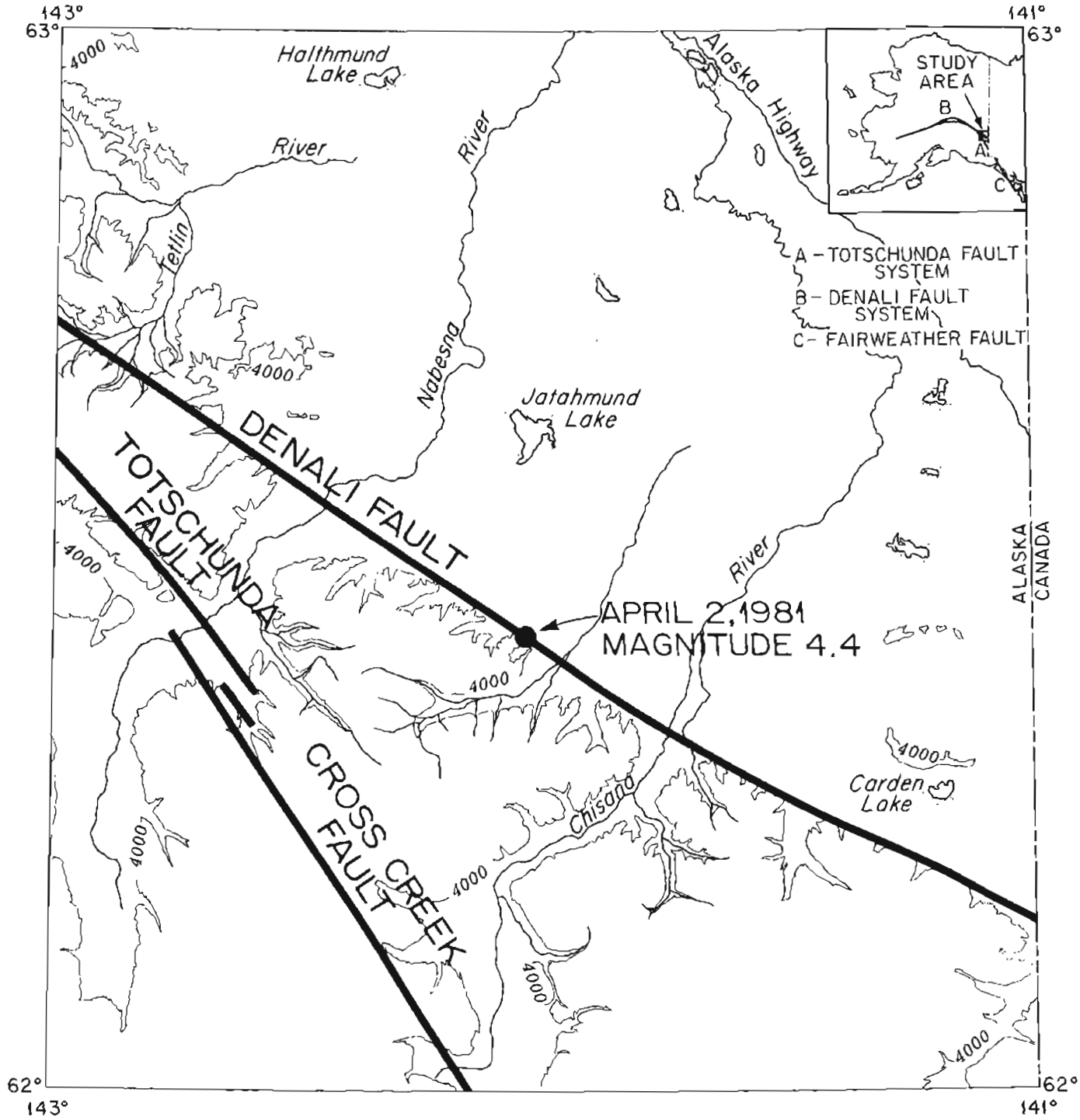

Figure 1. Location of epicenter of April 2, 1981 earthquake on the Denali fault, Alaska. Regional relationships with other interacting fault systems are shown in insert; the Cross Creek fault is part of the Totschunda fault system.

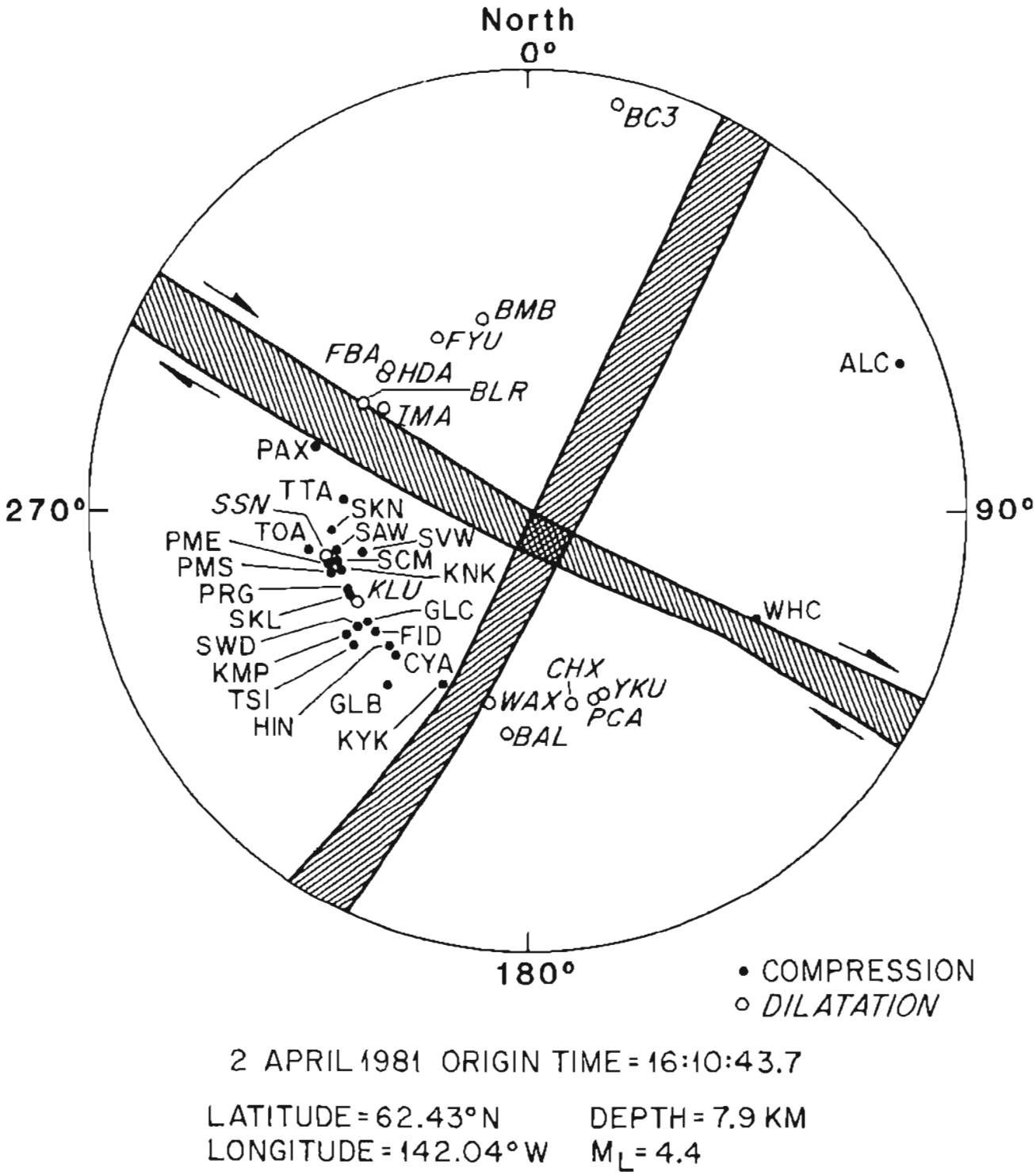

Figure 2. Fault-plane solution of April 2, 1981 earthquake on the Denali fault, Alaska. Cross-hatched areas mark error limits of nodal planes. Their apparent awkward configuration results from use of the Wulff equal-angle net. Inconsistent observations at stations SSN and KLU may be due to a combination of incorrect station calibration, scaling error, and other factors.

Without more sophisticated diagnosis, it is not possible to distinguish which plane represents the fault and which plane represents the perpendicular 'auxiliary plane.' Generally, an identification can be made by reference to the tectonic setting.

Possible solutions in figure 2 are a) left-lateral offset on a fault trending northeast-southwest, or b) right-lateral offset on a fault trending northwest-southeast. The latter solution is probably applicable because the trend of the northwest-southeast-striking plane (N. 60° W. $\pm$ 5°) parallels the Denali fault (Richter and Matson, 1971).

DISCUSSION

Richter and Matson (1971) note a marked decrease in Holocene fault activity southeast of Mentasta Pass and recognize the Totschunda fault as a possible new transcurrent fault connecting major strike-slip systems (including the Fairweather fault) in southeast Alaska. In fact, the Totschunda fault may be shunting lateral motion that was previously absorbed by the Denali fault near Mentasta Pass. The April 2 earthquake, however, seems to provide evidence that not all horizontal displacement is occurring along the Totschunda fault, and that this segment of the Denali fault may be more active than previously recognized.

ACKNOWLEDGMENTS

We express our appreciation to D.B. Stone, J.F. Meyer, R.D. Reger, and R.B. Forbes for their critical reviews and valuable suggestions and to D.L. Marshall for assistance in analyzing and processing the data. We also wish to thank the U.S. Geological Survey at Menlo Park, the Alaska Tsunami Warning Center at Palmer, and the Earth Physics Branch of the Department of Energy, Mines, and Resources in Ottawa, Canada, for providing their station data. This research was supported by State of Alaska funds appropriated to the Geophysical Institute, University of Alaska, Fairbanks.

REFERENCES CITED

Boucher, Gary, and Fitch, T.J., 1969, Microearthquake seismicity of the Denali fault: Journal of Geophysical Research, v. 74, p. 6638-6648.

Byerly, Perry, and Stauder, W.V., 1957, Motion at the source of an earthquake: Publications of the Dominion Observatory, v. 20, no. 2, p. 255-261.

Forbes, R.B., Pulpan, Hans, and Gedney, Larry, 1976, Seismic risk and the Denali fault: Prepared for Gulf Interstate Engineering Company, Geophysical Institute, University of Alaska, 52 p.

Forbes, R.B., Smith, T.E., and Turner, D.L., 1974, A solution to the Denali fault offset problem: Alaska Division of Geological and Geophysical Surveys Annual Report, 1973, p. 25-27.

Page, R.A., and Lahr, John, 1971, Measurements of fault slip on the Denali, Fairweather, and Castle Mountain faults, Alaska: Journal of Geophysical Research, v. 76, p. 8534-8543.

Page, R.A., 1972, Crustal deformation on the Denali fault in Alaska 1942-1970: Journal of Geophysical Research, v. 77, p. 1528-1533.

Richter, D.H., and Matson, N.A., 1971, Quaternary faulting in the eastern Alaska Range: Geological Society of America Bulletin, v. 82, p. 1529-1540.

Savage, J.C., 1975, Further analysis of the geodetic strain measurements on the Denali fault in Alaska: Journal of Geophysical Research, v. 80, p. 3786-3790.

Stout, J.H., Brody, J.B., Weber, F.R., and Page, R.A., 1973, Evidence for Quaternary movement on the McKinley strand of the Denali fault in the Delta River area, Alaska: Geological Society of America Bulletin, v. 84, p. 939-947.

Tobin, D.G., and Sykes, L.R., 1966, Relationship of hypocenter of earthquakes to the geology of Alaska: Journal of Geophysical Research, v. 71, p. 1659-1667.

TRIASSIC PALEOMAGNETIC DATA AND PALEOLATITUDES FOR WRANGELLIA, ALASKA

By D.B. Stone[1]

INTRODUCTION

In the early 1970s, it became apparent from both geological evidence (Jones and others, 1972) and paleomagnetic data (Packer and Stone, 1972) that at least parts of Alaska had moved relative to North America. Similar conclusions were also drawn for parts of western Canada (Monger and Ross, 1971; Irving and Yole, 1972).

The subsequent compilation of a considerable amount of basic information---including the paleomagnetic data for Alaska by Stone and Packer (1977, 1979), Stone and others (1981), Panuska and Stone (1981), Hillhouse (1977), and Van der Voo and others (1980)---supports the theory of relative movement between Alaska and the rest of North America. Much of the paleomagnetic data (Beck, 1980) from western North America can be explained according to this theory. Along with the recognition that large-scale relative motion had occurred in Alaska and western North America, came the awareness that the areas involved were composed of many geologically distinct terranes. These terranes have different stratigraphies, and where observed, the boundaries between them are tectonic. Currently, in excess of 50 tectonostratigraphic terranes have been delineated in Alaska and adjacent parts of Canada (Jones and Silberling, 1979; Jones and others, 1981).

A key terrane in Alaska is Wrangellia, defined by Jones and others (1977) and shown in figure 1. Wrangellia is not confined to Alaska; areas of British Columbia and northwestern continental U.S. as far south as eastern Oregon are involved.

Paleomagnetic data from the Middle or Upper Triassic Nikolai Greenstone of the Wrangell Mountains (Hillhouse, 1977) and the correlative Karmutsen Volcanics of Vancouver Island (Irving and Yole, 1972) show that at time of extrusion the terrane was in equatorial latitudes. Low paleolatitudes have also been determined for other southern Alaska terranes (Stone and others, 1981).

[1]Geophysical Institute, University of Alaska, Fairbanks, Alaska 99701.

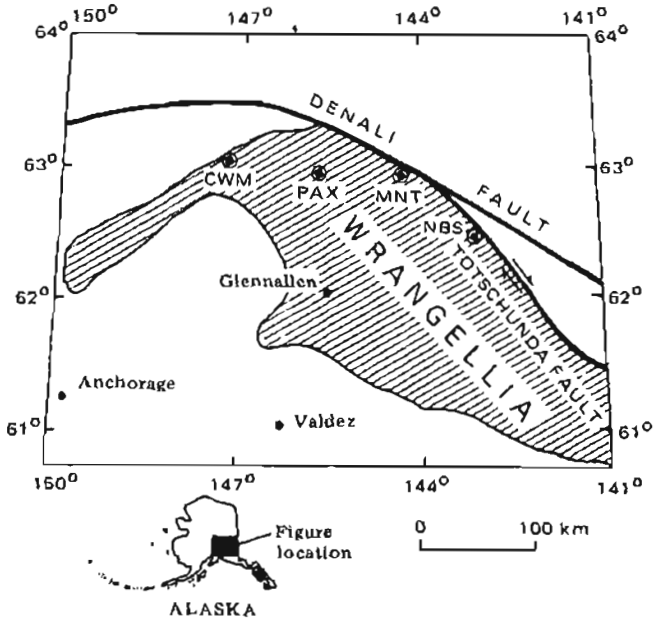

Figure 1. Wrangellia tectonostratigraphic terrane in Alaska. Sampling localities include Clearwater Mountains (CWM), Mentasta Mountains (MNT), Nabesna area (NBS), and Paxson Mountain (PAX).

PALEOMAGNETIC SAMPLE COLLECTIONS FROM WRANGELLIA

Since 1965, several collections of samples for paleomagnetic work were made from Wrangellia. All samples were collected as 2.5-cm-diameter cores drilled in the field. The cores were oriented by sighting on known geographic features, by sun compass, and (rarely) by magnetic compass alone.

Magnetizations were measured at the University of Alaska (Fairbanks) with a Foster spinner (Foster, 1966) or Schonstedt SM-1 magnetometer, or at the Woodward-Clyde and Associates paleomagnetic laboratory (Oakland, California) with a superconducting magnetometer. All samples were 'cleaned' with successively higher alternating magnetic fields.

The paleomagnetic data collected in the 1960s and early 1970s were difficult to interpret because of the prevalent concept of a fixed geography for the sampling areas. As a result of the recent acceptance of large-scale reorganizations of paleogeographies and the publication of the Triassic Wrangellia paleomagnetic pole (Hillhouse, 1977) based on the Nikolai Greenstone, older collections

have been remeasured and reinterpreted.

Because many of the lithologies, and hence magnetic properties, differ according to locality, not all samples react similarly to alternating demagnetization techniques. To select the best demagnetization level for a given site in a locality, a 'closest approach' technique was used (Stone and Packer, 1979). For a given sample, this involves selecting the demagnetization level that represents the resultant magnetic vector that could plausibly be the primary component and lies closest to the mean of the other samples. When enough demagnetization levels were available, the primary component was chosen on the basis of a Zijderveld plot (Zijderveld, 1967); only vectors on a path through the origin were selected.

PALEOMAGNETIC DATA

Mean data points for each locality described below and listed in tables 1-4 are calculated as:

a. A magnetic vector direction with respect to present north and present horizontal, that is, in a present geographic reference frame. If the present magnetic field lies within the confidence limits of this mean, a *flag* warns that samples here may have been remagnetized in the present field.

b. A magnetic vector direction with respect to present north and ancient horizontal, that is, in a stratigraphic reference frame. Ancient horizontal is determined by such indicators as bedding planes and compositional layering, as noted in the text. From the inclination of this vector, the magnetic paleolatitude of a site is easily calculated.

c. Paleomagnetic pole positions, which are locations of one end of the axis of the geocentric dipole that would have produced the observed paleomagnetic vector direction.

CLEARWATER MOUNTAINS (CWM)

The Clearwater Mountains are geologically and structurally complex, and consist of Cretaceous gneiss, schist, slate, and intrusive rocks and Jurassic argillite and associated metasedimentary rocks. Triassic metavolcanic rocks considered to be Nikolai Greenstone equivalents are also preserved. Flow units in the latter sequence were sampled for paleomagnetic measurements at two localities. The assignment of a Karnian (Upper Triassic) age is based on fossil evidence found in a limestone pod on strike with the flow units (T.E. Smith, 1979, oral commun.; Smith, 1981; Smith and Turner, 1973).

Table 1. *Clearwater Mountains; 2 localities*[a], *6 sites*[b]
(no measurements rejected)

	Geographic Vector[e] D	I	N[h]	Stratigraphic Vector[f] D	I	k[i]	α95[i]	VGP[g] φ	λ
CWM-1; long.[c] 213.0°; lat.[d] 63.1°									
flow 1	30	-4	7	36	-26	9.4	20.8	358	8
flow 2	40	4	7	42	-15	12.4	17.8	350	12
CWM-2; long. 213.2°, lat. 63.2°									
flow 1	348	-79	6	73	-33	19.8	15.4	327	-8
flow 1a[j]	234	-76	2	102	-49	11.0	29.8	307	-32
flow 2	19	-58	3	57	-23	281.9	7.3	338	3
flow 3	44	-74	3	78	-20	145.2	10.3	318	-4
CWM-1+CWM-2 Mean	30	-53	6	62	-29	11.7	20.4	334	-2

[a]Sampled area where rocks demonstrably belong to integral unit.
[b]Point in time, such as a single flow unit.
[c]Average longitude of site.
[d]Average latitude of site.
[e]Declination (D) and inclination (I) of magnetic vector before correction for dip.
[f]Declination (D) and inclination (I) of magnetic vector with respect to ancient horizontal.
[g]Virtual geomagnetic-pole longitude (φ) and latitude (λ) of pole position corresponding to stratigraphic vectors.
[h]Number of samples.
[i]Statistical parameters defined by Fisher (1953) and calculated for stratigraphic vectors.
[j]Opposite polarity from flow 1.

Table 2. *Mentasta Mountains; 3 localities, unknown number of sites over 200 m of vertical section*

MNT-1, -2, -3; long. 216.1°, lat. 62.96°

	Geographic Vector			Stratigraphic Vector				VGP	
	D	I	N	D	I	k	α95	ϕ	λ
MNT-1 (6m section)	73	-51	6	97	-56	80.8	7.5	318	-35
MNT-2[a] (10m section) A	81	27	8	77	-12	28.6	10.5	320	0
B	103	-35	12	145	-52	8.5	15.8	269	-53
MNT-3 (40m section)	95	60	16	76	20	21.0	8.2	314	16
Mean (excluding B data)	82	15	3	81	-16	4.4	38	318	-3
	85	34	30	79	-3	6.0	11.7	317	3

[a]MNT-12 is divided into two groups; MNT-2B is not included in final mean because it is more discordant than rejection criteria allow.

Table 3. *Nabesna; 2 localities, + 11 sites*

NBS-2; Lost Creek; long. 216.9°, lat. 62.6°; 8 m stratigraphic section; number of flows not determined

	Geographic Vector			Stratigraphic Vector				VGP	
	D	I	N	D	I	k	α95	ϕ	λ
Combined data	139	5	11	152	40	50.2	6.5	243	-2
NBS-5, -6, -7 Skookum Creek; long. 217°, lat. 62.4°									
NBS-5									
flow 5.1	290	82	3	278	57	19.6	28.6	140	36
flow 5.2	163	-34	2	163	-34	43.0	39.0	240	-45
flow 5.3	346	-1	3	348	-8	47.0	18.2	50	23
flow 5.4a	203	-31	1	187	-35	--	--	207	-47
flow 5.4b	13	-42	1	32	-34	--	--	7	5
flow 5.5a	0	-54	2	32	-49	90.8	26.5	9	-6
flow 5.5b	166	-38	1	151	-27	--	--	253	-38
flow 5.6	203	44	2	221	32	12.4	78	178	-4
flow 5.7	4	26		352	23	238	8	47	39
NBS-6									
flow 6.1	55	-54	4	68	-33	129.2	8.1	334	-6
flow 6.2	18	10	4	13	14	33.4	16.1	21	34
NBS-7									
flow 7.1	351	76	3	292	60	31.6	22.3	131	44
Mean[a] normal (N-up VGP)	10	21	5	9	-11	9.1	26.8	25	20
Mean reversed (S-up VGP)	183	-18	4	180	-19	5.6	42.7	217	-38
Mean normal + reversed	7	-5	9	5	2	7.3	20.5	30	28

[a]Final means exclude flows 5-1 and 7-1, which are considered to represent present field, and flow 6.1, which is more discordant than rejection criteria allow. Statistics on final means are for VGP's; remaining statistics are for stratigraphic vectors.

Table 4. *Paxson; 1 locality, 7 sites*

PAX; long. 214.3°, lat. 63.1°

	Geographic Vector			Stratigraphic Vector				VGP	
	D	I	N	D	I	k	α95	φ	λ
flow 1	106	12	3	103	4	21.3	27.4	292	-4
flow 2	102	14	2	103	-7	13.8	73.5	294	-9
flow 3[a]	289	75	4	354	69	145.2	7.6	54	79
flow 4	110	1	2	111	-5	58.2	33	286	-12
flow 5	101	6	3	101	-3	34.4	21.3	295	-6
flow 6	22	76	3	31	56	175.6	9.3	344	57
flow 7	78	45	2	69	29	115.7	23.4	316	23
Mean of flows 1,2,4,5	105	6	4	104	-2	155	7.4	292	-8

[a]Flows 3,6,7 were rejected; 3 and 6 are close to present field; flow 7 is more discordant than rejection criteria allow.

PALEOMAGNETIC DATA (CWM;1, -2)

These samples were collected and measured in 1972; new measurements and new statistics were calculated in 1979.

Although the length of time represented by this collection from six flow units is difficult to reliably estimate, the stratigraphic thickness (50 m) may indicate a sufficiently long time span to average secular variation of the field. The small number of sites for the two localities is probably the major contributor to the spread of the magnetic directions. What was originally called flow 1 from locality CWM-2 was subdivided into flows 1 and 1a on the basis of a polarity change. This subdivision does not conflict with the geology, because flow boundaries are not clearly defined in the exposures. The localities are about 6 km apart and approximately on strike with one another. The magnetic stability of the flows is indicated by the fact that both polarities of field are present (CWM-2, flow 1a).

To obtain the mean-flow direction for the final analysis, the closest approach of all samples was used. The flowmeans and overall mean are shown in figure 2 and the basic information is shown in table 1.

MENTASTA MOUNTAINS (MNT)

The Mentasta Mountains are divided into two geologic provinces by the Denali fault. North of the fault the section consists of regionally metamorphosed sedimentary rocks, which generally dip steeply to the southwest. South of the fault the rocks are very weakly metamorphosed and dip at moderate angles to the northeast. Paleomagnetic samples were taken from Triassic amygdaloidal basalts mapped as Nikolai Greenstone (Richter, 1967, 1976) that crop out south of the fault and uncomformably overlie the Permian Mankomen Formation, which consists of argillite, shale, limestone, and chert. The Nikolai Greenstone is conformably overlain by massive limestone, limy siltstone, and sandstone of probable Late Triassic age (Richter, 1976).

The Triassic basalts form a ridge approximately 8 km west-northwest of Mentasta Village; exposure is intermittent. Paleomagnetic samples were collected from three localities along the ridge. No interbedded sediments were observed, and the attitude of the flow units was determined from vesicular layering. The internal consistency of the attitude of this banding and its similarity to that of the adjacent sediments are strong indicators that it represents ancient horizontal.

PALEOMAGNETIC DATA (MNT)

Original paleomagnetic measurements on these samples are reported by Packer (1972). Additional demagnetization levels were applied to the original data, and figure 2 shows the means of all data as selected by the closest-approach methods. At locality MNT-2, two discrete sets of vector direction were subdivided into sample sets A and B (top and bottom of section, respectively). However, several samples indicated both directions during demagnetization, and we conclude that two components of magnetization were present. Because the B directions were discordant with respect to other localities, they are not included in the final mean. Locality means are shown because it was not possible to accurately identify the number of flow units at each locality. The mean of both localities and samples and the sample mean used in the final compilation are shown in table 2.

NABESNA (NBS)

Samples were obtained from three localities in the Triassic Nikolai Greenstone (Richter, 1976). In the Nabesna area, the formation underlies Triassic limestone containing subordinate interbeds of banded sandstone and siltstone, calcareous siltstone, silty

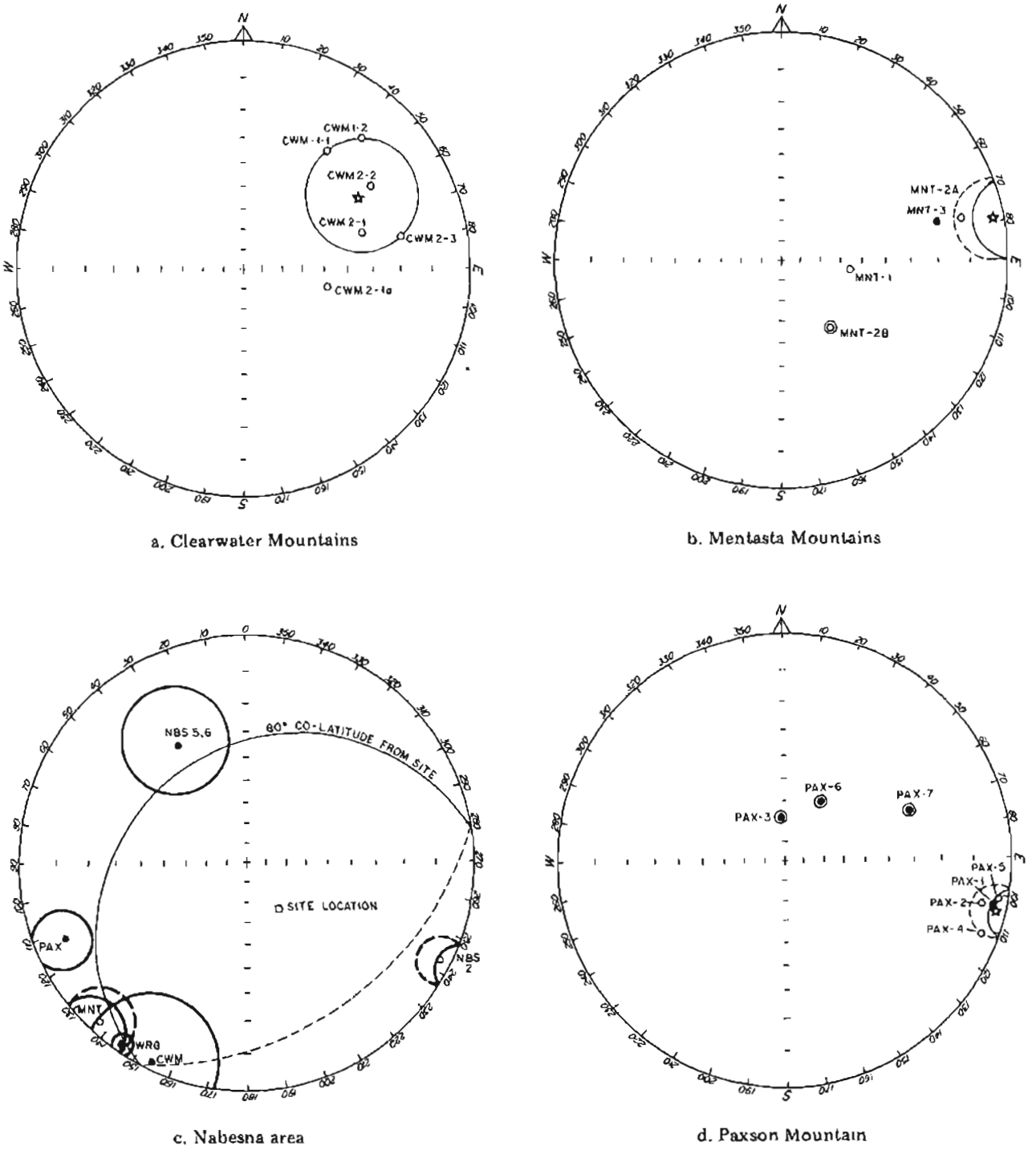

a. Clearwater Mountains

b. Mentasta Mountains

c. Nabesna area

d. Paxson Mountain

Figure 2. Paleomagnetic data for Clearwater Mountains, Mentasta Mountains, Nabesna area, and Paxson Mountain.

limestone, and calcareous mudstone.

Locality NBS-2 is located about 9 km north of the Nabesna road on the east side of Lost Creek; the rocks dip about 45° NW (Packer 1972). Localities NBS-4, -5, and -7 are located on Skookum Creek near Devil's Mountain Lodge. The attitudes of sites NBS-5 and -7 were determined from a distinctive purple-red-shale unit interbedded with the flows.

PALEOMAGNETIC DATA (NBS)

Initial results for NBS-2 and -4 are reported in Packer (1972) and Chantry-Price (1967), respectively; results from NBS-5 and -7 are not previously reported. The NBS-2 and -4 data have been reevaluated. The results and mean of the NBS-2 reevaluation and the data from NBS-5, -6, and -7 are shown in table 3 and in figure 2. The latter data show both normal and reversed polarities that are antiparallel within their confidence limits. Data selection was based on the closest-approach technique. In addition, flows 5.1 and 7.1 were rejected because they are magnetized along the present field, and flow 6.1 was rejected because it was beyond the discordance cutoff of 40°.

PAXSON MOUNTAIN (PAX)

Paxson Mountain, located near the junction of the Richardson and Denali Highways, was mapped by Stout (1976) as a gray-green to olive metabasalt he calls the Paxson Mountain Basalt. He considers it lowermost Mesozoic in age, and probably equivalent to the Nikolai Greenstone. Numerous dacite porphyry dikes of Tertiary age cut the basalt.

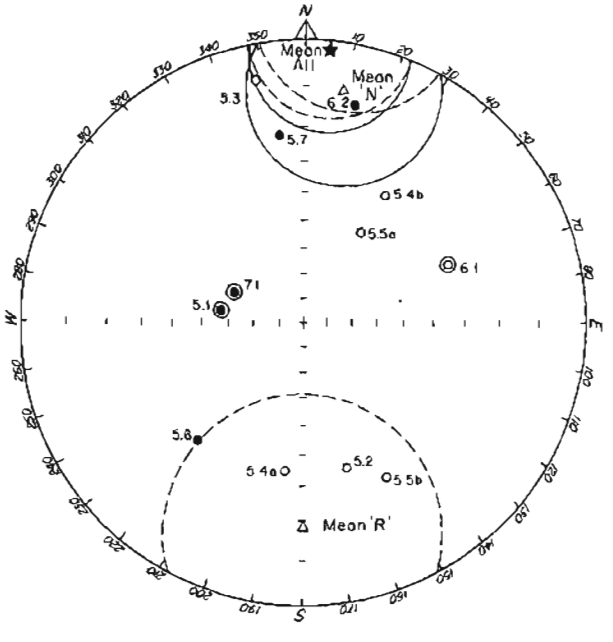

Figure 3. Polar stereographic projection of mean virtual geomagnetic poles and mean pole (WRG) of Hillhouse (1977). Circles of confidence are at 95 percent level (Fisher, 1953).

Three to six samples were collected from each of a series of seven flows exposed near the Denali Highway. Accurate attitudes were difficult to obtain, but the flows were estimated to dip at about 20° NE (38° east of north), which compares favorably with attitudes mapped by Stout (1976).

PALEOMAGNETIC DATA (PAX)

The original measurements on these cores are reported by Chantry-Price (1967). Additional demagnetization levels have been measured and the statistics recalculated using the closest-approach method.

Of the seven flows, four show consistency and shallow inclination for the magnetic vector. Three steeply magnetized flows displayed erratic behavior during demagnetization, and two of these approximate the present field direction. Therefore, the data from these three flows were not included in the final mean. Figure 2d shows the individual combined flow mean; locality information is listed in table 4.

RECONSTRUCTION

Paleogeographic reconstructions are traditionally formed by the superposition of paleomagnetic poles of the same age. According to the dipole hypothesis, only one pair of poles can exist at any given time. Thus, if the poles from different areas are separated, relative motion between them is implied. Superposition of the poles yields the relative paleolatitude of two areas, but does not constrain their relative longitudes with respect to the paleomagnetic pole.

In addition to the problems of constraining paleolongitude, there is also an inherent uncertainty in the location of the paleopole position for any given locality. First, any tilting of the ancient horizontal is assumed to have occurred as a simple rotation---which can be similarly corrected---about the present strike of bedding. Thus, any tectonic activity that produces more than one axis of folding or tilting can introduce serious errors in the paleomagnetic pole positions. Second, local rotation of tectonic blocks about a vertical axis---as might be expected for blocks caught between two transcurrent faults---will be seen as a dispersion of the paleomagnetic poles.

In contrast, paleomagnetic-latitude data are derived solely from the inclination of the magnetic vector relative to ancient horizontal.

The mean paleomagnetic pole positions for the sampled localities and the approximate location of the area sampled [with an enclosing circle of equal colatitude (80°)] are shown in figure 3.

If the paleolatitude derived from the paleomagnetic data is the same for each site, then the paleomagnetic

Table 5. *Summary of paleomagnetic vectors and equivalent pole positions.*

	N	Stratigraphic Vector D	I	k	α95	VGP φ	λ	Paleo-λ p. λ
CWM-1,-2	6	62	-29	11.7	20.4	334	-2	4:15:30
MNT-1,-2,-3	30	79	-3	6.0	11.7	317	3	-8:-1:4
NBS-2	11	152	40	50.2	6.5	243	-2	18:23:28
NBS-5,-6	9	5	2	7.3	20.5	30	28	-10:1:11
PAX	4	104	-2	155	7.4	292	-8	4:1:2
WRG[a]	50	255	21	18.3	4.8	146	2	8:11:14
Mean VGP excluding NBS-2,-5,-6	4	259	3	19.0	21.6	137	-2	-13:-2:10

[a]Data from Hillhouse (1977).

poles will fall on the same small circle of colatitude. The scatter of poles around that circle of equal colatitude can be caused by tectonic rotation or by multiple tilting of the locality.

In figure 3, marked longitudinal scatter of paleomagnetic poles is coupled with a consistent grouping. Both the widespread geographic distribution of sampling localities and the fact that the two most discordant localities at Nabesna (NBS) are very close to the Totschunda fault system (with its additional potential for local rotation), indicate that the grouping represents a mean pole. The mean and circles of confidence of the pole have been calculated with Fisher statistics (Fisher, 1953), although strictly speaking they apply only to circular distributions of vector directions. Thus, the quoted error limits should be used only as guides and not as an accurate assessment of the confidence limits.

Because the polarity of the sampled field is unknown, the paleomagnetic pole positions for the new data in tables 1-4 are listed in the central Atlantic Ocean (~long. 320°), but the overall mean pole listed in table 5 is in the southwest Pacific Ocean (~long. 140°). On the basis of evidence from Permian-age rocks (Panuska and Stone, 1981), the southwest Pacific Ocean is the preferred location for the ancient pole position equivalent to today's magnetic north pole.

CONCLUSIONS

The mean poles in table 5 indicate that Wrangellia must have been very close to, and probably north of the equator when the basalt that forms the Nikolai Greenstone was erupted. These data substantiate the conclusion of Hillhouse (1977) and fit well with data from older (Panuska and Stone, 1981) and younger (Stone and others, 1981) rocks. The combined data suggest southward latitudinal motion between Permo-Triassic and Middle Jurassic time, followed by a systematic northward motion of Wrangellia from about Middle Jurassic time to the present.

This systematic south-then-north motion, if real, is critical to the interpretation of the geology of Alaska, because it indicates that the present geography of Alaska is geologically very young.

ACKNOWLEDGMENTS

I would like to acknowledge the help of Bruce Panuska in the preparation of the data and manuscript, D.R. Packer and Woodward-Clyde and Associates for assistance with data collection and processing, and the University of Newcastle upon Tyne for initiating the project. I appreciate the critical reviews of Sherman Grommé (U.S. Geological Survey) and John Decker (DGGS). Most financial support came from National Science Foundation grants GA-1216 and EAR-00817.

REFERENCES CITED

Beck, M.E., 1980, Paleomagnetic record of plate margin tectonic processes along the western edge of North America: Journal of Geophysical Research, v. 85, p. 7115-7131.

Chantry-Price, R.E., 1967, A paleomagnetic investigation of some post-Carboniferous rocks from Alaska: University of Newcastle upon Tyne, unpublished M.S. thesis, 130 p.

Fisher, R.A., 1953, Dispersion on a sphere: London, Proceedings of the Royal Society, series A217, p. 295-305.

Foster, J.H., 1966, A paleomagnetic spinner magnetometer using a fluxgate gradiometer: Earth and Planetary Science Letters, v. 1, p. 463-466.

Hillhouse, J.W., 1977, Paleomagnetism of the Triassic Nikolai Greenstone, McCarthy Quadrangle, Alaska: Canadian Journal of Earth Science, v. 14, p. 2578-2592.

Irving, E., and Yole, R.W., 1972, Paleomagnetism and the kinematic history of the mafic and ultramafic rocks in fold mountain belts: Ottawa, Department of Energy, Mines, and Resources, v. 42, p. 87-95.

Jones, D.L., Irwin, W.P., and Ovenshine, A.T., 1972, Southern Alaska - a displaced continental fragment: U.S. Geological Survey Professional Paper 750A, p. B213-B219.

Jones, D.L., and Silberling, N.J., 1979, Mesozoic stratigraphy - the key to tectonic analysis of southern and central Alaska: U.S. Geological Survey Open-file Report 79-1200, 37 p.

Jones, D.L., Silberling, N.J., Berg, H.C., Plafker, George, 1981, Map showing tectonostratigraphic terranes of Alaska, columnar sections, and summary description of terranes: U.S. Geological Survey Open-file Report 81-792.

Jones, D.L., Silberling, N.J., and Hillhouse, J.W., 1977, Wrangellia - a displaced terrane in northwestern North America: Canadian Journal of Earth Science, v. 14, p. 2565-2577.

Monger, J.W.H., and Ross, C.A., 1971, Distribution of fusilinaceans in the western Canadian Cordillera: Canadian Journal of Earth Sciences, v. 8, p. 259-278.

Packer, D.R., 1972, Paleomagnetism of the Mesozoic in Alaska: Fairbanks, University of Alaska, unpublished Ph. D. dissertation, 160 p.

Packer, D.R., and Stone, D.B., 1972, An Alaskan Jurassic paleomagnetic pole and the Alaskan orocline: Nature, v. 237, p. 25-26.

Panuska, B.C., and Stone, D.B., 1981, Late Paleozoic paleomagnetic data for Wrangellia; resolution of the polarity ambiquity: Nature, v. 293, p. 561-563.

Richter, D.H., 1967, Geology of the Upper Slana - Mentasta Pass area, south-central Alaska: Alaska Division of Mines and Minerals Geologic Report 30, 25 p.

Richter, D.H., 1976, Geologic map of the Nabesna Quadrangle, Alaska: U.S. Geological Survey Miscellaneous Geologic Investigations Map I-932.

Smith, T.E., 1981, Geologic map of the western Clearwater Mountains, central Alaska: Alaska Division of Geological and Geophysical Surveys Geologic Report 60, 72 p.

Smith, T.E., and Turner, D.L., 1973, Geochronology of the McLaren metamorphic belt, south-central Alaska: A progress report: Isochron/West, no. 7, p. 21-25.

Stone, D.B., and Packer, D.R., 1977, Tectonic implications of Alaska Peninsula paleomagnetic data: Tectonophysics, v. 37, p. 183-201.

_____, 1979, Paleomagnetic data from the Alaska Peninsula: Geological Society of America Bulletin, v. 90, p. 545-560.

Stone, D.B., Panuska, B.C., Packer, D.R., 1981, Paleolatitudes versus time for southern Alaska: Journal of Geophysical Research [in press].

Stout, J.H., 1976, Geology of the Eureka Creek area, east-central Alaska Range: Alaska Division of Geological and Geophysical Surveys Report 46, 32 p.

Van der Voo, R., Jones, D.L., Gromme, C.S., Eberlein, G.D., Churkin, Michael, 1980, Paleozoic paleomagnetism and northward drift of the Alexander terrane, southeastern Alaska: Journal of Geophysical Research, v. 85, p. 5281-5296.

Zijderveld, J.D.A., 1967, A.C. demagnetization of rocks; analysis of results, *in* Collinson, D.W., Creer, K.M., Runcorn, S.K., eds., Methods in paleomagnetism: Amsterdam, Elsevier, p. 254-286.